Recent advances in hydrogel-based drug delivery systems for enhanced cancer therapy: A review

Materials Today Communications 48 (2025) 113615

Contents lists available at ScienceDirect

Materials Today Communications

journal homepage: www.elsevier.com/locate/mtcomm

Recent advances in hydrogel-based drug delivery systems for enhanced cancer therapy: A review

Fatemeh Davodabadi [a], Saman Sargazi [b,c,d,*], Francesco Baino [e,*]

[a] Department of Medical Nanotechnology, School of Advanced Technologies in Medicine, Tehran University of Medical Sciences, Tehran, Iran
[b] Cellular and Molecular Research Center, Research Institute of Cellular and Molecular Sciences in Infectious Diseases, Zahedan University of Medical Sciences, Zahedan, Iran
[c] Genetics of Non-communicable Disease Research Center, Zahedan University of Medical Sciences, Zahedan, Iran
[d] Department of Clinical Biochemistry, Faculty of Medicine, Zahedan University of Medical Sciences, Zahedan, Iran
[e] Institute of Materials Physics and Engineering, Department of Applied Science and Technology, Politecnico di Torino, Corso Duca Degli Abruzzi 24, Turin 10129, Italy

ARTICLE INFO

Keywords:
Hydrogels
Drug delivery systems
Biocompatible materials
Cancer therapy

ABSTRACT

Hydrogels have been identified as a strong group of biomaterials that improve the performance and selectivity of drug delivery applications, especially in cancer treatment. This review systematically summarizes the state of the art in hydrogel-based systems over the past few years, focusing on the multiple types of stimuli sensitivity, such as thermo-, pH-, redox-, and light-sensitivity, which enable targeted drug release in different tumor regions. This comprehensive review article distinguishes between natural and synthetic hydrogels and assesses their potential as drug delivery systems. A focused discussion is presented to detail their uses in various types of cancers, including breast, ovarian, prostate, lung, liver, and gastric cancer, to demonstrate the versatility of hydrogels in enabling site-specific and prolonged drug delivery with minimal off-target effects. Still, issues concerning mechanical solidity, drug encapsulation capability, biocompatibility, and intricate regulatory procedures slow down the translation from bench to bedside. In turn, future studies can minimize the challenges above and enhance the properties of hydrogels to achieve the highest therapeutic efficacy and practical applicability. This review will serve as a valuable reference for researchers and clinicians interested in utilizing hydrogel technology to enhance the current approach to cancer therapy and promote the development of personalized treatment methods.

1. Introduction

According to a recent report, cancer affects approximately 1 in 5 men or women in their lifetime [1]. Across countries with different socio-economic statuses, cancer burdens vary significantly [2]. Globally, breast, lung, colon, and prostate cancer are the most common cancers. Incidence of breast cancer is the highest, but lung cancer is the leading cause of death [3].

To manage this life-threatening disease, early detection and effective treatment are essential. The main challenges in cancer therapy include limitations of conventional chemotherapeutic agents, lack of targeting drugs, and drug resistance [4,5]. In spite of the fact that many cancer types initially respond to chemotherapy, they can eventually become resistant to it [6]. Drug-resistant cancers and the ability of cancer cells to develop resistance to traditional treatments point to the need for more research and treatment development [7]. Drug resistance can be reversed through the use of nanoparticles (NPs) as delivery systems that target key factors involved in cancer development and function [8].

A new area of therapeutic research involves nanomedicine drugs based on active targeting, which offer new avenues for cancer treatment. For several years, Doxil® and Abraxane® have been used as first-generation nanomedicine drugs by modulating their physicochemical properties for passive targeting [9,10]. To selectively target overexpressed receptors on specific tumor cells, antibodies [4], small organic molecules [5,6], and peptides [7] have been conjugated to the surface of NPs. Then, using carriers, anti-tumor drugs can kill tumor cells [9,11]. In past studies, the effectiveness of nanocarriers in various fields of cancer treatment was reviewed, such as drug delivery [8,12,13], vaccines [14], theranostics [15], delivery of oligonucleotides (i.e., small interfering RNAs (siRNAs), long non-coding RNAs (lncRNAs) and microRNAs (miRNAs)) for targeted therapies [10,16], and thermodynamic approaches [17]. Despite their numerous advantages for targeted delivery,

* Corresponding author.
E-mail addresses: davodabadii.fateme@gmail.com (F. Davodabadi), sgz.biomed@gmail.com (S. Sargazi), francesco.baino@polito.it (F. Baino).

https://doi.org/10.1016/j.mtcomm.2025.113615
Received 29 April 2025; Received in revised form 9 August 2025; Accepted 17 August 2025
Available online 19 August 2025

NPs suffer from several major disadvantages, including burst release and poor bioadhesion [18]. As a result, long-term use is discouraged. Researchers are employing a combination of nanoparticles and hydrogels to address this limitation and create more effective drug delivery systems (Fig. 1).

Another practical drug delivery approach is using hydrogels, which act as water-swollen networks. Hydrogels are a special class of polymers that may contain smaller molecules or colloidal particles and can be cross-linked chemically or physically. Hydrogel-based drug delivery systems continue to grow in popularity [19,20]. Different designs can be achieved with hydrogels depending on the molecules that make up the material, their functionality, and their shape, such as i) multiple drug codelivery [21–23], ii) theranostic systems [24,25], and iii) controlled and programmed release [26,27]. Due to their hierarchy of accessible micro- and nano-environments (hydrophobic or hydrophilic), they serve as a versatile delivery platform for drugs, and some have even reached the clinic. They also offer numerous possibilities, including the attachment and combination of ligands with nanoparticles [19].

In principle, hydrogels have the potential to revolutionize cancer treatment strategies. Firstly, water-based hydrogels can replicate both soft and hard tissues, creating an environment that resembles biological conditions [28]. Moreover, they encapsulate drugs, safeguarding them against degradation, extending their effectiveness, and allowing for sustained release through mechanisms such as diffusion, matrix degradation, or external or internal triggers. Peptides, recombinant proteins, and other biopharmaceutical agents, such as polynucleotides and monoclonal antibodies [23–26], as well as siRNA [27–30], can be delivered via hydrogels because they are hydrophilic [29,30]. In nanocomposite gels, hydrogels can also solubilize hydrophobic drugs depending on their architecture, for example, by combining polymer nanoparticles [31,32]. The second advantage of hydrogels is their wide range of sizes, including macrogels, microgels, and nanogels. Hydrogels are prescribed in different ways, including oral delivery, in situ implantation, pulmonary delivery, in situ injection, and intravenous injection. As a result, the hydrogel material provides controlled and continuous delivery of drugs, thereby minimizing drug requirements and systemic side effects [33]. The hydrogel system can also release anti-cancer active substances on demand depending on internal and external environmental factors. There are several key differences between the microenvironment of tumors and healthy tissues, including temperature, pH, redox potential, and reactive oxygen concentration. Using stimuli-responsive hydrogels to detect tumor tissue and release drugs on demand reduces damage to normal tissue [34].

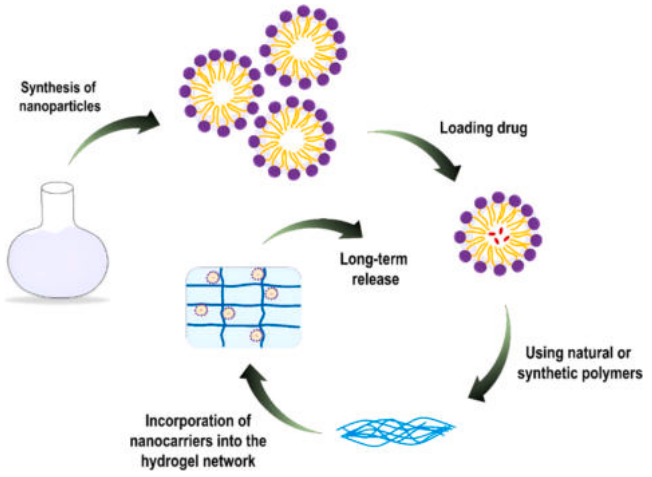

Fig. 1. Using nanocarriers and hydrogels to produce a drug delivery system with better efficiency (this system combines the advantages of both nanocarriers and hydrogels). In addition, it reduces the limitations of using nanoparticles, such as the burst release.

A number of recent studies have focused on the potential of hydrogel systems for cancer treatment [35–39]. For example, Mohammadzadeh et al. discuss recent advances in using hydrogels as immunotherapeutic and cell delivery platforms, highlighting their potential to overcome current limitations [40]. Using smart hydrogels for breast cancer bone metastasis, Chen et al. highlight their potential in gene delivery and immunomodulation of the microenvironment [41]. As reviewed by Chang et al., the use of hybrid hydrogels in the treatment of gynecologic cancers could advance precision therapy and regenerative medicine [42]. Unlike prior reviews in this field, our current study provides a comprehensive analysis of hydrogels, highlighting significant research advancements and key features of both natural and synthetic hydrogels, as well as stimuli-responsive hydrogels designed explicitly for drug delivery applications, which have attracted considerable attention in recent years. A central focus of our review is the potential of hydrogel-based carriers and drug reservoirs to overcome the limitations inherent in traditional therapeutic approaches, enabling targeted, localized, and modulated drug delivery to treat more than ten various cancers. The concluding section of this paper discusses clinical studies and addresses the challenges associated with developing and applying hydrogels in clinical trials. Furthermore, AI was discussed as a way to reduce existing challenges in hydrogel design and drug delivery.

2. Hydrogel-based systems

Hydrogels contain a dense matrix of hydrated intermeshed polymer chains in an aqueous solution that forms a swollen matrix [43]. It is estimated that between 20 % and 99 % of the weight of the polymer matrix is water [44]. Stimulation changes the local properties of a polymer. Stimuli commonly used include temperature, pH, oxidation potentials, electromagnetic power, and light. In general, polymeric hydrogels are liquids with low viscosities. When properly stimulated, polymers can change their drug site and form semisolid gels that are reversible to their original state [45]. Section 2 begins by providing a detailed overview of various polymers employed in the fabrication of hydrogels for cancer therapy. Subsequently, these hydrogel-based systems are classified according to the specific stimuli to which they respond.

2.1. Thermo-sensitive hydrogels

In response to changes in body temperature, the sol-gel transition of these hydrogels maintains drug retention in the tumor microenvironment. Their architectures require a delicate balance between hydrophobic and hydrophilic monomers to produce a thermal response [46,47]. As a result of phase separation, low dissolution temperatures are represented by the lower critical solution temperature (LCST), whereas high dissolution temperatures are represented by the upper critical solution temperature (UCST) (Fig. 2). LCST is the temperature at which thermally responsive polymers undergo a phase transition, and the material can be dissolved at a low temperature.

At higher temperatures, molecules precipitate out of the solution and undergo sol-gel transitions. Thermally responsive polymers undergo phase transitions below the upper critical solution temperature (UCST), and they cannot dissolve at low temperatures but can be dissolved above this temperature. Because heat-responsive polymers with a lower LCST can form hydrogels only above the LCST, which is closer to human body temperature, these polymers have good prospects for biomedical applications. Various polymers with polysaccharides have UCST and cannot react at physiological temperatures, such as Kara gum, cold glue, agarose, and starch [48]. A hydrogel forms as the LCST temperature is reached, causing the polymer to shrink and become hydrophobic and insoluble. Due to this, polymers near the critical temperature undergo phase changes from soluble to insoluble [49]. Heat-responsive polymers interact molecularly at high temperatures due to the presence of hydrophobic molecules. The polymer chains are exposed to water

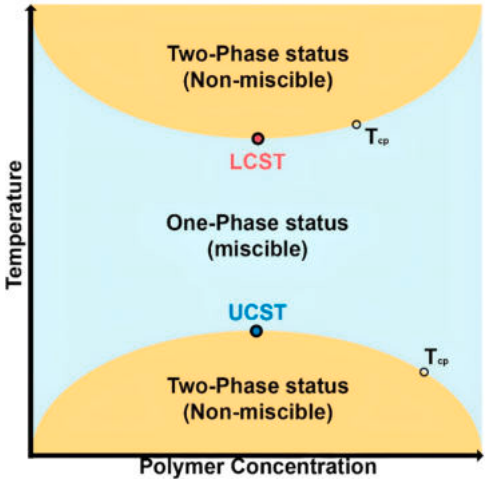

Fig. 2. LCST and UCST. Polymer concentration affects the phase transition temperature of LCST polymers. As a result, LCST refers exclusively to the lowest temperature, while the temperature above LCST that induces a phase change is often referred to as T_{cp}. LCST: Lower critical solution temperature, UCST: upper critical solution temperature, T_{cp}: cloud point temperature. Reprinted from [52] under the terms and conditions of the Creative Commons Attribution (CC BY) license (https://creativecommons.org/licenses/by/4.0/).

molecules, which swell the polymer to form a hydrogel [50]. Thermodynamically, the transition from sol to gel is relocated because of the freedom of motion [51]. Interactions between molecules, such as hydrogen bonds and hydrophobic interactions, can lead to phase separation [49].

2.2. pH-sensitive hydrogels

This type of hydrogel consists of polymers with acidic and basic groups that ionize at varying pH levels (Fig. 3) [44]. The polymer backbone provides mechanical stability in this formulation, while the ionizable component is responsible for pH sensitivity [53]. The molecular structure of hydrogels can be tailored to control the mechanical, responsive, and diffusive properties [54]. pH-sensitive hydrogels change the amount of dissociated carboxylic ions based on solution pH. In pH-sensitive hydrogel sensors, the refractive index and volume of the hydrogel are changed by altering pH [55,56]. Hydrogels with varying water contents vary in size and refractive index. Since pure water has a lower refractive index than hydrogel in its shrunken, unexposed state, swelling can result in a negative shift of refractive index [53].

2.3. Redox-sensitive hydrogels

Because intracellular and extracellular compartments have vastly different redox potentials, redox-responsive hydrogels can release drugs inside cells [58]. Redox-responsive hydrogels can be achieved by using cross-linkers containing disulfide, and several methods exist to produce them. The first method involves the use of crosslinking precursor polymers with disulfide bonds [59–61]. During or after cross-linking, small-molecular-weight active species can be loaded into these hydrogels through physical encapsulation or noncovalent interactions.

Conversely, macromolecular compounds should be loaded during cross-linking unless they interact noncovalently with the hydrogel surface, since they are too large to diffuse and penetrate. By covalently attaching proper loads to hydrogels via disulfide bonds, high specificity and loading capacity can also be achieved [58]. The covalent bonding of lysozyme between redox-cleavable crosslinkers in dextran hydrogels was reported to maintain lysozyme activity. Glutathione (GSH) reduces disulfide bonds, rapidly releasing immobilized lysozyme [60]. Compared to disulfide and diselenide bonds, succinimide thioether bonds have been relatively less studied in the literature. The most common application of succinimide thioether bonds in hydrogels is as a crosslinking agent [62–65], but they have also been used in micelles [66] and hybrid hydrogel-liposome systems [67]. PEG polymers are often used as building blocks for hydrogels that incorporate succinimide thioethers. Succinimide thioether cross-links were formed using a variety of PEG groups [62–65].

2.4. Light-sensitive hydrogels

Light irradiation alters the structure and conformation of light-responsive hydrogels [68,69]. The intensity, wavelength, exposure

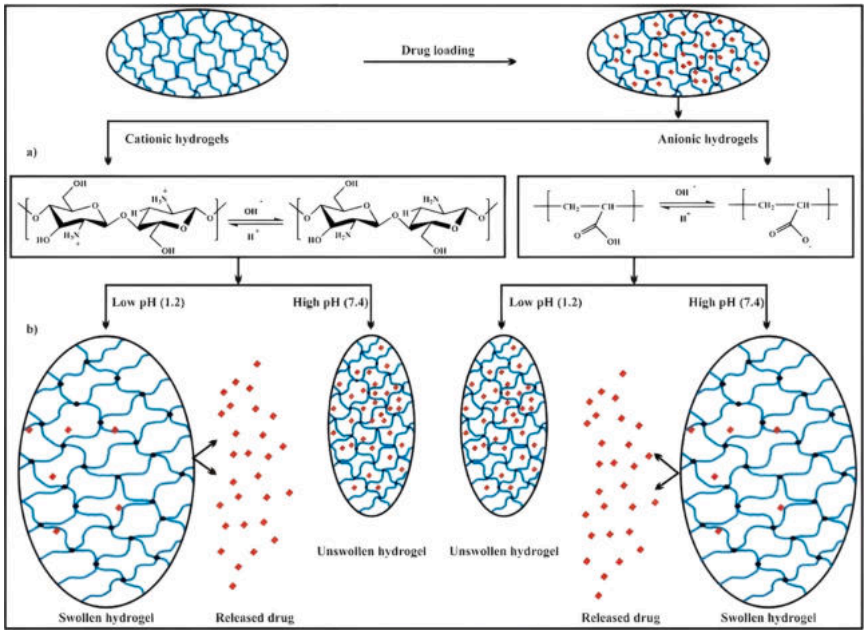

Fig. 3. Mechanism of cationic and anionic hydrogels. (a) Hydrogel chains ionize based on pH, and (b) Swelling and drug release are pH-dependent. Reprinted from [57] under the terms and conditions of the Creative Commons Attribution (CC BY) license (https://creativecommons.org/licenses/by/4.0/).

time, and beam diameter of an external stimulus, such as light, can be easily controlled and are readily acquired, making them effective and noninvasive. In the past decade, light has become increasingly crucial for controlling drug delivery accurately and spatiotemporally [70]. The polymer structure of light-responsive hydrogels can be modified with photosensitive moieties. A reversible or irreversible reaction may be caused by the use of photosensitizers [69]. Hydrogels can undergo partial or complete de-crosslinking, degradation, swelling, or shredding when light cleaves, isomerizes or dimerizes photosensitive groups [71].

The three types of light-controlled drug delivery systems are photoisomerization, photochemical, and photothermal. Photoisomerization in hydrogels involves conformational changes from the trans to the cis form under light irradiation. It is during this process that hydrogels open their pores, allowing drugs to diffuse out of their matrices. This process does not break the chemical bonds of hydrogels; it can usually be reversed and repeated [72]. The hydrogel network structure and configuration can be altered by photochemical reactions, leading to drug release [73]. Photocleavage is one of the most common photochemical reactions for controlled drug delivery. This method incorporates light-cleavable linkers into the hydrogel structure to create nanoparticles [74,75]. Drugs are covalently attached to hydrogel networks using photocleavable linkers, preventing unwanted release [76,77]. During photothermal reactions, light energy is converted into heat energy, which disrupts thermally sensitive drug carriers [78,79]. Two components are needed for the reaction: a photosensitizer that converts light into heat and a temperature-sensitive material that releases the drug when the temperature changes [71].

2.5. Electro-Responsive Hydrogels

Hydrogels and nanohydrogels that are electrically sensitive or electroactive undergo precise conformational changes, expanding or contracting in response to an electric field [80,81]. The shape of the gel and its position relative to the electrodes determine how electro-responsive hydrogels respond to an electric field. The central axis of the hydrogel bends when it lies parallel to the electrodes (but does not touch them), whereas deswelling occurs when it lies perpendicular to them [82]. By controlling the mechanical response of polyelectrolyte hydrogels to an electric field, the release of drugs can be precisely regulated. During gel formation or after the gel has been formed, drug molecules can be incorporated into the network by incubating the gel in a drug solution. A variety of small and large, charged and uncharged guest molecules have been electro-stimulated to be released. Typically, drugs are released when an electric field is applied, and the delivery is stopped or reduced when the field is removed [83]. Forced convection, electrophoresis of charged drugs, diffusion, syneresis water, and erosion of electro-erodible gels are the main mechanisms of drug release [84].

2.6. Magneto-responsive hydrogels

A magneto-responsive hydrogel is a polymeric network embedded with magnetic particles, such as iron oxide or other ferrimagnetic materials [85,86]. Magnetic hydrogels are field-responsive because of the embedded magnetic particles [87–90]. Fe_3O_4, cobalt ferrite ($CoFe_2O_4$), and carbonyl iron (CI) are common magnetic particles. The type, size, composition, and distribution of magnetic particles have a significant impact on the mechanical properties and behavior of hydrogels [90–97]. Under localized magnetic fields, the hydrogel releases therapeutic agents at specific sites, improving precision and treatment effectiveness [98]. Additionally, when exposed to alternating magnetic fields, the magnetic nanoparticles in these hydrogels generate heat, which is utilized in hyperthermia therapy to treat cancer non-invasively [99–101].

2.7. Entity-responsive hydrogels

Furthermore, hydrogels can also respond to specific entities such as metal ions, small molecules, proteins, and glucose in addition to physicochemical stimuli [102–104]. The responsiveness of hydrogels makes them highly promising for biosensing and environmental monitoring [98]. For example, using boronic acid-glucose complexation, Dong et al. reported the development of an injectable and glucose-responsive hydrogel that was able to release an encapsulated model drug in response to glucose [105]. In another study, it has been reported that a glucose-responsive hydrogel dressing system stimulated wound healing in rats with methicillin-resistant Staphylococcus aureus wounds [106].

2.8. Multi-stimuli responsive hydrogels

Biomedical applications of multi-stimuli responsive hydrogel systems include targeted drug delivery, tissue engineering, environmental remediation, and multifunctional sensors [98]. Drug delivery is more versatile and specific when multiple stimuli are combined. In addition to responding to numerous stimuli, hydrogels derived from special polymers can detect minute changes in their environment with great precision. As soon as the hydrogel is exposed to the stimuli, its constituents are released [107]. As a result, they have synergistic effects compared to single-stimulus hydrogels. Specific effects include complex shape transformations, directional motion, and synergistic chemo-magnetism hyperthermia in the treatment of cancers [108]. In addition to enhancing therapy efficacy, this delivery also reduces chemotherapy side effects.

3. Types of hydrogels

3.1. Natural hydrogel

Natural hydrogels derive from biological materials, such as hyaluronic acid, collagen, fibrin, gelatin, amino polysaccharide chitin, chitosan, cellulose, naturally occurring anionic biopolymer alginate, agarose, and elastin [109]. The advantages and limitations of some representative hydrogels of this group are depicted in Fig. 4.

Collagen forms a triple helix and is one of the most abundant proteins in the body. When collagen biopolymers are cross-linked with alginate, oxazolidine, or hyaluronic acid, their mechanical strength can be increased [110,111]. A collagen-binding domain (CBD) is responsible for the interactions between proteins and collagen [112]. It is possible to target the release of CBD-associated biomolecules into the tumor collagen scaffold by engineering antibodies, drugs, or cytokines that contain CBD, thereby reducing off-target effects, minimizing systemic toxicity, and increasing localized retention. Combining collagen-derived

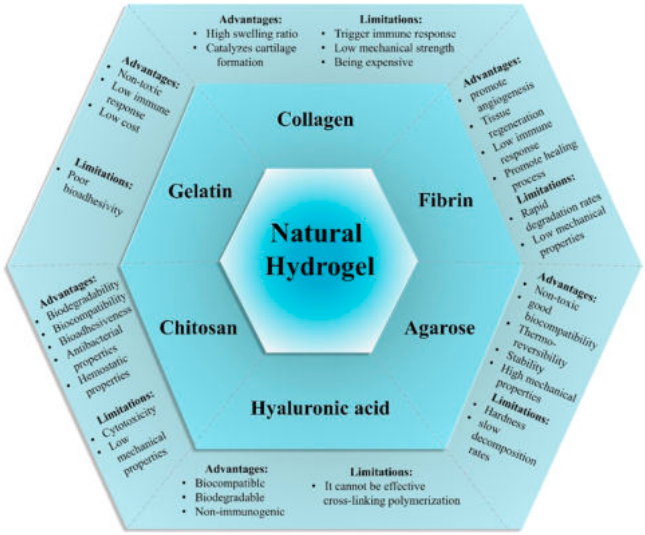

Fig. 4. A brief overview of natural hydrogels used in biomedicine.

hydrogels with CBD has also been investigated to improve in situ drug delivery. Using collagen hydrogel implants containing CBD and interferon-alpha 2b, immunotherapeutic drugs can be delivered locally and in a temporally controlled way [113].

Hyaluronic acid (HA) has three chemical groups: hydroxyl, carboxylic, and N-acetyl, which can be modified chemically. HA is synthesized by various cells, including fibroblasts [114]. In addition to its high water-binding capacity, HA is non-toxic, biodegradable, cytocompatible, and nonimmunogenic [115]. Research has demonstrated the potential for using HA-based nanomaterials to treat cancer, including polymeric drug-conjugated HA, micelles, polymersomes, hydrogels, and inorganic NPs (Fig. 5) [116].

Fibrinogen and thrombin can be combined and heated at 37°C to produce fibrin-based hydrogels. Therefore, altering the fibrinogen concentration can readily modify the mechanical properties of these fibrin gels. As a biomaterial, fibrin is famous for engineering adipose, dermal, and cardiovascular tissues since it is biocompatible and easy to manipulate [117]. When fibrin hydrogels are degraded by plasmin or other cell-produced enzymes, they can lose their mechanical stiffness in an uncontrollable and unpredictable manner. In 3D cultures, these hydrogels have not been widely used due to their low stability and opacity. PEGylated fibrin hydrogels with increased transparency and stability have recently been developed [118].

In either alkaline (type B) or acidic (type A) conditions, gelatin is a natural polypeptide extracted from animal collagen and partially hydrolyzed. Gelatin is characterized by its superior physicochemical and biological properties, such as its abundance, relatively low cost, biocompatibility, and biodegradability, as well as its ability to adhere to cells, low immunogenicity, and ease of chemical modification. These properties are the reasons why it has received increasing attention for use in industrial and biomedical applications. This polymer has crosslinking properties due to its accessible amine, carboxyl, and hydroxyl functional groups. Furthermore, it is antimicrobial and antioxidant [119–121]. Gelatin suffers from poor mechanical strength and relatively rapid degradation, which are two crucial limitations in the frame of biomedical applications. It is possible to solve these issues by crosslinking gelatin and fabricating hydrogels chemically hybridized from gelatin [122,123].

Chitosan is recognized for its biocompatibility, biodegradability, bioadhesiveness, antibacterial characteristics, and hemostatic abilities, making it valuable in tissue engineering and RNA delivery applications [124]. It is of interest as a local therapy because it stimulates wound healing by modulating inflammation [125]. The basic pH of chitosan promotes its gelling due to its polycationic nature [126]; when tumors and tissue become acidotic, chitosan gel precursors spread locally [127, 128]. The problem with using chitosan hydrogels is that the crosslinker, known as the dialdehyde, which is usually glutaraldehyde, can be toxic to humans [129].

Agarose, a linear polysaccharide derived from red marine algae, is inexpensive, inert, and readily available. In addition to its excellent biocompatibility, optimal gelling characteristics, and tunable mechanical properties, it is a superb biomaterial for manufacturing scaffolds for tissue engineering [130,131]. However, its poor bioadhesivity limits its use as an ECM-mimicking material [132].

The crosslink network of elastin is formed from its soluble precursor tropoelastin, resulting in an insoluble polymer. Amorphous elastin and microfibrils form the elastic fibre, which acts as a scaffold for elastin to deposit. As a result of its elasticity, elastin is frequently used for building scaffolds to replace skin as well as vascular grafts [133]. Biocompatibility and biodegradability are two of the interesting properties of elastin, which is a natural component of the ECM. It is therefore necessary to purify elastin from the elastic fibers formed during its synthesis. There is a possibility of contamination during this purification process, which can lead to immune responses by the body, and elastin tends to calcify during this process. For 3D cell cultures, drug and gene delivery, highly porous hydrogels derived from elastin are studied [134–136].

Brown algae cell walls and some bacteria capsules contain alginate polysaccharide [137]. α-L-gluconate and β-D-mannuronate are the two monomers making up its structure [138]. Alginate has nontoxic and noninflammatory properties for medical applications. However, it exhibits poor cell adhesion and poor mechanical characteristics. The use of alginate has been explored in contact with different tissues, including the liver, nerves, heart, and cartilage [139]. In order to treat chronic osteomyelitis, pH-sensitive silk fibroin (SF)/sodium alginate hydrogel scaffolds containing teicoplanin and phenamil-loaded SF nanoparticles were developed, assuring 40 and 35-day drug release profiles of phenamil and teicoplanin [140].

From various agricultural wastes, cellulose is produced in large quantities and is widely used, affordable, and biodegradable. Cellulose, a polymer of glucose, is the primary component of plants and natural fibers such as flax and cotton. Hydrogels can be created by dissolving native cellulose with N-methylmorpholine-N-oxide monohydrate or ionic liquids [141]. An anionic polymer compound, carboxymethyl cellulose (CMC), has a molecular weight of thousands to millions Da, is odorless, tasteless, and hygroscopic [142]. CMC gel, or colloidal solution, forms when dispersed in water. Due to low toxicity and immunogenicity, intelligent responsiveness [143], biocompatibility, and

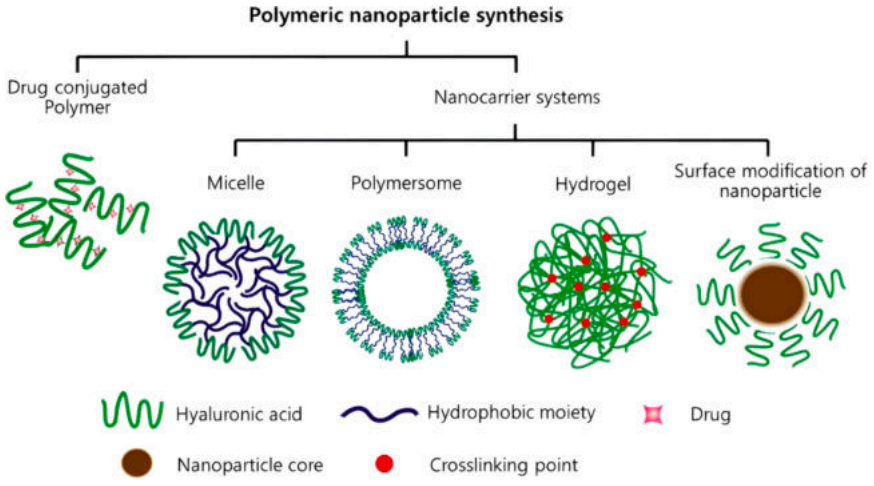

Fig. 5. HA-based nanomaterial formulations. Nanomaterials based on HA for cancer treatment include polymeric drug-conjugated HA as well as micelles, polymersomes, hydrogels, and inorganic nanoparticles. Reprinted from ref [116] under the terms and conditions of the Creative Commons Attribution (CC BY) license (https://creativecommons.org/licenses/by/4.0/).

biodegradability [144], CMC-based hydrogels have attracted extensive research attention as auspicious materials for use as drug carriers in clinical fields [145]. Drug delivery can be achieved by using a variety of hydrogels synthesized using CMC with additives such as tamarind gum, gelatin, xanthan gum, graphene oxide, chitosan, polyacrylamide, etc [146]. For example, a hydrogel containing CMC and xanthan was prepared using monochloroacetic acid as the cross-linker and proposed as a carrier for the slow delivery of cefmenoxime drug through gastrointestinal path and transdermal systems [147].

3.2. Synthetic hydrogels

Several materials make up synthetic hydrogels, including polyethylene glycol (PEG), polyvinyl alcohol (PVA), polylactide (PLA), polyacrylamide, poloxamer 407 and 188, poly(N-isopropylacrylamide) (PNIPAM), polyvinylpyrrolidone (PVP), and Polyacrylic acid (PAA) (Fig. 6). By physically or chemically crosslinking many functional polymers, synthetic hydrogels typically have a higher mechanical strength than natural hydrogels, allowing them to be used in a broader range of applications [109].

There are many applications for PEG, including tissue regeneration and drug delivery. A PEG-based biomaterial is biocompatible, does not stimulate immune responses, and is highly soluble in water. Due to its properties, PEG has been used in various formats, including bulk, thin solid films, hydrogels, and nanoparticles [148]. Due to its non-toxic nature, PEG is also highly stable during internal body circulation. PEG can be chemically functionalized with diverse target groups, such as imines, orthoesters, acetals, and ketals [148]. Tumor microenvironment can induce the release of cargo drugs in response to pH, temperature, and redox changes. Additionally, PEG hydrogels can enhance permeability and retention (EPR) by precisely controlling the nanoparticle size [149]. PEG-based materials offer these advantages for developing localized and on-demand drug delivery strategies.

The hydrophobic polyester PLA, along with its copolymers, is widely used in biomedical applications [150]. Copolymerizing PLA with hydrophilic polymers like PEG changes its physical properties. Biphasic copolymers form micelles that are tunable by changing both the PLA and PEG molecular weights [151,152]. A tri- and multi-block copolymer of PEG and PLA was synthesized, opening the door to PLA use for hydrogels [153]. PEG-PLA hydrogels exhibit thermo-responsive properties due to their copolymer ratio, which offers numerous possibilities. These hydrogels are typically soluble at room temperature and gel at 37°C, which is the body temperature [154]. The copolymer type and chain length of PLA-PEG polymers have a significant impact on water molecule access to PEG and drug release rate. Due to stronger hydrogen bonds between chains, an increase in PEG content reduced chain mixing energy and slowed drug release [155].

Due to its reversible sol-gel transition with temperature, its ability to increase the solubility of hydrophobic compounds, extended release of payloads, biodegradability, excellent safety profile, and clinical potentials in the biomedical field, $PLGA_{1500}$-*b*-PEG_{1000}-*b*-$PLGA_{1500}$ triblock copolymer hydrogel (ReGel) is among the most popular polymer-based hydrogels [156,157]. PLGA segments that are hydrophobic physically associate to form thermosensitive hydrogels. Most triblock copolymers form individual loops at low temperatures, joining two hydrophobic PLGA segments together in the center of each loop. Several loops will share the hydrophobic PLGA center (microsome formation) as low temperatures approach [158,159].

There are other thermosensitive polymers, such as poly(N-isopropylacrylamide) (PNIPAM), that are also popular in research [160]. A hydrophilic amide group and a hydrophobic isopropyl side chain make up this compound, which has a LCST of 32°C [161,162]. At room temperature, PNIPAM solutions take on a sol state, and at body temperature, they can take on a gel state [163]. PNIPAM is therefore an excellent candidate for applications in biomedical areas, including drug delivery, tissue engineering scaffolds, and wound dressings [164–166]. Drug molecules can easily be loaded into hydrogels by directly dissolving them in the solution at a lower temperature, then raising the temperature to above the LCST to gel them. Furthermore, maintaining fine control over the temperature can result in site-specific drug delivery [167].

Physical hydrogels based on PVA have superior mechanical and biocompatibility properties [168,169]. In biotechnology and biomedicine, these materials have been used for decades to immobilize enzymes and whole cells, convert biomass, and engineer tissues. By freezing and thawing polymer solutions, cryogellation produces robust and biocompatible PVA materials [168]. Biomedical engineers have primarily overlooked the application of PVA cryogels due to their inability to fulfill the specific criteria necessary for nanomedicine, including precise nanoscale dispersion and controlled release of therapeutic agents. However, recent advances in nanotechnology and polymer science, such as the synthesis of polymers with precise molecular weight control, novel bioconjugation methods, and controlled supramolecular associations, have enabled the development of PVA-based hydrogels into

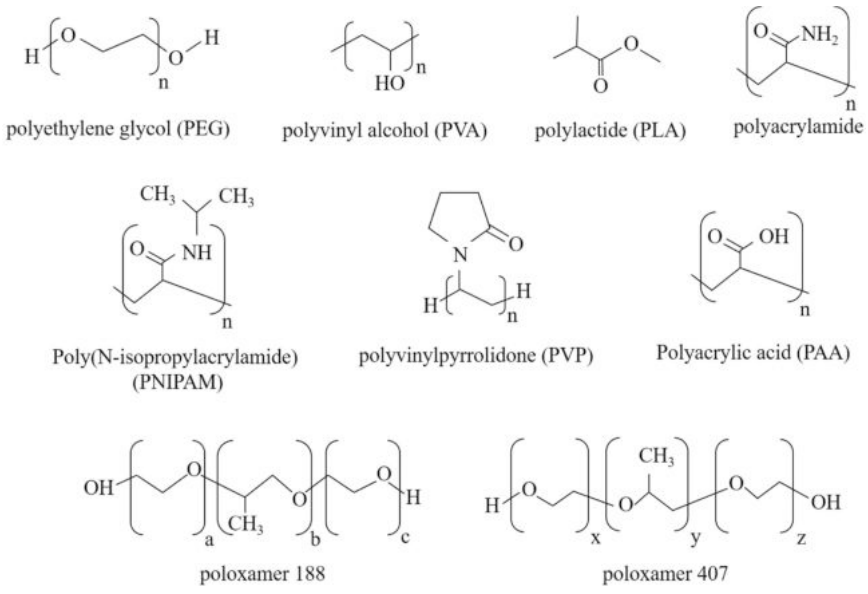

Fig. 6. The chemical structure of materials making up synthetic hydrogels.

stand-alone biomedical materials [170].

The polyacrylamide hydrogel comprises 95 % water and 5 % polyacrylamide [171]. In particular, Chinese medical facilities have been using polyacrylamide injections for breast augmentation for more than 10 years. Despite the Chinese State Food and Drug Administration's ban on the clinical use of polyacrylamide on April 30, 2006, its long-term consequences may not become apparent for several decades [172].

Water-soluble PVP is another biocompatible polymeric hydrogel used for many biomedical applications [173], [174,175], including contact lenses, drug delivery systems, scaffolds for tissue engineering, and wound dressings [173,174,176–178]. When applied as a surface coating, PVP hydrogel increases its hydrophilicity, reducing protein adsorption [179,180]. As a result, decreased protein adsorption limits the adhesion of cells and the activation of blood platelets [181].

PAA is a super-absorbent polymer capable of absorbing and retaining large quantities of water. Each repeating unit of the polymer PAA contains a single carboxylic acid group, resulting in a higher concentration of ionic groups than any natural polymer. The abundance of carboxylic acid groups in PAA makes this polymer highly amenable to chemical and physical modifications for developing biofunctional surfaces [182]. Using highly conductive PAA hydrogels, a wide range of reactive sensors can be developed by reversibly swelling/decaying in response to changes in surrounding conditions such as pH, organic solvents, light, electric fields, temperature, and humidity [183]. On the other hand, pure PAA hydrogels have significantly lower biocompatibility and biodegradability than natural hydrogels [184]. For the delivery of quercetin anticancer drug to MCF-7 cells, a novel PAA-based hydrogel coated with γ-alumina modified with PVP was synthesized; pH-sensitive drug delivery based on this system was achieved orally, nasally, ocularly, and parenterally [185].

Another class of appealing materials is that of poloxamers, which are nonionic triblock copolymers available under the trademark Pluronics® [186]. Poloxamer 407 (P407) is one of the most studied poloxamers because of its good solubilizing capacity, low toxicity, and drug release characteristics, as well as its compatibility with many biomolecules [187,188]. Due to their ability to be liquid at room temperature and viscous at body temperature, thermosensitive gels based on P407 have an excellent potential for the treatment of periodontal disease [189, 190]. However, periodontal treatments with P407 have been limited due to short in situ residence times. Other biocompatible polymers could be incorporated into the P407 formulation to increase the strength and mucoadhesion, ensuring sustained release of the dispersed drugs [191]. Biocompatible block copolymer Poloxamer 188 (P188), a poly(ethylene oxide)–poly(propylene oxide) copolymer, is FDA approved [192]. When P407 and P188 are combined, gelation temperature can be controlled and gel strength increased as well [193].

3.3. Hybrid hydrogels

Bioengineering and drug delivery applications have demonstrated remarkable versatility with hybrid hydrogels that combine natural and synthetic polymers with nanoscale additives [194–196]. In hybrid hydrogels, multiple materials (natural or synthetic) or crosslinking mechanisms are incorporated, and this design allows materials to respond to more than one type of external stimuli [197–199]. The natural/synthetic hybrid hydrogels have a high water content, a high degree of flexibility, and is biocompatible and swells well [200]. The advantageous applications of hybrid hydrogels include: i) Using hybrid hydrogels, chemotherapeutic agents are encapsulated within a polymeric network to maintain sustained, local concentrations of the drug in tumor cells without causing systemic side effects; ii) By implanting or injecting hybrid hydrogels, we can create an in situ depot that slowly releases chemotherapeutics or immunomodulators, aiming to target microscopic foci that would otherwise remain untreated; iii) When loaded with radioprotective nanoparticles or antioxidant compounds, this hydrogels can reduce damage to adjacent normal tissues during and after radiation [42].

Hydrophobic drug delivery and intestinal targeted drug delivery are excellent uses of natural/synthetic hybrids [201]. A CMC-PEG hydrogel film was prepared with citric acid as a non-toxic crosslinking agent to deliver ketoconazole, a hydrophobic drug. Hemocompatibility and cytocompatibility of the hydrogel films were excellent. Enhanced loading and controlled release of poorly soluble drugs were achieved using CMC-PEG hydrogel films [202]. The xylan was crosslinked and copolymerized with N-isopropylacrylamide (NIPAm) and acrylic acid (AA) using UV irradiation to produce a temperature- and pH-dual-responsive hydrogel. There was a cumulative release rate of around 90 % and 26 % of acetylsalicylic acid in intestinal and gastric fluids, respectively [203]. Moreover, injectable hydrogels can achieve accurate and targeted local delivery and are more effective in preventing infection than traditional hydrogels using minimally invasive techniques. Therefore, it can be used to develop and improve natural/-synthetic hybrid hydrogels for drug delivery [204]. Using pH-sensitive and dynamic hydrazone linkages at 37 °C, injectable polymeric hydrogels were synthesized combining oxidized pullulan and 8-arm PEG hydrazine. Such hydrogel systems provided 28 days of sustained release of PEG-Dexamethasone conjugate in a pH-sensitive manner. At pH 6.5 and 7.4, 74.5 % and 55.1 % PEG-dexamethasone conjugate was released [205].

4. Hydrogels for targeted cancer therapy

Blood circulation quickly removes a chemotherapy drug administered directly into the bloodstream, preventing its accumulation and allowing tumor tissue to be eradicated for a prolonged period [206]. Several chemotherapeutic drugs can be released around tumor tissues after being wrapped in hydrogels to avoid multiple injections and maintain a high drug concentration locally [207–209]. A catheter or syringe can be used to inject hydrogels into the body [210]. Hydrogels can potentially load more chemotherapy drugs; in this case, multiple or dual chemotherapy reduces side effects and dosages compared to single chemotherapy [211]. Hydrogels have gained increasing popularity in recent years for tissue engineering and regeneration, with more trials being conducted to deliver chemotherapy drugs in situ using these biomaterials.

4.1. Breast cancer

At present, 2.3 million new cases of female breast cancer are expected annually, representing 11.6 % of all cancers. Globally, 666,000 deaths are caused by this disease, and actually, the most common cancer death is due to breast cancer in 112 countries [1]. Breast cancer is caused by both internal and external factors [212]. A poor lifestyle, an unfavorable environment, and social-psychological factors all contribute to its occurrence. A genetic mutation or family history accounts for 5–10 % of breast cancers, while modifiable factors account for 20–30 % of this disease [213].

In a study, niosomes encapsulating tamoxifen citrate (TMC) were prepared using liquid film hydration techniques. These products were then incorporated into thermoresponsive Pluronic hydrogels. The polymer formulation was adjusted correctly to ensure that the gelation temperature of the hydrogel ranged between 34 °C and 37°C. This TMC-containing hydrogel allowed for the sustained release of the drug and was found to be more effective than free TMC in reducing tumor size *in vivo*. The high viscosity and flexibility of TMC-loaded niosomal thermosensitive hydrogels were crucial in controlling the release of the drug from the gels [214]. A PLGA-PEG-PLGA thermoresponsive hydrogel was used in another study to provide local delivery of herceptin, thereby decreasing its systemic effects, including cardiotoxicity. The mixture of hydrogels was created using the blending method. Strong fluorescence signals were maintained at the injection site for four weeks after injection with the hydrogel system, as shown in Fig. 7 [215].

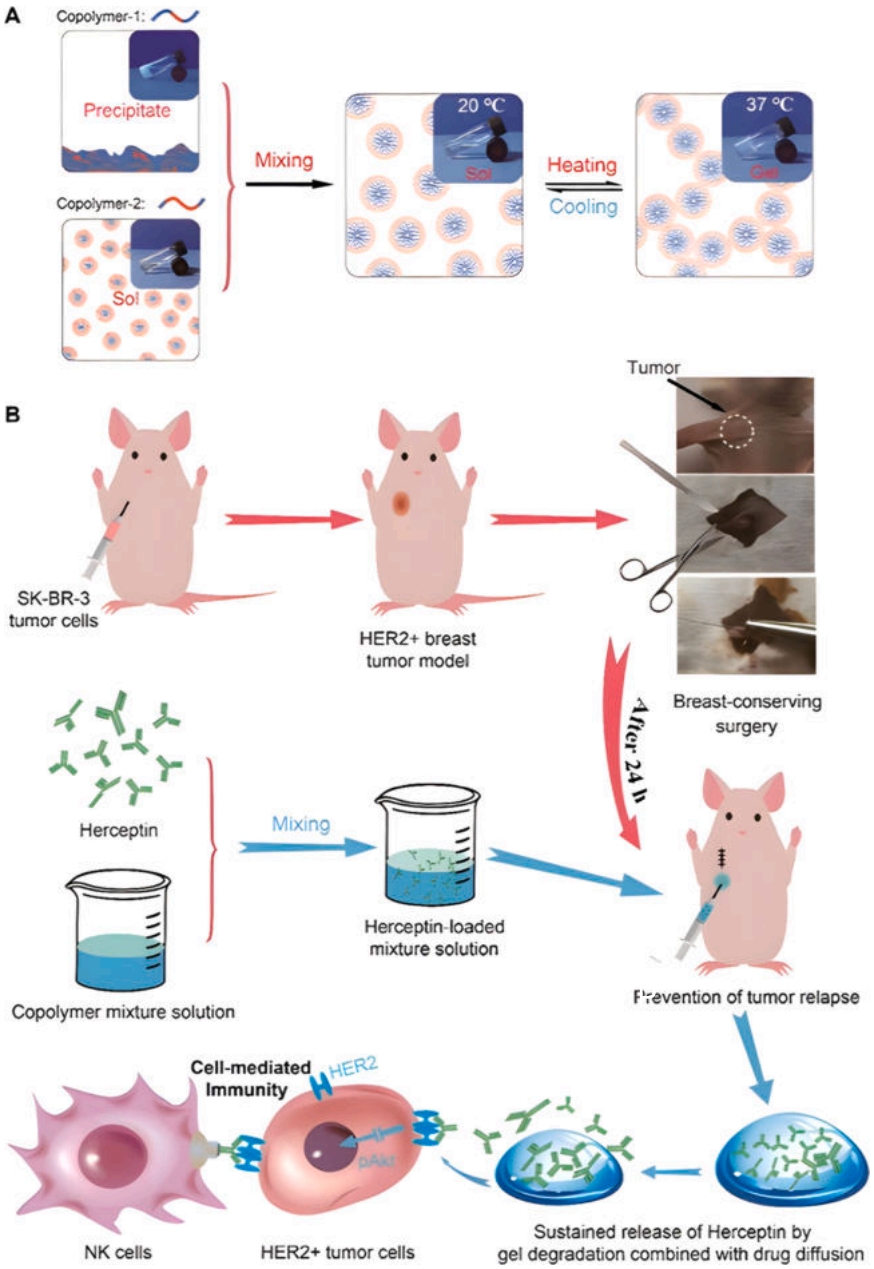

Fig. 7. Schematic of the Herceptin-loaded hydrogel used after breast-conserving surgery for preventing HER2 + breast tumor recurrence. Breast tumors with HER2 + were treated with a hydrogel loaded with herceptin. Low temperatures cause micelles to form in aqueous solutions. During the sol-gel transition, micellar aggregation induced by hydrophobic interactions creates a percolated micelle network at high temperatures. A hydrogel containing herceptin was hypodermically injected 5 mm away from the site of the tumor excision. Herceptin was sustained for an extended period due to gel degradation and drug diffusion. The effects of sustained herceptin delivery inhibited pAkt signaling and stimulated NK cell-mediated immunity. NK: natural killer cells. Reprinted from ref [215] under the terms and conditions of the Creative Commons Attribution (CC BY) license (https://creativecommons.org/licenses/by/4.0/).

Polyamidoamine (PAMAM) dendrimers and PEG hydrogels have been proposed for the sustained delivery of hydrophobic anticancer drugs (silibinin, camptothecin, MTX). The solubility of silibinin, camptothecin, and MTX increased by 37-fold, 4-fold, and 10-fold in the presence of vinyl sulfone-functionalized PAMAM dendrimers. After 48 h, MTT assays of J82 and MCF7 cells treated with various doses of drug-encapsulated hydrogels revealed cytotoxicity for all three drugs. In spite of its lower solubility, camptothecin exhibited higher cytotoxicity to both cell lines than silibinin and MTX, achieving 95 % cell death [216].

Scientists prepared graphene oxide-conjugated folic acid (GOFA) for the targeted delivery of DOX. The pH-sensitive properties of graphene oxide are being used to release drugs. GOFA-DOX was encapsulated in a poly(N-isopropylacrylamide)-chitosan-poly(N-isopropylacrylamide) hydrogel designed for intratumoral delivery (Fig. 8**A**). A slow degradation time of up to 3 weeks is also observed for HACPN. Intratumoral delivery of GOFA-DOX/HACPN enables tumor cells to absorb GOFA-DOX through interactions with GOFA and the folate receptor. Cells treated with GOFA-DOX (30 %) showed a higher apoptosis rate than cells treated with DOX (8 %) and GO-DOX (11 %) (Fig. 8**B**). Based on tissue biopsy examinations and blood analysis, GOFA-DOX/HACPN delivered intratumorally did not induce acute toxicity (Fig. 8**C**) [217].

For the delivery of 5-FU, a hybrid pH-sensing hydrogel was prepared by combining CuBTC with PVA and borax for crosslinking. In both HeLa and MCF-7 cells, the hydrogel exhibited excellent biocompatibility. At pH 5.2, the hydrogel swelled more than at pH 7.4, indicating a greater

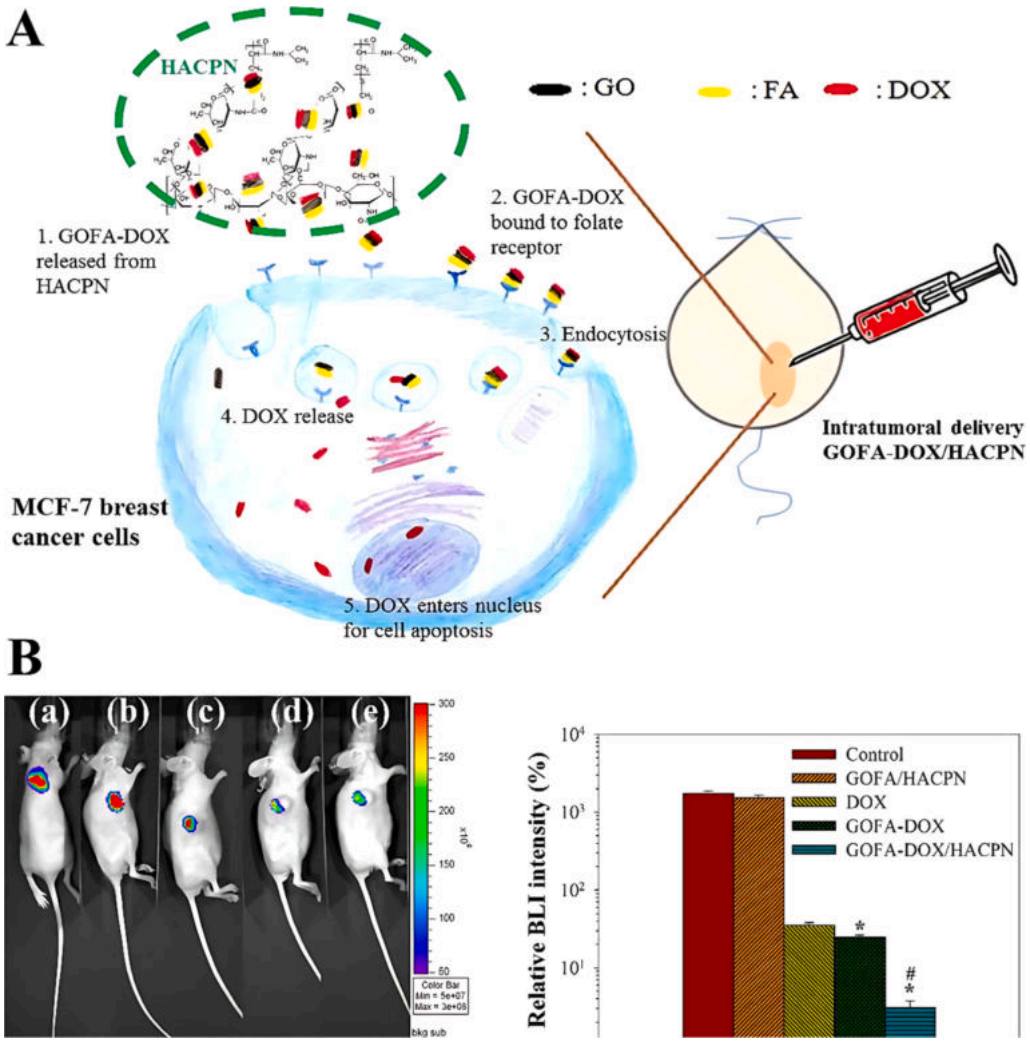

Fig. 8. **A)** In mice, GOFA-DOX/HACPN was delivered intratumorally to induce an antitumor effect. **B)** Between the GOFA/HACPN treatment group and the control group without any drugs, there was no significant difference in BLI signal. At 21 days, the intensity of the combinatory GOFA-DOX/HACPN signal decreased to 3.1 %. GO: graphene oxide, FA: folic acid, DOX: doxorubicin, HACPN: hyaluronic acid-chitosan-g-poly(N-isopropylacrylamide). Reprinted from ref [217] under the terms and conditions of the Creative Commons Attribution (CC BY) license (https://creativecommons.org/licenses/by/4.0/).

ability to absorb and hold water. At pH 5.2, the release of 5-FU in the 6 h, 24 h, and 36 h samples was 15.4 %, 54.2 %, and 84.4 %, respectively [218]. In addition to hydrogels responsive to temperature and pH, gellan gum-based redox-responsive implantable hydrogels have been developed for the treatment of HER2 + breast cancer. Acetate and phosphate buffers were used in this study to synthesize hydrogels that were also crosslinked with l-cysteine at various concentrations. Modifying the cross-linking density of the HGGs enables customization of the rate at which taxane is released from PTX-loaded HGGs after tumor resection *in vivo*. Taxane was delivered through glutathione-responsive mechanisms. All hydrogel samples exhibited a minor initial burst release after 6 h, which is characteristic of biodegradable polymers. PTX release ratios from non-crosslinked HGGsAB@PTX and HGGsPBS@PTX were 45 and 35 %, respectively, whereas PTX release ratios from cysteine crosslinked HGGsAB[3LCys]@PTX and HGGsPBS[3LCys]@PTX were 33 and 25.5 %. In the following 72 h, approximately 49 % of the taxane was released from crosslinked AB hydrogels, while about 38 % was released from crosslinked PBS hydrogels (Fig. 9)[219].

Nanoparticles of bovine serum albumin (BSA) loaded with PTX were synthesized (PTX@BN). Then, cross-linked PTX@BN was combined with o-phthalaldehyde (OPA)-terminated poly(ethylene glycol) (4aPEG-OPA) via a condensation reaction between OPA and the amines in BSA to fabricate the hydrogel. *In vitro*, the nanocomposite hydrogels loaded with PTX allowed the sustained release of PTX over 30 days, as predicted by the Korsmeyer-Peppas model. As compared to free PTX solutions, PTX@BN-loaded hydrogel significantly enhanced antitumor efficacy and prolonged animal survival in mice with C26 or 4T1 tumors [220].

In treating breast cancer, stimuli-responsive hydrogel systems, which respond to temperature, pH, and redox changes, have been shown to be effective. In addition to long-term release, these drug delivery systems also have reduced drug toxicity; however, a more in-depth understanding of their potential use in local or intra-tumor treatment is needed.

4.2. Ovarian cancer

A total of 4.7 % of all cancer deaths in 2020 will be caused by ovarian cancer (OC). OC ranks eighth among cancers affecting women [221] and is the most lethal gynecological tumor globally. In most countries, OC patients still have a 5-year survival of less than 50 % of cases despite improvements in surgical techniques and maintenance therapy [222]. As a result of inadequate screening methods and frequent development of chemoresistance, disease recurrence often occurs and is primarily due to late disease diagnosis [223,224].

Hyun et al. developed an injectable drug delivery system for OC therapy comprising a visible light-curable glycol chitosan hydrogel

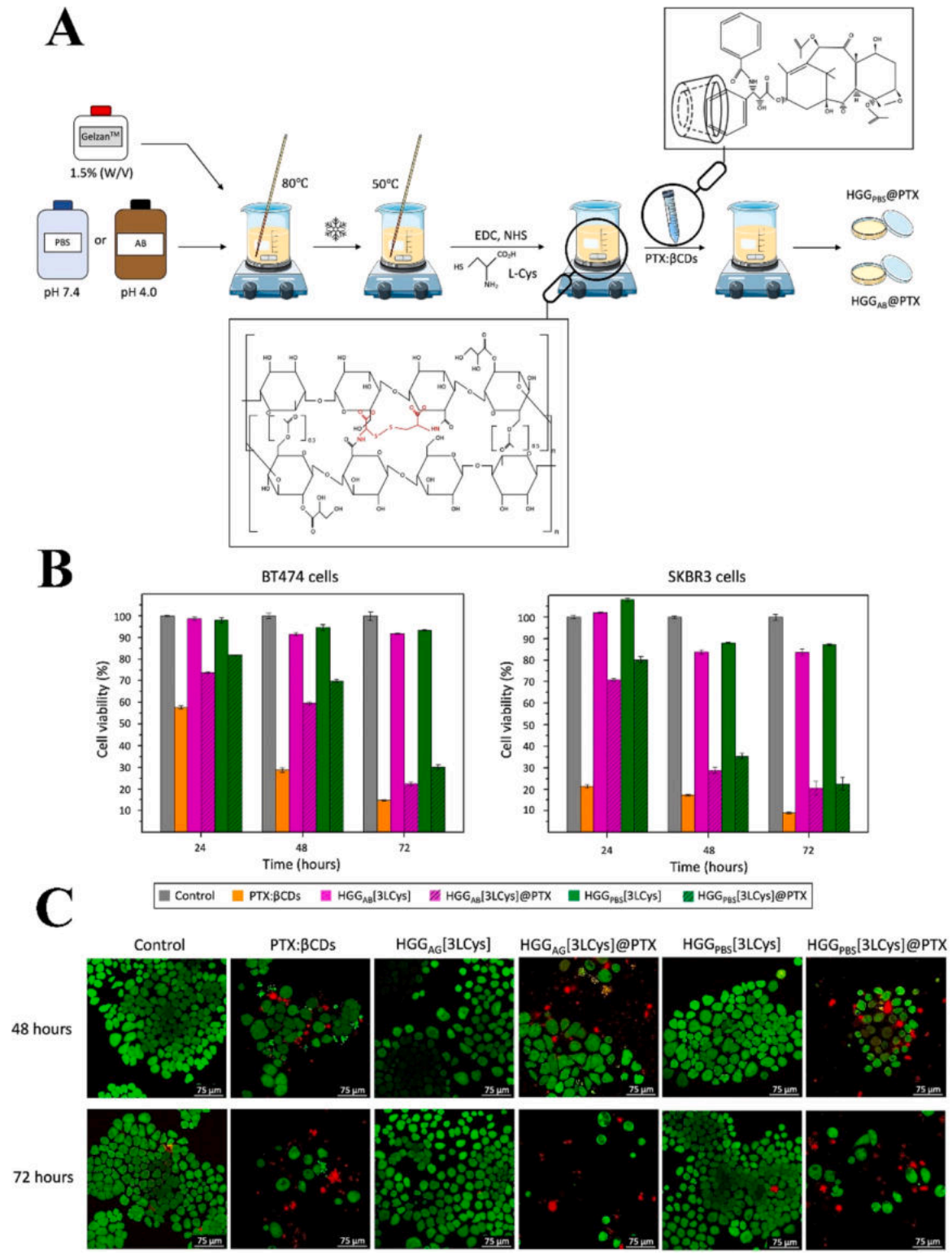

Fig. 9. A) PTX: CD complexes loaded on HGG patches crosslinked with different concentrations of l-Cys. **B)** The biocompatibility of HGG was assessed using the HS5 and BT474 cell lines. After 72 h of incubation with HGGs [3LCys], both cells had a viability greater than 90 %. **C)** After exposure to HGGs [3LCys], CLSM images of HS5 and BT474 cells were obtained. Calcine AM (green) and propidium iodide (red) were used to determine the survival and death of cells. Additionally, both HGGs [3LCys] did not cause cytotoxicity in the live/dead CLSM assays for 24 h. as neither BT474 nor HS5 cells lost viability compared with untreated cells. PTX: paclitaxel, HGG: GG hydrogels. Reprinted from ref [219] under the terms and conditions of the Creative Commons Attribution (CC BY) license (https://creativecommons.org/licenses/by/4.0/).

containing PTX-complexed β-cyclodextrin (GC/CD/PTX). The CD/PTX complex enhanced the water solubility of PTX. GC/CD/PTX released PTX over 7 days, yielding a lower cancer cell viability percentage *in vitro* than free PTX (Fig. 10)[225]. In another study, alginate was modified by introducing hydroxyl groups, rendering it a functional linear polymer. As crosslinkers, PLGA and PEG triblock copolymers were selected for their biocompatibility, biodegradability, flexibility, and viscosity. Over one week, this hydrogel-OxPt system released 78.8 % of oxaliplatin [226].

In another experiment, a biocompatible DOX-loaded supramolecular hydrogel was constructed using presynthesized DOX-2N-β-CD, Pluronic F-127, and α-CD, exploiting host-guest interactions among the molecules (Fig. 11). The DOX release was found to be dependent on pH and, specifically, favored by an acidic pH: for example, at pH 7.4, two hydrogels released 48.50 and 10.66 % of the drug, while at pH 5.5, the same hydrogels were able to release 66.33 and 15.56 % of DOX, respectively, which revealed and acceleration in the release rate [227].

In a study by Serini et al., cisplatin was delivered to ovarian cancer cells via a hydrogel composed of hyaluronic acid and folic acid. The release of cisplatin was gradual and particularly effective due to the hydrogel's ability to swell at physiological pH. Compared to the administration of free cisplatin, GEL-CIS had a greater inhibiting effect on OC metastatic spread, a lower resistance of cancer cells to the drug, and a significant modulation of epithelial-mesenchymal transition proteins [228]. Shen et al. developed an injectable and thermosensitive polymer-platinum(IV) conjugate hydrogel to deliver cisplatin and paclitaxel (PTX) for prolonged periods. Conjugate hydrogels strengthened after PTX was introduced, resulting in reduced sol-gel transition temperatures. According to *in vitro* experiments, the loaded drugs were released in a sustained manner over a period of 2.5 months [22]. An experimental system for sustained drug delivery of docetaxel-containing nanoparticles (Doc-NMs-hydrogel composites) was developed by Xu et al. After encapsulation in MPEG-PCL, the drug was incorporated into a Pluronic F-127 hydrogel. At the same dose, Doc-NMs-hydrogel composites induced apoptosis and inhibited cell growth more effectively than the other groups [229].

Despite its promising potential, intraperitoneal chemotherapy (IP) is not yet widely available as a post-surgical treatment for ovarian cancer (OC). PTX nanocrystals (PNC) were developed for IP chemotherapy of ovarian cancer as cross-linkable hydrogel deposits in situ. PNC-gel-treated mice had a lower maximum tolerated dose than PPT-gel-treated mice, suggesting that PNC dissolves and is absorbed more quickly. PPT-gel inhibited SKOV3 cell proliferation more effectively than PNC. Compared to Taxol, PNC-gel significantly increased the survival rate of mice with tumors [230]. ES-2-luc xenograft mice were also implanted with a hydrogel that exhibited excellent therapeutic and diagnostic properties after IP administration, allowing for improved peritoneal surgery. McKenzie et al. examined the properties and release profiles of poly-(D, L-lactide-co-glycolide)-block-poly-(ethylene glycol)-block-poly-(D, L-lactide-co-glycolide) thermosensitive hydrogels (TheranoGel) containing paclitaxel, rapamycin, and LS301. TheranoGel slowly released these three drugs at 37°C [231]. This strategy of co-delivering multiple drugs can enhance the effectiveness of treatment by inducing more apoptosis and cell death in ovarian cancer cells. In addition, temperature-responsive hydrogels are also ideal for IP due to their ability to release drugs for an extended period at 37°C.

4.3. Prostate Cancer

Among men, prostate cancer)Pca(is recognized as one of the most significant health issues and a leading cause of cancer-related mortality [232]. There is a threefold difference in incidence rates between transitioned and transitioning countries, but a much smaller difference in mortality rates [1]. There are a limited number of lifestyle and

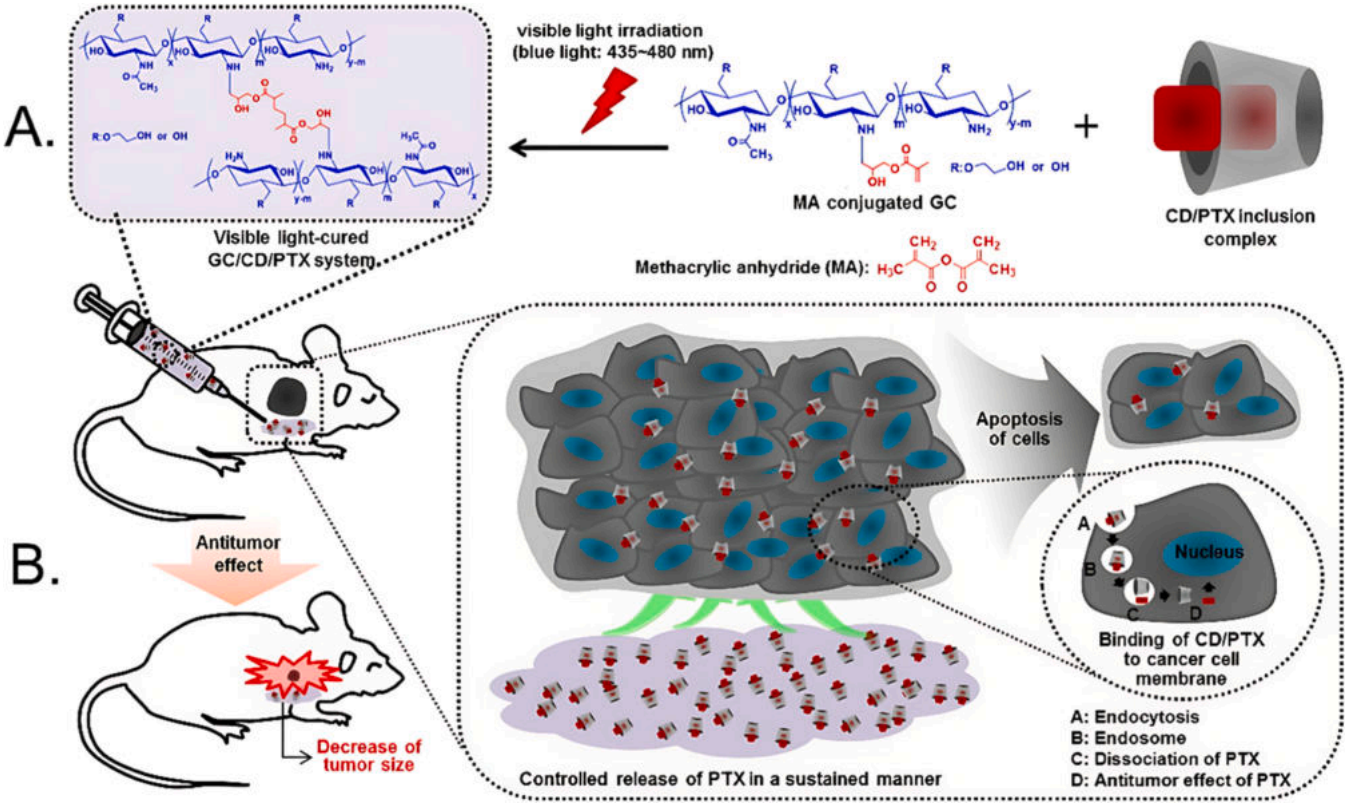

Fig. 10. (A) A process for preparing GC/CD/PTX. (B) Newly developed nanoformulations were examined *in vivo* on mice bearing ovarian cancer. PTX: paclitaxel, GC: glycol chitosan, CD: cyclodextrin. Reprinted from ref [225] under the terms and conditions of the Creative Commons Attribution (CC BY) license (https://creativecommons.org/licenses/by/4.0/).

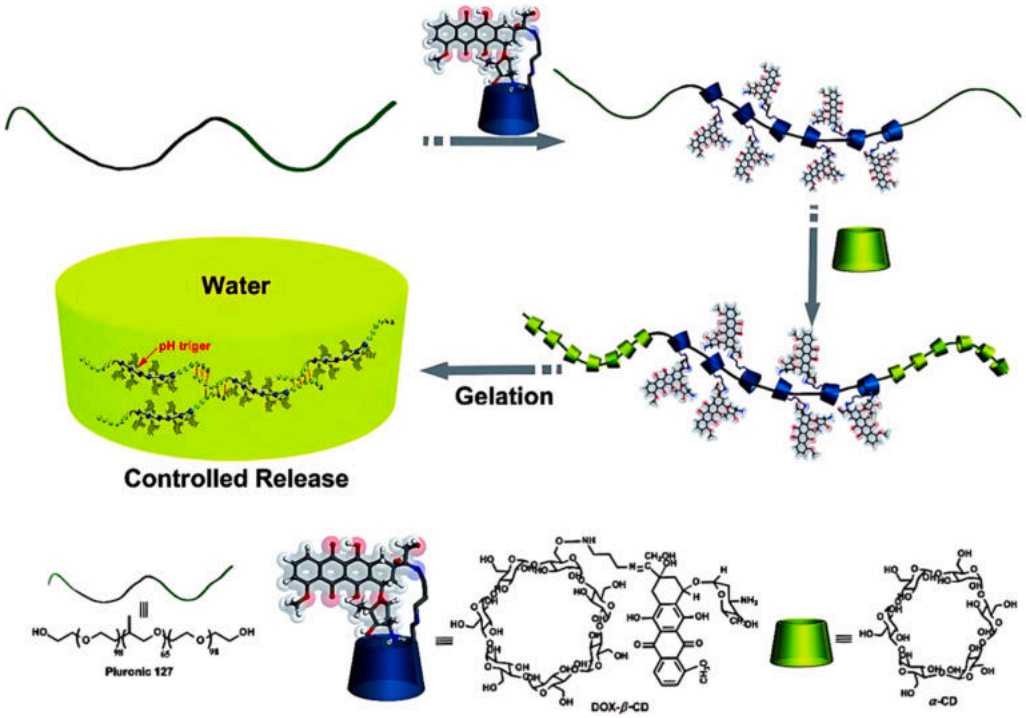

Fig. 11. The process of manufacturing biodegradable and injectable hydrogels loaded with DOX. α-CD: α-Cyclodextrin, β-CD: β-cyclodextrin, DOX: Doxorubicin. Reprinted from ref [227] under the terms and conditions of the Creative Commons Attribution (CC BY) license (https://creativecommons.org/licenses/by/4.0/).

environmental factors associated with Pca. Only genetic mutations, age, and family history have been established as risk factors for this condition. Smoking, obesity, and some nutritional factors may also contribute to disease [233]. By using mono(ethylene glycol) methyl ether methacrylate (MEO3MA), acrylic acid (AAc), and di(ethylene glycol) methyl ether methacrylate (MEO2MA), a series of hydrogel nanoparticles (PMOA nanoparticles) was created. AAc increases the LCST and gelation temperature due to its high electrostatic properties. By recruiting and trapping circulating cancer cells, an Epo gradient can reduce or delay cancer metastasis [234]. It has been demonstrated that alginate-g-PNIPAAm hydrogels can sustain the release of micelles encapsulating DOX for an extended period. Slowly released micelle-DOX improved cancer cell killing by increasing cellular uptake of DOX in multidrug-resistant AT3B-1 cells (Fig. 12) [235]. Despite the limited number of prostate cancer studies, we can conclude that hydrogel-based delivery systems can decrease drug resistance and tumor metastasis; nevertheless, more research is needed.

4.4. Colon cancer

The number of deaths and new cases associated with colorectal cancer is projected to reach 904,000 and 1.9 million in 2022, respectively. Colorectal cancer ranks third in terms of incidence, yet it holds the second-highest mortality rate [1]. In countries going through significant transitions, colorectal cancer incidence rates have been continuously rising [236,237]. Overweight and obesity have increased in such settings due to behavioral and dietary changes, along with a relatively higher intake of animal-based foods. The risk of developing disease is higher when you drink alcohol, smoke, consume red or processed meat, and have a high body fat percentage. Supplements, whole grains, fiber, dairy products, and physical activity are believed to be protective against colon cancer [238].

The effectiveness of MoS_2 nanoflowers (MoS_2 NF) oxidized dextran hydrogels (OD) and doped chitosan hydrogels (CS) for colon cancer therapy has been demonstrated. Electrostatic attraction and hydrogen bonding combined 5-fluorouracil (5-FU) with polyethylenimine (PEI)-decorated MoS2 nanofibers (NF) and were used to encapsulate the compound in 1-tetradecanol (1TD). Methotrexate (MTX) was co-encapsulated in CS/OD hydrogels by Schiff base reaction and electrostatic attraction. Since CS and OD are electrostatically attracted to one another, the hydrogels readily released MTX and TD/5-FU/PEI/MoS2 at pH 7.3. Biocompatibility and effective inhibition of colon cancer cells were proved through cytotoxicity testing of the sequential delivery system [239]. Additionally, an AlgNB/MoS_2/5-FU adhesive hydrogel was proposed as an injectable 2D-MoS_2-integrated photothermal and drug-delivery implant suitable for treating colorectal cancer. As a result of the superior dispersibility of the MoS_2 nanosheets in the hydrogel, they exhibited a highly efficient NIR-triggered photothermal effect. By triggering PTT and delivering the 5-FU drug, the injectable adhesive AlgNB/MoS2/5-FU hydrogel inhibited the proliferation of SW480 cells and promoted colorectal tumor regression *in vivo* [240].

In another study, a Schiff base reaction was used to combine chitosan-grafted-dihydrocaffeic acid (CS-DA) and oxidized pullulan (OP) to form multifunctional hydrogels. pH-dependent equilibrium swelling ratios, morphologies, and rheological properties were observed *in vitro* for the hydrogels, along with good injectability. DOX was released from the hydrogels, which effectively kills HCT116 cells. Aside from DOX, amoxicillin showed good antibacterial properties *in vitro* when encapsulated in hydrogels. These hydrogels demonstrated good adhesion to mucosal surfaces, making them suitable for local drug delivery [241]. The Cs/AMPS/AAc terpolymer hydrogel was synthesized and loaded with 5-FU, specifically targeting colon cancer. AAc and AMPS hydrogels synthesized by radiation based on Cs are pH-sensitive amphiphilic hydrogels that deliver 5-FU to the colon and prevent stomach Cs leakage. The pH-sensitive AMPS/AAc based on 1 % Cs showed maximum swelling at pH 7 and low swelling at pH 1. In 30 min, 5-FU is released at pH 1 by 1.55 % and at pH 7 by 25.3 %. Around 96 % of the 5-FU is released after 7 h at pH 7 [242]. Using ethylene glycol dimethacrylate (EGDMA), the itaconic acid (IA) and methacrylic acid (MAA) monomers were chemically crosslinked to form a robust hydrogel designed to release 5-FU and leucovorin calcium (LV) at the colonic site. At pH levels of 1.2 and 7.4, multiple assays were conducted on

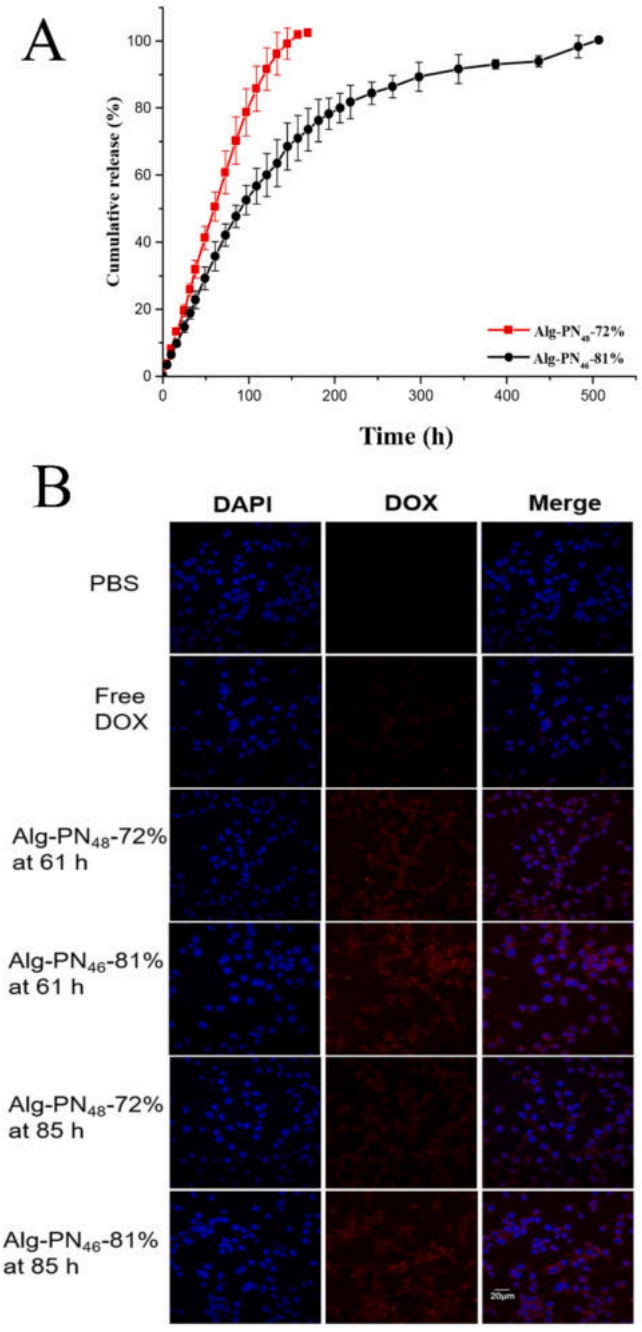

Fig. 12. A) For Alg-PN48–72 % and Alg-PN46–81 % hydrogels, controlled and sustained releases of DOX were achieved for 7 days and 20 days, respectively. Burst releases were not significant. With a higher content of PNIPAAm in AlgPN46–81 %, the formed gel is stiffer and more robust, allowing the drug to be released gradually over a longer period. B) AT3B-1 (MDR+) cells are shown in confocal microscope images, which display the cellular distribution of DOX (red). The nuclei of the cells were stained with DAPI (blue). Alg: alginate, PNIPAAm: poly(Nisopropylacrylamide), DOX: Doxorubicin. Reprinted with permission from ref [235].

swelling, drug loading, and drug release. Compared with pH 1.2, co-polymeric hydrogels demonstrated enhanced swelling and drug release at pH 7.4. Additionally, formulations with a greater concentration of IA exhibited increased swelling and drug release. Studies on rabbits have found that these co-polymeric hydrogels are non-toxic and biocompatible [243]. Using guar gum (GG), polyvinyl alcohol (PVA), chitosan (CS), and tetra-orthosilicate (TEOS), Zarbab et al. developed a blended biopolymeric hydrogel loaded with MTX. In PBS with a pH of 7.3, 96 % of the drug loaded in the hydrogel was released after 7 h and 25 min. MTX-loaded hydrogels were non-hemolytic and anti-proliferative against HCT-116, significantly reducing cell viability compared to free MTX [244]. Sheng et al. have proposed a dual-drug delivery system. Alginate and sodium carboxymethylcellulose (CMC) were crosslinked with Ca2 + in this system to co-entrap the MTX-loaded $CaCO_3$ and aspirin (Asp). The ability to deliver dual pH-responsive drugs was even more critical. Hydrogels helped protect MTX from absorption in the stomach and small intestine, ensuring its effectiveness in the colon. The pH difference between the small intestine and the colorectum allowed ASP in the small intestine and MTX in the colorectum to be delivered [245]. In order to enhance drug release control and therapeutic efficacy, galactomannan (GM) and sodium alginate (SA) hydrogels were reinforced with Fe_3O_4 magnetic nanoparticles (MNPs). During in vitro drug release studies, pH-sensitive behavior was observed: $<$ 14 % of the drug was released at pH 1.2 and $>$ 88 % at pH 7.4. Inhibition of Gram-negative *Escherichia coli* (over 94 %) and Gram-positive Staphylococcus aureus (over 99 %) was achieved using the system [246]. Pectin-co-poly(MAA) hydrogels were also proposed for the oral delivery of 5-FU with minimal invasion of the upper gastrointestinal tract. Hydrogels containing more pectin were prepared strategically to degrade entirely in the colon. The grafting of methacrylic acid imparted pH responsiveness, whereas cross-linking polymerization was achieved simultaneously with benzoyl peroxide [247]. A mild redox polymerization process generated Hal-embedded nanocomposite hydrogels containing sodium hyaluronate and poly(hydroxyethyl methacrylate). 5-FU was encapsulated into Hal using an equilibrium swelling method, followed by pulling and breaking the vacuum. Compared to conventional hydrogels, these nanocomposite hydrogels released 5-FU in a pH-dependent controlled manner [248]. A new hydrogel was developed by Sarkar et al. by mixing 5′-guanosine monophosphate disodium salt with 1,4,5,8-naphthalene tetracarboxylic acid tetra potassium salt. Over a pH range of 3–6, the composite hydrogelated, and at pH levels greater than 5, the gel transformed into a sol. In 100 h at pH 7.4, 82 % of DOX from DOX-Gel hydrogel was released. When DOX-gel was administered, the tumor volume declined 87.5 % over 21 days, which is a significant improvement compared to the use of free DOX (46.0 % tumor reduction) [249]. Using a solution polymerization technique, an intelligent polymeric network composed of hydroxypropyl–β–cyclodextrin and maltodextrin was developed for the site-specific delivery of cytarabine in the colon. Hydrogel degradation *in vitro* was markedly higher at intestinal pH than acidic pH. The biocompatibility of the fabricated network was confirmed through toxicology studies, which revealed no ocular, skin, or oral toxicity. As a result, the hydrogel networks could deliver cytarabine to the colon in a practical, prolonged, and site-specific manner [250].

A self-healing hydrogel with intrinsic antitumor properties was produced using DOX coupled to oxidized carboxymethylcellulose (CMC) (CMC-Ald). $NaIO_4$ oxidized CMC into CMC-Ald. A coupling reaction was used to graft the DOX onto the CMC-Ald. Different samples had UV–Vis spectra ranging from 380 to 620 nm. CMC-Ald contained no chromophores, and its curve showed no significant absorption. However, an absorption characteristic of DOX around 485 nm was observed when DOX was grafted onto CMC-Ald. Camptothecin (CPT) was coupled with DOX in these systems to treat tumors synergistically and prevent burst release. Both *in vitro* and *in vivo* tests showed that this system reduced biotoxicity [251]. Carrexo et al. developed thermoresponsive hydrogels from NIPAM, modified with maleic acid and 4-penten-1-ol, and cross-linked with TEGDE and PEGDE. At body temperature, the transition from sol to gel in hydrogels takes place. A NIPAM/4-penten-1-ol-based hydrogel decreased swelling and prolonged DOX release [252].

In summary, using natural polymers as a delivery system for colon cancer drugs is the most common method for drug delivery. Effective drug delivery for colon cancer necessitates systems capable of retaining the therapeutic agent in the acidic pH of the stomach, followed by its subsequent release in the alkaline environment of the colon. This has been demonstrated through the application of hydrogel systems. Drugs

can achieve a sustained therapeutic effect by releasing them over an extended period, reducing the need for re-administration. Furthermore, strengthening these systems promotes good adhesion to the colon mucosa, which is suitable for local treatment.

4.5. Brain cancer

As per the 2020 estimates from the Global Cancer Observatory, cancers of the brain and central nervous system represent a significant share of the worldwide disease burden, comprising 1.9 % of all cancer cases and 2.5 % of cancer-related deaths, making it the leading cause of death in this category [253]. Following systemic administration, lipophilic and hydrophilic molecules can be delivered to brain cells by using nanocarriers [254]. Multiple hydrophobic drugs may be delivered simultaneously and controllably to a brain tumor by using nanocarriers – also in the form of nano-hydrogels, either surgically or intramuscularly [255,256].

According to Lin et al., magnetic resonance imaging (MRI)-traceable ultra-thermosensitive hydrogels were prepared from aqueous solutions within 4 s at 28°C, exhibiting rapid gelation ability for the simultaneous delivery of hydrophobic (PTX) and hydrophilic (EPI) drugs using bovine serum albumin nanoparticles (BSA NPs). In gliosarcoma-bearing mice, BSA/PTX nanoparticles incorporating hydrogel Gd/EPI improved survival rate of 63 or 69 days without recurrence [257] (Fig. 13).

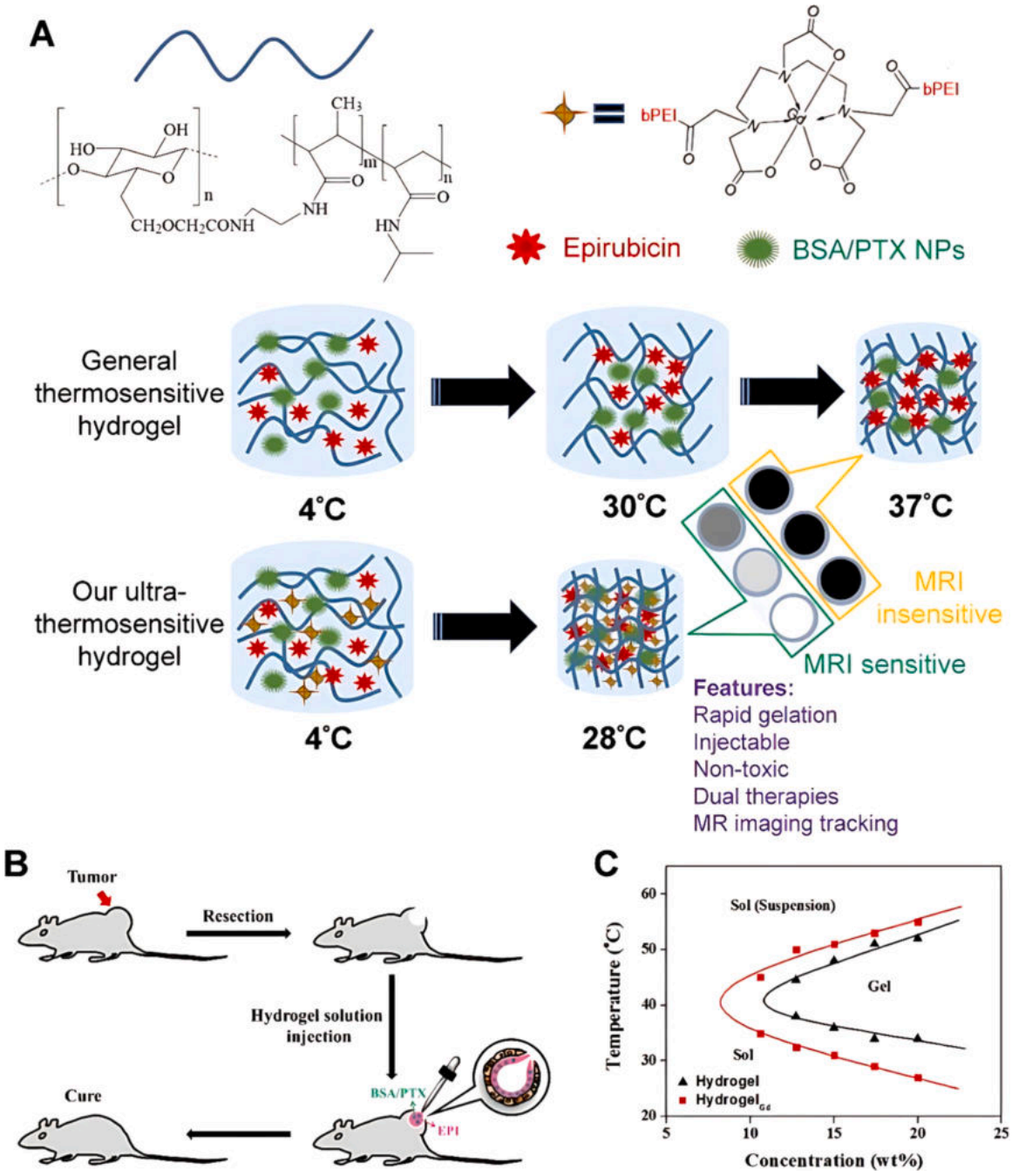

Fig. 13. **(A)** A schematic illustration of the formation of hydrogel-based systems at various temperatures. **(B)** After surgery, BSA/PTX nanoparticles incorporated into a hydrogel Gd/EPI inhibit local tumor growth and prevent recurrence. (C) Hydrogel and hydrogel $_{Gd}$ sol-gel phase transition diagram. PTX: Paclitaxel, EPI: epirubicin, BSA: bovine serum albumin, MRI: magnetic resonance imaging. Reprinted from ref [257] under the terms and conditions of the Creative Commons Attribution (CC BY) license (https://creativecommons.org/licenses/by/4.0/).

Using iron ions (Fe^{3+}) and guar gum succinate (GGS) as cross-linkers, a novel one-pot method for synthesizing hydrogels has been developed. Hydrophilic levofloxacin was continuously released from this system over 31 h; after 24 h of treatment with various doses of GGS–PAA–Fe^{3+} hydrogel, glioblastoma cells exhibited nuclear fragmentation, chromatin condensation, and an increase in DAPI-positive cells [258].

A hydrogel system was created by Kim et al. and monitored with MRI. A thermosensitive/magnetic poly(organophosphazene) (PPZ) hydrogel loaded with PEGylated cobalt ferrite (P-$CoFe_2O_4$) nanoparticles could serve as an imaging platform, and SN-38 (an active metabolite of irinotecan) was used as a chemotherapeutic agent. To treat brain tumors, MLTH was stereotactically injected. Biodegradable MLTH underwent a reversible sol-gel phase transition near body temperature. An ongoing biodegradation of the platform caused the SN-38 to diffuse spontaneously over a few weeks. A sustained drug release was demonstrated by monitoring the hydrogel concentration and long-term biodegradation *in vitro*. Over 22 days, it inhibited tumor growth in U87 MG tumor-bearing mice. Additionally, GBM areas, both treated and untreated, were visible in MR images [259].

Xu et al. prepared and optimized a thermosensitive gel delivery system for combating glioblastoma containing monomethoxy(polyethylene glycol) and poly(D, L-lactide-co-glycolide) (mPEGPLGA). These nanocomposite gel systems enabled the sustained release of PTX and TMZ and, compared to other formulations, inhibited the growth and induced apoptosis more significantly in U87 and C6 cells [260]. Fourniols et al. proposed a polyethylene glycol dimethacrylate (PEG-DMA) injectable hydrogel to deliver TMZ locally and sustainably. Their goal was to develop a new injectable delivery system that would 1) fit into the cavity of the resection, 2) polymerize in situ using a commercial device, 3) deliver anti-cancer drugs directly to the invaded parenchyma, and 4) significantly reduce recurrence rates. There was rapid photopolymerization in the hydrogel (<2 min), and within the first 24 h, 45 % of TMZ was released linearly, followed by a logarithmic release of 20 % over the first week. *In vivo* biocompatibility studies showed that microglia did not undergo apoptosis in mice treated with this hydrogel, while the release of TMZ from the hydrogel significantly reduced tumor weights [261].

Arai et al. evaluated thermoreversible gelation polymers (TGP) for the treatment of malignant gliomas via local drug delivery. A continuous application of a hybrid system combining polymeric microspheres and liposomes, referred to as sphere-DOX and lipo-DOX, respectively, was employed. *In vitro* studies demonstrated that both delivery systems could sustain the release of doxorubicin (DOX) for up to 30 days. *In vivo* evaluations indicated that the TGP-sphere-DOX formulation effectively inhibited tumor growth for 32 days, while the TGP-lipo-DOX formulation resulted in a more prolonged inhibition, lasting 38 days [262].

In summary, the application of hydrogels for drug delivery in treating brain cancer has demonstrated significant advancements. These hydrogels facilitate the targeted delivery of therapeutic agents, and their progress can be monitored via magnetic resonance imaging (MRI), thereby providing critical insights into the delivery mechanisms employed. Furthermore, evidence suggests that this innovative treatment approach is associated with improved survival rates and reduced tumor growth, underscoring its potential as a promising strategy in oncological therapeutics.

4.6. Lung cancer

According to a recent report, lung cancer is projected to lead to more than 1.8 million deaths and 2.5 million new cases globally; it was also estimated to account for one in every eight cancer diagnoses and one in every five cancer-related deaths worldwide [1]. Research has established a clear link between smoking and lung cancer; moreover, tobacco use is associated with various other diseases, leading to the terms "cigarette epidemic" and "tobacco epidemic" to describe this widespread health issue [263,264]. The intensity, duration, type, and degree of inhalation of tobacco smoke also differed historically and geographically [265,266].

Using hyaluronic acid-tyramine as a carrier, Wang et al. synthesized an endostatin (ES)-loaded hydrogel-based drug delivery system (ES/HA-Tyr). Radiotherapy combined with ES/HA-Tyr had low systemic toxicity and exerted significant anti-angiogenic and anti-tumor effects. The sustained release of ES significantly inhibited the growth of HUVEC cells. Overall, the ES/HA-Tyr treatment increased local drug concentrations, decreased blood drug concentrations, and reduced systemic toxicity. Additionally, tumor microvessel density was reduced with ES/HA-Tyr, pericyte coverage increased, hypoxia was decreased, and radiotherapy response was synergistically increased [267].

Another hydrogel-based drug delivery system (CS-NSA/A-HA) was developed using chitosan modified by nitrosalicylaldehyde and aldehyde hyaluronic acid. This hydrogel, as a dual drug-loaded system, was loaded with cisplatin and DOX incorporated separately. In A549 cells, cytotoxicity studies confirmed that the dual-loaded carrier showed superior activity to the single-loaded carrier [268]. Using lyophilization, DOX was encapsulated in a biopolymer hydrogel scaffold made of a gelatin/sodium carboxymethyl cellulose mixture. The viability and proliferation of A549 cells significantly decreased in contact with this system due to sustained DOX release (Fig. 14) [269].

Anlotinib-loaded hydrogel (AL-HA-Tyr) was investigated in a second study to determine its antitumor effects and the reduction of toxicity to healthy cells. *In vitro*, it inhibited the proliferation of HUVEC cells. Additionally, tumor growth and angiogenesis were reduced: in vivo findings indicated that AL–HA–Tyr significantly reduced organ toxicity and lowered the expression of Ki67 and VEGF-A in tumor cells compared to AL. As a result, this led to a marked increase in the survival rate of the mice [270].

An *in situ* gel-based dual drug delivery system was developed by combining thermosensitive hydrogels containing diamminedichloroplatinum (DDP) (PEG–PCL–PEG–PEG/DDP, PECE/DDP) with polymeric micelles containing PTX (MPEG–PCL/PTX, abbreviated as PDMP). In BALB/c nude mice, PDMP inhibited tumor growth and prolonged survival time. Compared to another group treated with free drugs, the PDMP-treated group survived 53 days longer [271]. An interpenetrating network system (IPN) comprising PEG-diacrylate, AuP, and modified gelatin was also proposed as a drug delivery system. According to *in vitro* experiments, AuP was released from the IPN in a first-order kinetic manner. Comparing IPN loaded with AuP to IPN alone, the hydrogel-based system demonstrated higher toxicity against cancer cells, inhibiting tumor growth and reducing angiogenesis in mice [272].

Li et al. developed a triple-combination nanosystem for concurrent chemotherapy, gene therapy, and phototherapy using multifunctional RNA nanohydrogels. Three lung cancer inhibitor microRNA hairpins were integrated into a single RNA nanoparticle using DNA nanotechnology and rolling circle transcription, which simultaneously silenced three mRNAs. DOX and 5,10,15,20-tetrakis porphyrin were carried by RNA NH and delivered to cancer cells. In cancer cells resistant to multiple drugs, microRNAs, DOX, and TMPyP4 worked together synergistically. RNA NHs containing the aptamer sequence S6 modified with cholesterol showed cancer-specific cellular targeting [273]. Therefore, by combining three different drugs, the nanosystem can overcome multidrug resistance resulting from gene malfunctions during the chemotherapy process. In another study, Meng et al. utilized boronate ester-linked COFs (COF-1) to construct advanced drug delivery systems characterized by high specific surface areas, lipotropism, and structural tunability. COF-1@DOX was a lipophilic COF that encapsulated DOX and immobilized the functional protein drug ribonuclease A (RNase A-COF-1@DOX) on its surface. An albumin-oxygenated hydrogel network could be cross-linked into the pores of COFs to deliver RNase A and DOX *in vivo* (RNase A-COF-1@DOX gel). It also provided a platform for developing more effective and targeted therapeutic approaches for

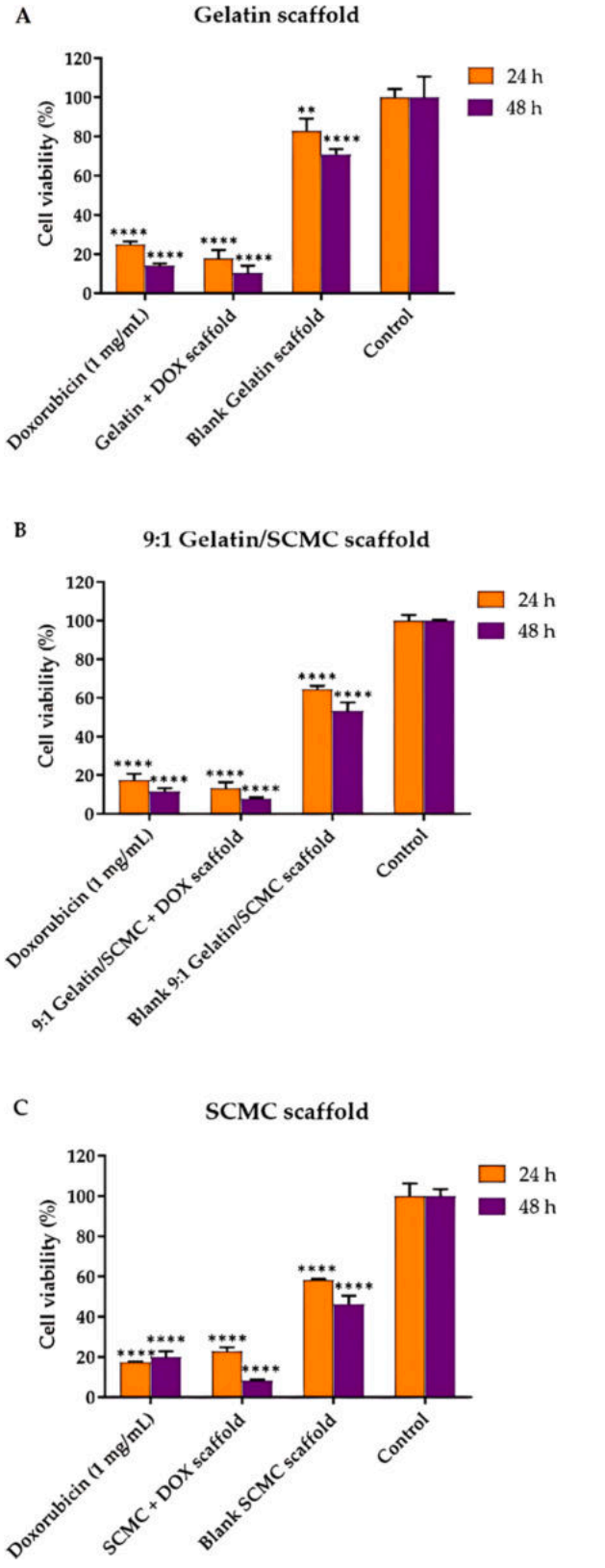

(caption on next column)

Fig. 14. A549 cell viability after treatment with (A) gelatin, (B) 9:1 gelatin/SCMC, and (C) SCMC scaffolds containing DOX. Porous hydrogel scaffolds could be utilized to deliver DOX locally to tumors. Around 30 % of DOX was released in 24 h from the scaffold, indicating that DOX is released to tumors sustainably. In the 24- and 48-hour periods following scaffold application, MTT assays were used to measure the viability of A549 lung cancer cells. After exposure to DOX scaffolds, A549 cells showed a significant decrease in cell number. Data are expressed as mean ± S.D., ** indicated $p < 0.01$, and **** indicated $p < 0.0001$. Reprinted from ref [269] under the terms and conditions of the Creative Commons Attribution (CC BY) license (https://creativecommons.org/licenses/by/4.0/).

other forms of cancer in addition to COF-based systems for lung cancer treatment [274].

In summary, research on natural hydrogels for lung cancer treatment primarily focused on hyaluronic acid and chitosan. The findings from these investigations support the conclusion that multifunctional hydrogel systems are viable options for enhancing therapeutic outcomes through gene therapy, drug delivery, and phototherapy.

4.7. Liver cancer

The global death toll from liver cancer is estimated to be three-quarters of a million in 2022; after lung and colorectal cancer, it ranks third in cancer death and sixth in new cases [1]. Risk factors associated with hepatocellular carcinoma include obesity, aflatoxin exposure, smoking, heavy alcohol consumption, and type 2 diabetes [275].

An intravenously administered norcantharidin/DOX-coloaded nanoparticle system was developed by Gao et al. HepG2 cells treated with this dual drug-loaded hydrogel demonstrated remarkable anti-proliferative activity. *In vivo* studies revealed that this system was able to reduce tumor growth with minimal side effects and effectively extend the survival times of mice. Immunohistochemistry showed significantly reduced Ki-67 and CD31 expression in the drug-loaded hydrogel group [276]. In another study, PEG and polypropylene glycol (PPG) were cross-linked with polydimethylsiloxane (PDMS) oligomers to form hydrogels with a hydrophobic core and a hydrophilic surface, enhancing DOX solubility. In vitro studies with HepG2 cells demonstrated the promise of DEP-2 (Fig. 15)[277].

Embelin/PECTgel was a thermosensitive injectable hydrogel system developed by Peng et al. and demonstrated higher cytotoxicity against H22 cells in vitro compared to free embelin. *In vivo*, Embelin/PECTgel transformed from a liquid to a gel within a few seconds [278] and was a promising candidate for treating advanced hepatocellular carcinoma in humans. A Pluronic F127 hydrogel was blended with resveratrol microspheres and DDP to create a thermosensitive system that induced cancer cell apoptosis and arrested the cell cycle at the G1 phase *in vitro* against H22 cells. A drug-loaded F127 hydrogel was administered intraperitoneally to mice, resulting in the induction of tumor cell death, a reduction in microangiogenesis, and an extension of survival time. In this way, intraperitoneal chemotherapy becomes more effective. Moreover, immunohistochemical staining showed that F127 hydrogel drugs were not toxic to major vital organs [279]. Researchers prepared DOX-loaded micelles using a glycol chitosan-Pluronic F127 conjugate (GC-PF127), which was obtained by amidating the terminal carboxyl groups of PF127 with glycol chitosan (GC). DOX/GC-PF127 micelles had a size of 150 nm. DOX concentrations in tumor tissues were significantly elevated after hydrogel injection peritumorally into H22 mice-bearing tumors, while healthy tissues had reduced DOX concentrations. Following three intravenous injections of a similar total DOX dose, tumors in the mice treated with free DOX grew slowly. In contrast, just two intravenous injections of the drug-containing hydrogel were sufficient to suppress tumor growth, which was almost eliminated by a single peritumoral injection [280].

Graphene sheets (GNS), PVA, and CS co-polymeric hydrogel were loaded with MTX for in vitro liver cancer treatment. In 6 h, around 97 %

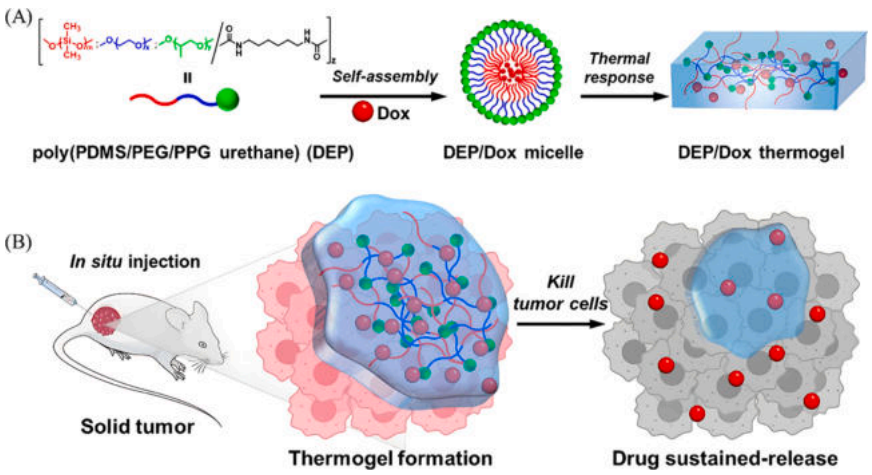

Fig. 15. PDMS-based polyurethanes that form hydrogels at the tumor site enhance the antitumor effect of DOX. (A) Preparation of DEP thermal gel and its molecular structure. (B) After in situ injection, the drug slowly releases from the thermal gel to achieve effective antitumor activity. DOX: Doxorubicin, DEP: poly(PDMS/PEG/PPG urethane)_ Reprinted from [277] under the terms and conditions of the Creative Commons Attribution (CC BY) license (https://creativecommons.org/licenses/by/4.0/).

of the drug was released. In addition to not promoting HepG2 cell growth, the hydrogels were not hemolytic. Hydrogels with GNS were reported to ensure improved drug delivery in cancer microenvironments while reducing adverse effects on healthy cells [281].

FER-8 peptide hydrogels were developed by Reza et al. to target tumors and deliver PTX. FER-8 peptide hydrogels formed at pH 7.4 exhibited high drug-loading capacities; however, at acidic pH conditions, degradation occurred more rapidly. The peptide hydrogel at pH 5.5 released PTX for almost a week and was more effective in inhibiting tumor growth than free drugs *in vitro*. Intratumoral administration of HG-PTX results in prolonged retention (96 h) at the tumor site [282]. According to another study, Xu et al. encapsulated DOX in biodegradable and pH-responsive hydrogels (pH 7.4–5.6) made from amorphous calcium carbonate (ACC) nanoparticles stabilized with poly(acrylic acid). Doping NPs with Sr^{2+} or Mg^{2+} in appropriate amounts could further enhance drug delivery to tissues with a less acidic microenvironment (pH 7.7–6.0). High drug encapsulation efficiency (>80 %), 62 ± 10 nm sizes, good serum stability, and high loading capacity (>9 %) are all characteristics of the DOX-loaded NPs. Intracellular uptake assays and zebrafish models provide evidence of tumor inhibition and decreased acute toxicity. Furthermore, the particles enhance tumor suppression by optimizing pharmacokinetics and increasing drug accumulation [283]. DOX was also encapsulated into a hydrogel composed of N-carboxyethyl chitosan (CEC) synthesized in an aqueous solution via a Michael reaction and dibenzaldehyde-terminated poly(ethylene glycol) (PEGDA). Benzaldehyde groups from PEGDA were covalently linked to amine groups from CEC in the hydrogels, resulting in rapid self-healing. DOX was released from different pH PBS solutions *in vitro* to confirm the pH responsiveness of the hydrogel. At physiological pH, DOX was released more slowly than at acidic pH. A comparison of pH 6.8 and pH 5.5 showed no significant differences among the groups. A pH 4.0 group released the drug faster than a pH 6.8 or 5.5 group. Approximately 96 % of DOX was released after 4 days of incubation in PBS at pH 4.0 with CEC/PEGDA20 hydrogel, and the hydrogels showed good cytotoxicity when tested on L929 cells [284]. Sodium alginate/chitosan/hydroxyapatite nanocomposite hydrogels were cross-linked using gamma irradiation for use as drug delivery systems for DOX. When pH 7.4 and 5 were applied to the nanocomposite after 24 h at 37°C, DOX was released from the nanocomposites [285]. Hydrogels encapsulating DOX and cisplatin were formed using aldehyde-pullulan (A-Pul), ε-poly-L-lysine (ε-PL), and branched polyethylenimine (BPEI). The hydrogel degradation and drug release rates are higher at pH 7.0 than at pH 7.4. It was observed that mice treated with cisplatin and DOX hydrogels showed the most effective tumor inhibition, suggesting a synergistic anticancer effect of the two drugs. Furthermore, the hydrogels showed excellent biocompatibility and safety *in vivo* when tested against Huh-7 cells [286].

As a result, pH-responsive hydrogels are highly effective for drug delivery in acidic tumor microenvironments. Temperature-responsive hydrogels used in intraperitoneal chemotherapy have also been shown to enhance apoptosis in liver cancer cells, thereby improving their efficacy.

4.8. Gastric cancer

Stomach cancer ranks as the fifth most prevalent and lethal disease globally, with more than 968,000 new cases and over 660,000 deaths reported worldwide in 2022 [1]. Over the past half-century, stomach cancer rates have steadily declined in most populations due to improvements in food storage and preservation, as well as a decrease in the prevalence of H. *pylori* [287]. Despite this, recent studies suggest that rates are rising again among younger age groups [288,289].

In a study by Zhou et al., a thermo-sensitive hydrogel based on carbon nanotubes (SWNT) was developed as a photothermal transducer and drug delivery system. Despite SWNT-hydrogel being nontoxic, NIR radiation induces cell death through pro-apoptosis due to hyperthermia. Combining DOX-SWNT-hydrogel with NIR radiation significantly reduced tumor growth in mice without causing organ toxicity [290]. As a result of the developed system, chemotherapeutic drugs are more effective, and systemic adverse reactions are minimized, which offers immense potential for treating gastric cancer.

The first-line treatment for gastric cancer is the administration of diamminedichloroplatinum (DDP). A DDP-complexed hydrogel (DDP-Gel) was prepared by Qian et al. and evaluated for its efficacy in treating gastric cancer. There was an improvement in body weight and survival time in mice treated with DDP-Gel. Compared to free DDP, DDP-Gel inhibited tumor growth and metastasis more effectively [291]. DDP was also encapsulated within a cross-linkable HA-based hydrogel *in situ* in another exciting experiment. Gelation time was affected by the concentrations of two polymers, HA-aldehyde and HA-adipic dihydrazide. Over four days, DDP was released from the hydrogel. Hydrogel-conjugated DDP was associated with a decrease in peritoneal nodule weight, whereas free DDP did not significantly affect tumor growth [292]. A temperature-sensitive hydrogel based on PDLLA-PEG-PDLLA (PLEL) was developed to deliver 5-FU + DDP intraoperatively. The 5-FU + DDP/PLEL combination inhibited cell

proliferation and triggered apoptosis in MKN45-luc cells. When injected, dual-drug hydrogels showed superior anti-tumor effects compared to single-drug hydrogels and free 5-FU and DDP. At 24 h, the cumulative release of 5-FU was approximately 62.43 %, while at 28 days, it was approximately 92.42 %. On the other hand, DDP released 33.35 % and 47.42 % cumulatively at 24 h and 28 days, respectively. Their different water solubility and diffusion rates within the hydrogel may explain their differences in release rates [293] (Fig. 16).

For the treatment of peritoneal carcinomatosis of the stomach, a thermosensitive poly(organophosphazene) hydrogel containing docetaxel (DTX) was also developed. The tumor growth in mice treated with DTX-gel was significantly reduced compared to treatment using free drugs (either oral administration or intraperitoneal injection), and the survival rate was substantially longer. In a peritoneal carcinomatosis (PC) model, DTX-gel suppressed peritoneal metastasis by continuing the release of chemotherapy agents (Fig. 17) [294].

Based on the temperature-induced phase transition of PEG-modified bovine serum albumin, an injectable hydrogel encapsulating PTX-loaded red blood cell membrane nanoparticles (PRNP-gel) has been developed. A loading efficiency of 85 % and a loading content of 22 % were achieved. PTX was cumulatively released at a rate of 30 % for 6 days from the in-situ-forming hydrogel. This nanoparticle–hydrogel hybrid system enhanced local chemotherapy and reduced systemic toxicity [295]. It was also found that DDP and 5-FU co-delivery systems had the most significant suppressive effect [296].

4.9. Melanoma

Although accounting for just 10 % of all skin cancers, melanoma is responsible for 80 % of deaths related to skin cancer [297]. After decades of research, patients with melanoma benefitted from complex reconstructive procedures and precision medication [298]. The five-year mortality rate for melanoma is at 8.2 % [299]; however, the disease burden is increasing, and lymph node metastatic relapse is common in melanoma patients after their first surgery, requiring additional surgery and sophisticated targeted treatments [300].

Transdermal drug delivery is noninvasive, painless, and supports self-administration of the drug without professional assistance, thus improving patients' compliance when compared to parenteral drug delivery [301]. In addition, transdermal delivery ensures localized and long-acting drug distribution at the wound site by enabling the controlled release and permeation of drugs and therapeutic agents through the skin, while also preventing systemic toxic complications and optimizing bioavailability by bypassing pre-systemic metabolism [302]. The specific conditions for passive diffusion through the skin make it impossible for many active ingredients to penetrate the skin spontaneously. Ideally, a drug should have optimal characteristics for spontaneous skin penetration. Low molecular weight, good lipophilic balance, and low fusion point are all required features of the drug for this application. Indeed, the characteristics of the drug as well as of the hydrogel used for encapsulation are keys in designing suitable topical drug delivery systems using hydrogels [303]. The hydration effect of hydrogels enhances the penetration of therapeutics across the skin, facilitating transdermal drug delivery [304]. Due to these properties, hydrogels can effectively hydrate the stratum corneum, enabling the delivery of active ingredients to a greater extent [305]. By modulating the porosity, crosslinking degree, and swelling behavior of the hydrogel, drugs and therapeutic agents can be released under controlled conditions [306]. According to the study by Ni et al. [307], a hydrogel matrix containing dendritic lipopeptide-modified multistage targeted

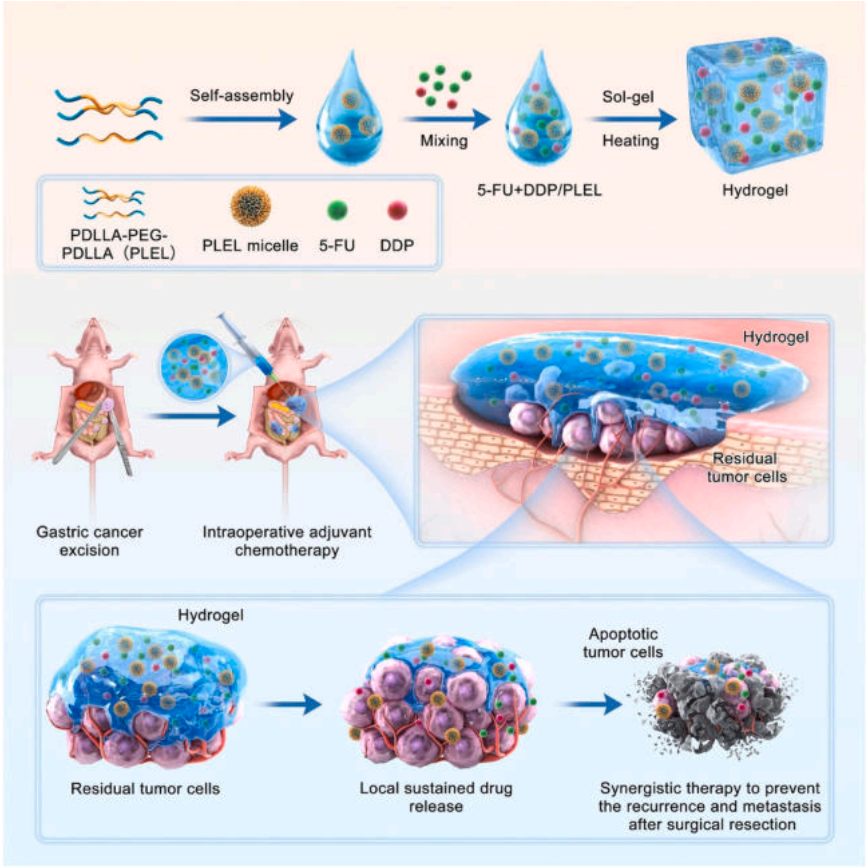

Fig. 16. A biodegradable thermosensitive hydrogel was used for intraoperative synergistic chemotherapy of gastric cancer to inhibit postoperative tumor recurrence and metastasis. 5-FU: 5-fluorouracil, DDP: cisplatin. Reprinted from ref [293] under the terms and conditions of the Creative Commons Attribution (CC BY) license (https://creativecommons.org/licenses/by/4.0/).

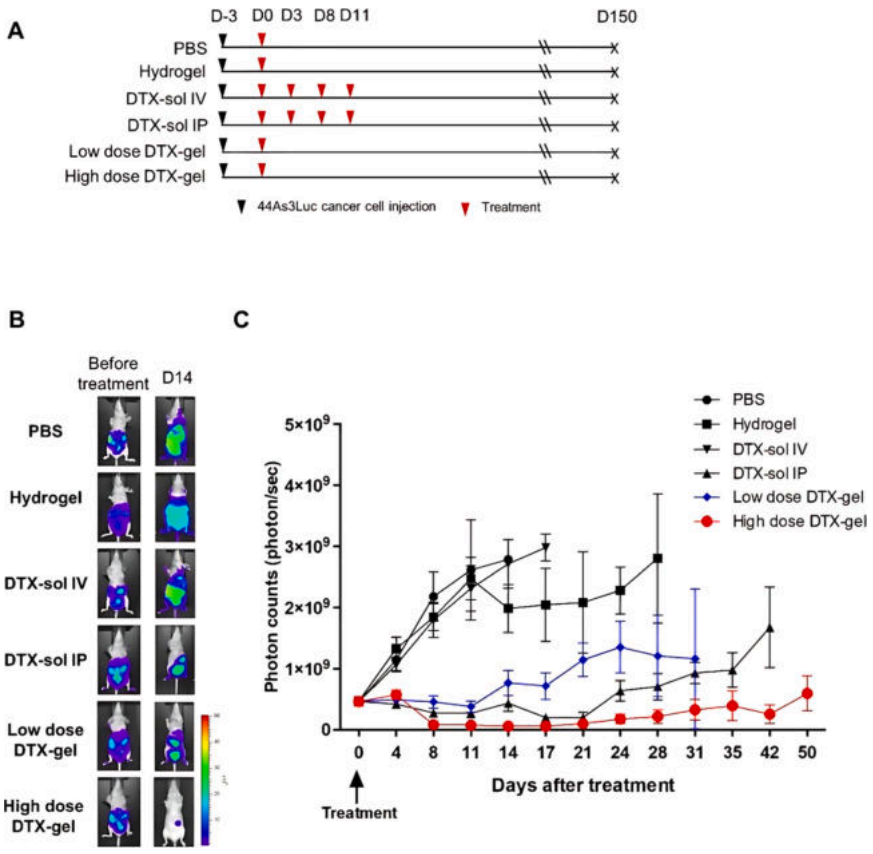

Fig. 17. Bioluminescence imaging was performed *in vivo* using a mouse model of peritoneal carcinomatosis. Bioluminescence images were obtained until 50 days after treatment. (A) Treatments include the injection of cells, PBS, hydrogel, IV or IP DTX-sol, and low- or high-dose DTX-gel. (B) A comparison between the groups of bioluminescence imaging. (C) Photon counts from bioluminescence images are analyzed. When DTX-gel was applied at low and high doses, photon counts were significantly reduced compared to control groups treated with PBS or hydrogel ($p < 0.001$). According to these results, DTX treatment with the hydrogel consistently and strongly suppresses PC growth. DTX: docetaxel, IP: intraperitoneal, IV: intravenous. Reprinted from [294] under the terms and conditions of the Creative Commons Attribution (CC BY) license (https://creativecommons.org/licenses/by/4.0/).

liposomes (Mtlips) allowed localized and sustained drug release. The ultra-deformability of Mtlips permits them to pass through the stratum corneum and into the epidermis, where melanoma was located. The high permeability of virus-mimicking Mtlip enhances the payload in tumor tissues. In addition to improving cell uptake efficiency, the positively-charged Mtlip may also accumulate selectively in mitochondria [307].

In another study, Sun et al. improved the solubility and stability of Cur by preparing cyclodextrin complexes for the treatment of melanoma [308]. Specifically, Poloxamers 407 and 188 were used to prepare an *in situ* hydrogel (ISG) embedding Cur. Cur-loaded ISGs had high transdermal efficiency and good therapeutic effect against melanoma, inhibiting the proliferation of melanoma cells in the G2/M stage, followed by apoptosis. [308]. Other Cur-embedding systems were also proposed for melanoma therapy: for example, Cur-loaded nanomicelles were incorporated into a thermosensitive hydrogel based on 16 % Kolliphor P407, which underwent a sol-gel transition at skin temperature (32–36°C) to enhance patient comfort and application efficiency. The nanomicellar dispersion released the maximum amount of Cur (11.38 %) within 48 h, with no significant further increase up to 72 h (11.12 %). On the contrary, the hydrogel formulations demonstrated a slower release of Cur, with amounts from 5.81 % at 48 h to 7.25 % at 72 h. Cur retention and distribution were improved by adding a thermosensitive hydrogel, which prolonged contact and promoted gradual release. Cur was effectively delivered to the basal epidermis, a target site for melanoma treatment [309]. Using poloxamers 407 and 188 as the matrix, Sun et al. prepared Cur's in situ hydrogels (ISGs). The extent to which drugs were released from ISGs *in vitro* depended on their dissolution. In contrast, ISGs containing Cur inclusion complexes had significantly greater effects due to the improved solubility of Cur. Cur caused apoptosis in melanoma cells by blocking cellular proliferation during the G2/M stage. ISGs of Cur inclusion complexes are promising treatments for melanoma [308].

Nasir et al. developed nanocomposite hydrogels (rGO-5FU-CMARX) to treat melanoma skin cancer using carboxymethyl arabinoxylan and 5-FU-loaded graphene oxide, and tested the system's efficacy with U-87 cell lines. Due to its surface area, a substantial amount of drug could be loaded in and released from rGO under photothermal phenomena. pH-sensitive rGO-CMARX nanocomposite hydrogels showed maximum drug release (93.10 %) in neutral media (pH=7.2), while minimum drug release (80.20 %) was found in acidic media (pH=6.4). According to this study, nanocomposite hydrogels could be useful in treating skin cancer [310].

A crosslinked sericin/dextran hydrogel (SDH) with controlled biodegradability and injectability has been synthesized by Liu et al. Subcutaneous injections of SDH loaded with DOX were administered to C57BL/6 mice. Following 12 days of significant weight loss, the degradation slowed. Approximately 70 days after injection, the degradation was nearly complete. Compared to the effects elicited by free DOX, the SDH-DOX hydrogel enhanced survival by approximately 33 % and inhibited tumor growth by approximately 50 % [311]. Luca et al. developed sustained and controlled-release hydrogels for DOX using combinations of dextran, chitosan, gelatin, and xanthan, as well as poly (acrylamide). The release of DOX occurred via diffusion, with minor contributions from hydrogel network relaxation. Hydrogels loaded with DOX significantly hindered the division of keratinocyte tumor cells and

promoted apoptosis in cutaneous squamous cell carcinoma cells, making them excellent for topical therapy. DOX-loaded hydrogels had a cell viability of 43–66 % after 24 h, whereas gelatin-based hydrogels had the lowest percentage. The trend continued 48 h after DOX exposure, and cell viability decreased to 26–38 %; then, 72 h later, it was 18–29 % [312]. Researchers have developed carboxymethylcellulose (CMC)-DOX nanosized complexes by forming supramolecular structures in aqueous solutions. A dual-responsive polymer-drug hydrogel network was created by chemically crosslinking CMC-DOX nanoparticulates with citric acid. *In vitro*, the distinct DS of CMC-tailored DOX release kinetics resulted in higher toxicity toward normal cells while active against cancerous melanoma cells [313]. Hybrid hydrogels were also created from AgNPs enclosed in CMC polymers and conjugated with DOX by Capanema et al. Colloidal nano-complexes were formed in aqueous media by reducing Ag^{+} ions in situ with a CMC polymer, which also served as a capping ligand and electrostatically bound to DOX. Experiments confirmed that DOX exhibited synergistic effects with AgNPs [314]. Based on the findings of these two studies, anticancer hydrogels containing colloidal polysaccharide-drug nanocomplexes offer promising perspectives for the transdermal delivery of chemotherapeutics.

4.10. Bladder Cancer

Worldwide, bladder cancer is estimated to result in more than 573,000 new cases and approximately 212,000 deaths nowadays [315]. In total, about 3 % of new cancer cases and about 2 % of cancer deaths can be attributed to this disease. A 5-year relative survival rate of around 77 % has been found in the US for bladder cancer, which ranks as the 10th most commonly diagnosed and 13th most common cause of cancer mortality around the world. When diagnosed early, bladder cancer is effectively treatable with relatively high survival rates [316]. Concerning bladder cancer, tobacco smoking is the leading risk factor. Compared to non-smokers, male smokers have a 3.3 times higher risk of bladder cancer, and female smokers have a 2.2 times higher risk [317].

A triblock PDLLA-PEG-PDLLA (PLEL) polymeric hydrogel-based drug delivery system was developed for the treatment of bladder cancer. In an animal study in mice, an intravenous injection of gemcitabine (GEM)-loaded PLEL hydrogel was performed, followed by subcutaneous injections of CpG-loaded PLEL hydrogel into the groin (Fig. 18). GEM released 57.7 % and 90.8 % after 24 h and 10 days, respectively. When injected intravenously, GEM/PLEL combined with CpG/PLEL kills tumor cells directly [318]. Employing such a dual-delivery system enhanced the therapeutic effect of GEM by prolonging its bladder retention and promoting continuous stimulation of the body's immune

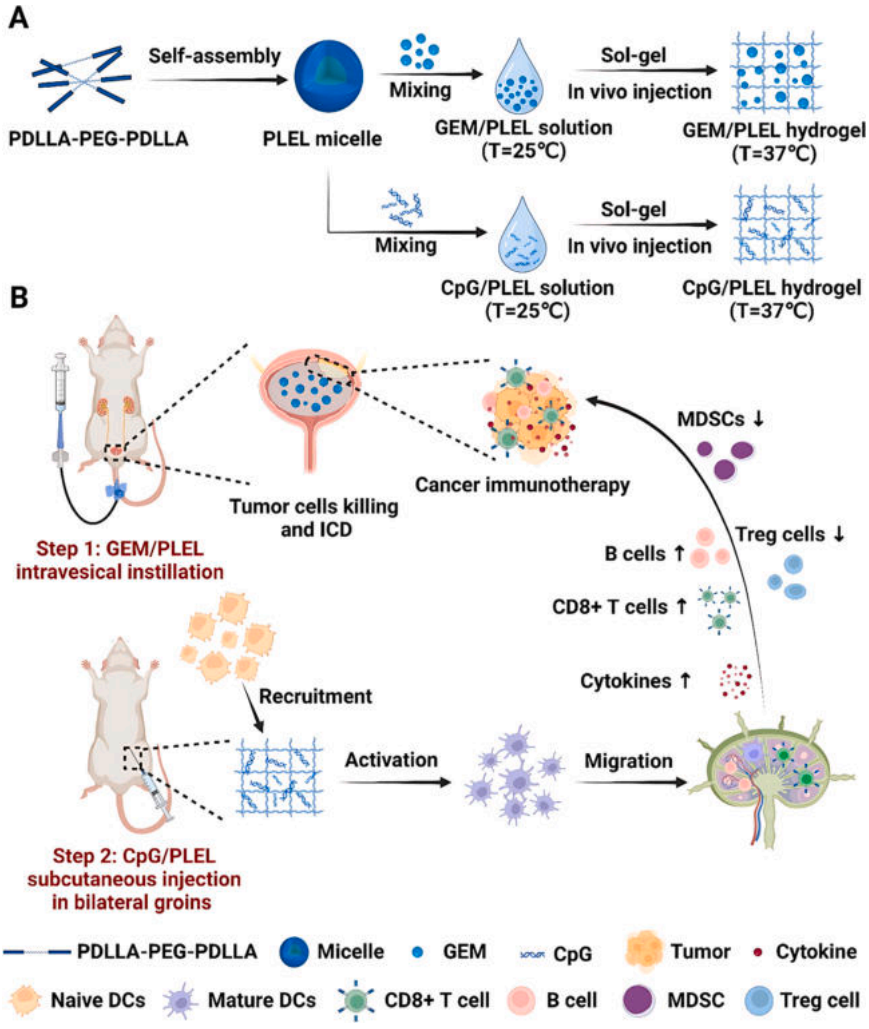

Fig. 18. (A) GEM/PLEL and CpG/PLEL hydrogel preparation. (B) Treatment of bladder cancer with chemotherapy and immunotherapy. Step 1: Instillation of intravesical GEM/PLEL. Step 2: CpG/PLEL are subcutaneously injected into the groin to boost tumor-specific immunity. GEM: Gemcitabine, CpG: cytosine-phosphate-guanine, MDSCs: myeloid-derived suppressor cells, PLEL: PDLLA-PEG-PDLLA, ICD: immunogenic cell death. Reprinted from ref [318] under the terms and conditions of the Creative Commons Attribution (CC BY) license (https://creativecommons.org/licenses/by/4.0/).

system through CpGs.

Novel polysaccharide supramolecular injectable hydrogel (CCA-1) was produced using cationic chitosan, anionic sulfobutyl β-ether-cyclodextrin (SBE-β-CD), and a trace amount of silver ions. The gel healed quickly and retained its elasticity and stickiness after injection. As carriers, CCA-1 hydrogels exhibited no apparent toxicity to normal or cancer cells, whereas CCA-DOX hydrogels had significant cytotoxic effects on bladder cancer cells. A drug release ratio of 22 % for CCA-DOX hydrogels was observed within the first 2 h, and a release ratio of 78 % was achieved after 48 h. CCA-DOX hydrogels released more drugs at pH 5.5 as compared with pH 7.4. Accordingly, 80 % of mice treated with the CCA-DOX system survived until day 12, and their bodies began to recover slowly after day 3 [319].

For making mucoadhesive HA-SH/PF127 nanogels, Pluronic F127 cores and thiolated hyaluronic acid shells were used. DOX was encapsulated in the core of the nanogel, thereby enhancing drug penetration into porcine bladder mucus without disrupting the mucus structure or bladder tissue in *ex vivo* studies. Significant toxicity of this system against both T24 and MB49 cells was reported [320]. Deguelin-loaded DMP nanoparticles (D/DMP) were formed by encapsulating deguelin in cationic poly(ethylene glycol)–poly(poliethoxyethylene glycol) (PPEG–PCL) hybrid nanogels (DOTAP). In this design, D/DMP nanoparticles were subsequently incorporated into a Pluronic F127 hydrogel. This entire system was capable of releasing the drug through two pathways: (i) slow release via surface erosion of the F127 hydrogel and (ii) release of D/DMP nanoparticles into the surrounding media, followed by the release of deguelin from the NPs [321].

Fe_3O_4 magnetic nanostructures were embedded in PEG-functionalized poly(N-isopropylacrylamide) hydrogels (HG(.When loaded with DOX and incubated with cancer cells, the system could subtly stimulate drug release at the site via an external radiofrequency field. DOX was released due to localized heat and mechanical vibrations of MNS, which caused the gel network to rupture. Incubation with HG-MNS-DOX for one *h* and exposure to RF for 24 h resulted in severe cell death, especially at higher fields. After 6 h following exposure to a high field, more than 80 % of cells were dead [322]. In order to deliver DOX to the bladder, magnetic hydrogel microspheres (DOX-mMSs) were developed using polyvinyl alcohol (PVA) and chitosan (CS). By tuning the externally applied magnetic field (AMF), magnetic nanoparticles (MNP) incorporated into the DOX-mMS matrix enable controllable retention in the bladder. By modulating urine pH, the pH-sensitive dissociation of CS and hydrazone bonds in DOX-mMSs could control the release of drugs. The cancer cell viability in the DOX-mMSs group after 72 h of incubation was only 7.3 %, demonstrating significant tumor cell death caused by DOX-mMSs [323].

In the comprehensive analysis of the examined studies, intravesical instillation was consistently employed as the administration method. Both CCA-1 hydrogel and HA-SH/PF127 nanogels exhibited significant binding affinity to the bladder mucosa. Regarding thermoresponsive characteristics, PLEL, D/DMP-F hydrogels, and HA-SH/PF127 nanogels demonstrated temperature sensitivity, whereas CS/SBE-β-CD/Ag+ hydrogels displayed responsiveness to pH variations. Furthermore, the HG-MNS-DOX system reported an exceptionally high cell death rate, approximately 95 %, thereby highlighting its potential efficacy in therapeutic applications. This comparative overview highlights the versatility of gel-based systems in targeted drug delivery and their implications for bladder treatment strategies.

4.11. Other cancers

Using N-(2-hydroxypropyl)methacrylamide (HPMA), researchers have synthesized biodegradable hydrogels that deliver DOX, vinblastine (a hydrophilic drug), and cyclosporine A (CsA) (a hydrophobic drug). Based on *in vitro* studies, hydrophilic drugs are released from HPMA-hydrogels primarily through diffusion and, to a lesser extent, through hydrogel degradation. Following implantation, hydrogels that degraded in 50 h released DOX for as long as 96 h. A concentration of 0.1–1 μg/mL of the drug was maintained in the bloodstream for at least 4 days. *In vivo* studies of HPMA-hydrogels in Bcl-1 leukemia demonstrated their therapeutic potential: compared to free DOX or a non-targeted polymeric drug (PK1), HPMA-hydrogels containing DOX significantly inhibited Bcl-1 leukemia. Cell lines overexpressing the P-glycoprotein (P-gp) were inhibited in vitro by DOX combined with CsA (as a P-gp blocker) via apoptosis [324].

In another experiment, an injectable hybrid nanocomposite made up of metal-organic frameworks (MOFs) and thermosensitive hydrogels was fabricated. DOX and celecoxib (Cel), both having antiangiogenetic activity, were co-loaded into the system (DOX/Cel/MOFs@Gel) for localized oral cancer therapy. Both drugs were released steadily and pH-responsively from this system, exhibiting enhanced toxic effects against both KB and SCC-9 oral cancer cells. *In vivo*, DOX and Cel displayed synergistic effects on tumor inhibition, inducing apoptosis and regulating angiogenesis. There was no evidence of persistent toxicity *in vivo* based on the biocompatibility test of the MOFs [325].

In situ controlled release of gambogic acid (GA) was used to treat oral squamous cell carcinoma (OSCC)-bearing mice. To improve the aqueous dispersibility of GA, thin-film hydration was employed to prepare GA-loaded mPEG2000-PCL micelles (GA-MIC). Then, poly(D,L-lactide)-poly(ethylene glycol)-poly(D,L-lactide) (PLEL) was synthesized for the preparation of thermosensitive hydrogels. Finally, an injectable therapeutic hydrogel was formed by mixing GA-MIC with PLEL. Using the thermosensitive GA-MIC-GEL, the hydrogel was formed within 24 s at 37 °C, facilitating local delivery and sustained release of GA. Upon testing in the OSCC mouse model, GA-MIC-GEL showed a significant improvement in both primary and long-term tumor remissions. GA-MIC-GEL downregulated PD-1 expression, increased the number of cytotoxic T cells, and reduced immunosuppressive cellular components, thereby enhancing the anti-tumor immunity of OSCC-bearing mice [326].

Head and neck cancer cells were treated with a self-assembling peptide hydrogel containing DOX and curcumin (Cur). The drug release rate was controlled based on the aqueous solubility of a dual drug-loaded peptide hydrogel. Hydrogel formulations that contain and release these drugs more significantly inhibited cancer cell growth compared to a simple combination of both drug solutions. In PBS pH 7.4, the hydrophilic DOX was released at 80 % within 4 h, while the hydrophobic CUR was released at 40 % within the same timeframe. DOX reached a plateau after 24 h with almost complete release, while CUR was released almost continuously for 19 days. The IC_{50} value of the peptide hydrogel-loaded CUR was the same as that of the plain CUR solution. Compared to a plain DOX solution, peptide hydrogel-loaded DOX achieved a 2.4-fold reduction in IC_{50} [327]. In order to synthesize an injectable intratumoral nanocomposite hydrogel delivery system, poly(lactic-co-glycolic acid) nanoparticles co-loaded with Erlotinib (Er) and Cur were incorporated into CS/ β-glycerophosphate hydrogels (optEr/Cur-NP-HG). A NP-loaded hydrogel formulation demonstrated a more pronounced modulation effect than optEr/ Cur-NP alone, enabling sustained and controlled drug release. The formulation of optEr/Cur-NP-HG21 demonstrated an impressive ability to retard tumor growth in a xenograft mouse model of Head and Neck Squamous Cell Carcinoma (HNSCC) [328]. Further details regarding the reviewed studies, such as stimulus type, administration methods, and other relevant parameters, are summarized in Table 1.

5. Clinical trials and FDA-approved formulations

At present, there are over 30 FDA- or European Medicines Agency (EMA)-approved injectable hydrogel-based products [330], of which only a minimal subset is specifically addressed to treat cancer (Table 2). In 2004, the FDA approved VANTAS® implants, which comprise diffusion-controlled polymer reservoirs containing (and releasing) histrelin acetate, a synthetic form of gonadotropin hormone. VANTAS® is used for the palliative treatment of advanced prostate cancer. The daily

Table 1
Overview of hydrogel-based drug delivery systems in the treatment of various cancers.

Cancer type	Hydrogel	Drug	Loading efficiency	Stimulus	In vitro	In vivo	Administration route	Outcomes	Ref
Breast cancer	Niosomes/poloxamers (P407/P188)	TMC	-	Temperature (34–37 °C)	MCF−7 and MDA-MB435 cells	mice	intratumorally	• A 90 % release of the drug from the niosomes occurred in six days • An increase of 2.8 fold in cellular uptake • After 72 h of exposure, cancer cells are killed more effectively • Drugs remaining at tumor sites for a prolonged period	[214]
	PLGA-PEG-PLGA	Herceptin	-	-	SK-BR−3 cells	mice	Hypodermic injection	• Herceptin was released consistently from the mixture-A hydrogel over 80 days • During the four-week observation period, the injection site maintained strong fluorescence signals • Hydrogels containing Herceptin were also influential in inhibiting tumor growth • Akt dephosphorylation and ADCC activity were highest in mice treated with 50 mg/kg Herceptin-loaded hydrogel,	[215]
	FA-GOFA / HACPN	DOX	51.2 %	37 °C / pH 7.4: 18.7 % and pH 5.5: 89.4 %	MCF−7 cells	BALB/c nude mice	intratumorally	• IC50 values of GOFA-DOX 7.3 mg/mL. • 30.3 % ratio of apoptotic cells. • Enhance the endocytosis and cytotoxicity of DOX in MCF−7 • Among the 21-day tumor inhibition ratios, 52 % were the highest • The GOFA-DOX showed 5 times more DOX being released at pH 5.5 than at pH 7.4 • GOFA-DOX/HACPN released only limited amounts of DOX at pH 7.4.	[217]
	gellan gum	paclitaxel:β-cyclodextrin	-	Redox	BT474 and HS5 cells	-	-	• After 72 h, 59.5–47 % of PTX was released • The HGGs were redox-responsive due to L-Cys-based crosslinking • Reduce the viability of BT474 and SKBR3 to 14 % and 9 %, respectively.	[219]
	CuBTC and PVA (borax serving as the crosslinking agent)	5-FU	-	physiological pH	MCF−7 and HeLa cells	-	-	• pH 5.2 showed a higher swelling ratio than pH 7.4, indicating a greater ability to absorb and hold water. • It can encapsulate 261.4 mM of 5-FU, which is 309 times more than dissolved in water.	[218]

(*continued on next page*)

Table 1 (*continued*)

Cancer type	Hydrogel	Drug	Loading efficiency	Stimulus	In vitro	In vivo	Administration route	Outcomes	Ref
	PAMAM dendrimer and PEG	silibinin, camptothecin, and methotrexate	-	-	J82 and MCF7 cell	-	-	• The 5-FU released 64.1 % after 48 h at a physiological pH 7.4. • The drug-encapsulated hydrogels release 30 %–80 % of their load after 1–4 days in water. • For silibinin, camptothecin, and methotrexate, drug solubility increases 37-fold, 4-fold, and 10-fold, respectively. • Both J82 and MCF7 cell lines show cytotoxicity after 48 h for all three drugs. • In both J82 and MCF7 cell lines, approximately 95 % of the cells were eliminated.	[216]
	4aPEG-OPA	PTX	-	-	C26 colon and 4T1 breast cancer cells	mice	peritumoral	• Over a 30-day period, the nanocomposite hydrogels sustained PTX release. • PTX@BN-loaded hydrogels significantly enhanced antitumor effects and prolonged the survival time of animals over free PTX solutions. • In order to make the drug-loaded hydrogel, PTX@BN was cross-linked with 4aPEG-OPA.	[220]
Ovarian cancer	GC	PTX-complexed beta-cyclodextrin (β-CD)	-	-	SKOV3 cell	mice	Locally	• The release of PTX was more rapid from GC/CD/PTX • When PTX is included in β-CD's cavity, its solubility is enhanced. • Within 5 h, initial bursts were observed. • There was a 3.33- and 2.38-fold decrease in cell viability compared with the other group. • Tumor volumes of the groups treated with GC/CD/PTX were fold lower on day 7 compared to other group. • The tumor tissue underwent necrosis.	[225]
	poly(alginate)-PLGA-PEG	OxPt	69.9 ± 0.9 %	-	.SKOV−3 cells	-	-	• Oxaliplatin degradation was 21.2 %, with 78.84 ± 6.28 % of the drug released over 1 week.	[226]
	α-CD β-CD and Pluronic F−127	DOX	-	pH	SKOV−3 cell	-	-	• At pH 7.4, 49.0 % of DOX was released from hydrogel 1 • At pH 5.5, the release of the drug was increased to 66.3 % for hydrogel 1 • To SKOV−3 cells, hydrogel 1 was less toxic than free DOX	[227]
	HA-FA	cisplatin	100 %	-	A2780wt and A2780cis cell	-	-	• From the third hour onwards, the release rate of loaded drugs decreased	[228]

(*continued on next page*)

Table 1 (*continued*)

Cancer type	Hydrogel	Drug	Loading efficiency	Stimulus	In vitro	In vivo	Administration route	Outcomes	Ref
								• Within 72 h, 90 % of the loaded drug was released. • EMT-related proteins were modulated in proliferation and expression.	
	PNC-HA	PTX	-	-	SKOV3 cell	mice	Intraperitoneally	• Increased killing efficiency and toxicity • Particle size reduction increased the absorption and dissolution rates of PTX.	[230]
	PLGA-b-PEG-b-PLGA	PTX, rapamycin, and LS301	-	Temperature (37 °C)	-	ES−2-luc xenograft mice	Intraperitoneally	• Within 48 h, three drugs reached 68–70 % release • After three days, the tumor burden decreased from 100 % to 7 ± 1 % in BLI. • Surgical outcomes in mice were improved. • Accurate delineation of tumor tissues in intraoperative NIR fluorescence images.	[231]
	Bi(mPEG-PLGA)–Pt(IV) (PtGel)	Cisplatin and PTX	100 %	temperature	SKOV−3 cell	BALB/c nude mice	intratumorally	• A sustained release of two drugs lasted for 2.5 months • Enhancement of PTX solubility by 1000-fold • Three weeks after administration, the tumor began to shrink, and the body weight increased.	[22]
	MPEG-PCL- Pluronic F−127	DOC	7 %	-	-	SKOV−3-bearing mice	-	• Induction of apoptosis • Inhibition of cell growth • raising local docetaxel concentrations • stabilizing and prolonging drug release • decreasing normal tissue toxicity	[229]
prostate cancer	PMOA	BSA and Epo	-	Temperature	PC3-KD cells	Balb/C mouse	subcutaneously	• In 11 h, PMOA released 50 % of the BSA. • There is good tissue compatibility with PMOA3 hydrogels.	[234]
	alginate-g-PNIPAAm	DOX	Alg-PN46–81 % and Alg-PN48–72 %	temperature	AT3B−1 cells	-	-	• alginate-g-PNIPAAm copolymers converted into micelles • Overcoming cancer cells' multidrug resistance • At 61 h, 81 % of DOX was released from Alg-PN46 hydrogels.	[235]
Colon Cancer	MoS2 NF doped CS/OD hydrogels	5-FU and MTX	-	pH	Colon cancer cell	-	-	• By electrostatic attraction, 5-FU was loaded into PEI/MoS2 • Electrostatic attraction and Schiff base reactions lead to the formation of CS/OD hydrogels.	[239]

(*continued on next page*)

Table 1 (*continued*)

Cancer type	Hydrogel	Drug	Loading efficiency	Stimulus	In vitro	In vivo	Administration route	Outcomes	Ref
								• pH 7.4 allowed the hydrogels to release MTX and TD/5-FU/PEI/MoS2. • MoS2 was found to be a powerful photothermal agent.	
	N-(2-aminoethyl)−4-(4-(hydroxymethyl)−2-methoxy−5-nitro-sophenoxy) butanamide (NB)-linked AlgNB and lipoid acid-modified- PEG-sulfur acid (LA-PEG-NH2) surface-modified MoS2 nanosheets (NH2-PEG-MoS2)	5-FU	20 %	-	SW480 cells	mice	intratumorally	• A NIR-triggered photothermal effect of the MoS2 nanosheets is highly efficient in the hydrogel and maintains superior dispersibility. • AlgNB's aldehyde group facilitates tissue adhesion to the hydrogel, enabling it to anchor and infiltrate tumor tissue. • A synergistic effect of PTT and 5-FU chemotherapy may inhibit DNA repair and enhance immune function. • Under 1.0 W cm−2 NIR irradiation, the AlgNB/MoS2/5-FU hydrogel killed approximately 75 % of cells	[240]
	GM and SA	DOX	-	pH	HT−29 cells	-	-	• Enhancing drug release control and therapeutic efficacy by using Fe3O4 magnetic nanoparticles. • A significant > 88 % release was observed at pH 7.2 compared to a release of 14 % at pH 1.2 • > 94 % inhibition of Gram-negative Escherichia coli • > 99 % inhibition of Gram-positive Staphylococcus aureus • Free DOX had an IC50 of 64 μg/mL, while DOX-loaded carriers had an IC50 of 128 μg/mL	[246]
	CS-DA-OP	DOX	0.32 % (w/w)	pH	HCT116 cells	rat	Subcutaneously	• Good antibacterial properties • 76 % of the DOX loaded into the hydrogels was released after 32 h • The CS-DA/OP6 hydrogel released 87 % of DOX after 60 h at pH 5.5 and 37 oC • The CS-DA/OP hydrogel exhibited mucoadhesive properties.	[241]
	Cs/AA/AMPS	5-FU	-	pH	-	-	-	• After 7 h, 96 % of the 5-FU drug was released at pH 7 • By γ-rays, amphiphilic hydrogels were prepared using CS and AMPS/AAc.	[242]
	MAA and IA through EGDMA	5-FU	-	pH	-	-	-	• Compared to lower pH 1.2, copolymeric hydrogels showed higher swelling and release at pH 7.4.	[243]

(*continued on next page*)

Table 1 (*continued*)

Cancer type	Hydrogel	Drug	Loading efficiency	Stimulus	In vitro	In vivo	Administration route	Outcomes	Ref
	GM/CS/PVA /Alg [illegible]	MTX and Asp	Asp: 91 % MTX: 68 %	pH	SW480 cell [illegible]	-	-	• At pH of 6.5 [illegible] 96 % of the drug MTX released [illegible] 7 h [illegible] 25 min • Decreased the cell viability [illegible] • [illegible] The MTX-associated side effects could be effectively reduced by decreasing the demand for MTX.	[245]
	pectin-co-poly(MAA)	5-FU	-	pH	-	Rabbit	orally	• Sustained release of drug • Drug release after 12-hour dissolution experiments ranged from 58 % to 60 % at pH 1.2 to over 90 % at pH 7.4.	[247]
	poly(HEMA)Hal SH nanocomposite	5-FU	-	pH	-	-	-	• Hal hydrogels showed 99 % release after 74 h. • Each hydrogel formulation releases 5-FU in accordance with its swelling behavior. • In intestinal fluid, 5-FU was released significantly more over 70 h. • 5-FU release in the gastric region was < 10 %,	[248]
	CMC-Ald /PAH	DOX and Camptothecin (CPT)	100 %	-	-	mice	intratumorally	• Coupled DOX prevented burst release • Reduction in biotoxicity • Improvement in antitumor properties	[251]
	5′-GMP disodium salt and NAP in 4:1 stoichiometry in aqueous media	DOX	-	pH	CT−26 cell	Balb/c mice	-	• The DOX release is ~approximately 82 % over 100 h at a pH ~of roughly 7.4. • A ~4.5-fold increase in internalization of DOX-Gel compared to DOX alone. • Following 21 days, tumor volume significantly reduced by ~87.5 %,	[249]
	HP-β-CD-g-MAA	Cytarabine	37.17–79.3 %	pH	-	Rabbit	orally	• The release of cytarabine lasted up to 24 h and was sustained. • The controlled drug release pattern ranged from 36.49 % to 95.77 % in the developed formulations. • Show no signs of abnormality or pathological distortion. • Prolonged t1/2, an increased MRT, and an increase in AUC for cytarabine	[250]
	PNiMaTH and PNiPenPH	DOX	5 %	temperature	Fibroblast	-	-	• Both hydrogels exhibit highly porous network structures at 25°C, whereas a layering and less porous morphology was observed at 37°C • PNiMaTH and PniPenPH released 31.5 % and 22.2 % of	[329]

(*continued on next page*)

Table 1 (*continued*)

Cancer type	Hydrogel	Drug	Loading efficiency	Stimulus	In vitro	In vivo	Administration route	Outcomes	Ref
								DOX, respectively, after a burst effect and rapid release for 12 h. • As a result of a more extended structure, PNiMaTH hydrogel was released rapidly since DOX molecules could not adhere to the nano-cavities formed on its surface.	
Brain cancer	PNIPAAmMA	EPI and PTX	39.1 ± 2.2 %	temperature	MBR 614 cell	C57BL/6 and Nu/Nu mice	intratumorally	• HydrogelGd/EPI-incorporated BSA/PTX NPs could release EPI (hydrophilic) and PTX (hydrophobic) drugs. • After 120 h, 78.9 % of EPI was released from hydrogelGd. • Mice survived an average of 63 or 69 days without tumor recurrence.	[257]
	MLTH	SN−38	-	temperature	NIH3T3 and U−87 MG cells	BALB/c-nu mice	intratumorally	• Over the 59 days, approximately 100 % of SN−38 from MLTH 1-#1 and MLTH 1-#2, and 70 % of SN−38 from MLTH 4 and MLTH 5, were released.	[259]
	mPEGPLGA nanocomposite	PTX and TMZ	-	temperature	U87 and C6 cell	-	-	• A composite gel subjected to zero-model showed PTX and TMZ to be released as NPs. • Exact proliferation inhibitory results showed significant differences in apoptosis rates between composite gel and other groups.	[260]
	TGP with PLGA microspheres and liposomes	DOX	-	temperature	U87MG and LN229 cell	mice	Locally	• Up to 30 days of DOX can be released • Inhibited tumor growth until day 32 and day 38. • U87MG cells were 90 % inhibited by TGP-DOX at 0.1 mg/mL. • Glioma growth was significantly reduced.	[262]
	PEG-DMA	TMZ	-	-	-	mice	Locally and intravenously	• A linear burst of 45 % of TMZ was released during the first 24 h • Release of 20 % over the following week. • Tumor weight loss • The lack of inflammation at the hydrogel implantation site	[261]
Lung cancer	HA–Tyr	ES	-	-	HUVECs	mice	intratumorally	• A more potent inhibitor of tumor growth • were lower HIF−1α positive cells were less prevalent • lower expression levels VEGF-A • In the first four days, ES was released suddenly	[267]

(*continued on next page*)

Table 1 (*continued*)

Cancer type	Hydrogel	Drug	Loading efficiency	Stimulus	In vitro	In vivo	Administration route	Outcomes	Ref
	CS-NSA/A-HA	CDDP and DOX	-	pH	A549 cell	-	–	• On the 14th day, the cumulative release of ES was 52.7 ± 3.9 % • The material is more effective as a dual-drug carrier than as a single-drug carrier. • A549 lung cancer cells were more effectively inhibited by the dual-drug carrier than by a single-drug carrier.	[268]
	HA–Tyr	AL	-	-	LLC cells and HUVECs	mice	intratumorally	• Reduced liver, kidney, and lung toxicity • Inhibition of HUVEC and LLC colony formation • A dose-dependent decrease in the number of surviving colonies in vitro. • Angiogenesis, migration, and invasion were inhibited • The ratios of Ki−67- and VEGF-A-positive cells were reduced.	[270]
	PDMP	CDDP and PTX	3.96 ± 0.03 %	temperature	A549 cells	BALB/c nude mice	intratumorally	• There was a significant increase in median survival time (53 days). • Ki−67 positive cells were reduced • suppression of cell proliferation and angiogenesis	[271]
	PEG –diacrylate (PEGdA) and modified gelatin	AuP	-	-	Normal lung fibroblast CCD−19Lu, lung tumor cells NCIH460 and A549	NCI-H460 Xenograft Model	injectable in situ gel	• Inducing tumor necrosis with AuP-containing hydrogel • After a 24 h initial burst, • A sustained release was achieved for 7 days, followed by a cumulative release of 65 % of loaded AuP • There was no significant weight loss during the treatment period, suggesting no systemic toxicity	[272]
	gelatin/SCMC	DOX	0.78 ± 0.07 %	-	A549 cells	-	-	• For all scaffold types, the drug encapsulation efficiency was around 100 %. • The burst release of DOX from hydrogel scaffolds • 30 % of DOX released within 24 h	[269]
	RNA NHs	microRNA and DOX	-	photo	A549, L02 and HeLa cells	BALB/c naked mice	intratumorally	• As a result of RNA NHs-T, intracellular ROS can accumulate, leading to cell death. • A549 cells treated with the negative control had a viability greater than 80 %.	[273]
	COFs + albumin-oxygenated hydrogel	RNase A and DOX	-	pH	-	mice	-	• A COF can deliver hydrophobic and hydrophilic proteins with different physicochemical properties in vivo, thereby	[274]

(*continued on next page*)

Table 1 (*continued*)

Cancer type	Hydrogel	Drug	Loading efficiency	Stimulus	In vitro	In vivo	Administration route	Outcomes	Ref
								escaping endosomal/lysosomal degradation and enhancing in vivo protein absorption. • Targeted delivery of proteins and small molecules in vivo	
Liver cancer	NCTD-NPs + Pluronic F127	DOX	8.80 ± 0.42 %	temperature	HepG2 cells	mice	intratumorally	• Within 168 h, DOX was released at a rate of 97 % • Enhanced cytotoxicity • Reduction of Ki−67-positive cells	[276]
	poly(PDMS/PEG/PPG) polyurethanes	DOX	-	temperature	HepG2 cells	BALB/c nude mice	in situ injection	• In the first 5 h, 20 % of the dose was released • Complete release on the 6 day. • Inhibited tumor growth by approximately 60 % compared to other groups • Lung, spleen, and kidney pathology showed no signs of injury or toxicity	[277]
	PECT	Embelin	10 %	temperature	H22 cells	mice	Intraperitoneally	• Approximately 32.34 % and 57.08 % of accumulated embelin were released after 48 and 504 h, respectively. • Necrotic, early apoptotic, and late apoptotic cell populations were significantly higher • A low dose of Embelin/PECTgel produced a significant antitumor effect	[278]
	Pluronic F127	CDDP	10 %	temperature	H22 cells	mice	Intraperitoneally	• Apoptosis is initiated • The cell cycle is arrested at the G1 phase • Only 28.4 % of the total drug load was accounted for by the F127 Gel RES-MS/DDP system in the first 8 h. • Increase in death rate (53.75 ×1.12 %) • Median survival time has increased (31 days)	[279]
	GNS, PVA and CS	MTX	-	Temperature and pH	HepG2 cell	-	-	• The maximum drug release was 97.34 % after 6 h. • CS-PVA-GNS hydrogels loaded with MTX had an IC50 of 5.87 μg/200 mL, while free MTX had an IC50 of 5.03 μg/200 mL. • > 80 % cell viability	[281]
	FER−8 peptide hydrogel	PTX	-	pH	H22 cells	mice	intratumorally	• Prolonged retention (96 h) at the tumor site • Reduced systematic side effects • In mice, paclitaxel doses of 10 mg/kg inhibited tumor cell growth by 12 days after treatment	[282]

(*continued on next page*)

Table 1 (*continued*)

Cancer type	Hydrogel	Drug	Loading efficiency	Stimulus	In vitro	In vivo	Administration route	Outcomes	Ref
	ACC/PAA	DOX	> 80 %	pH	SMCC−7721 Cells	zebrafish and mice	tail vein injection	• After 3 h of incubation with the hydrogel, the fluorescence intensity of treated cells increased 1.5 times, with pH decreasing from 7.4 to 6.6 • Better cancer cell-killing effect.	[283]
	glycol chitosan-Pluronic F127 micelles	DOX	86 % and 88 %,	pH	H22 cells	mice	intratumorally	• There was an increase in tumor cell uptake of loaded DOX in extracellular pH below 7.4. • Increase in antitumor activity • Lifetime is longer • Decrease of systemic toxicity	[280]
	CEC	DOX	-	pH	L929 and HepG2 cells	rat	subcutaneously	• Self-healing hydrogels could prolong their lifespan • After 7 days, CEC/PEGDA20 hydrogel in PBS at pH 7.4: 42 %, at pH 5.5: 92 %, and pH 6.8: 89 % of DOX was released; after 4 days and at pH 4.0: 96 % of DOX was released	[284]
	SA/CS/HAP	DOX	-	pH	-	-	-	• At pH = 5, drug release was up to 95 % • At pH = 7, drug release was up to 60 %.	[285]
	ε-PL/A-Pul/BPEI	CDDP and DOX	-	pH	Huh−7 cells	mice	intratumorally	• Compared with pH 7.4, degradation and drug release were faster at pH 7.0 • The cell inhibition rate of standard and • At 12 h, 76 % of CDDP+DOX were released • While CDDP's anticancer activity was metastable with time, DOX's anticancer activity increased	[286]
Gastric cancer	SWNT-GEL	DOX	-	temperature	BGC−823 cell	Balb/c nude mice	intratumorally	• Released approximately 50 % of DOX cumulatively. • After 27 days, the average growth ratio of tumor volume in the free DOX group reached 166 %, while in the DOX/SWNT-GEL group, it shrank to 61.3 %.	[290]
	SCMC	CDDP	-	-	-	BLAB/C node mice	orally	• The ID50 of CDDP-Gel was 13.2 times higher than that of CDDP. • Survival time is longer • Enhance antitumor efficacy • Decrease of systemic toxicity and tumor metastasis • At higher doses than CDDP (10 mg/kg) or CDDP-Gel (73.6 mg/kg), mice died, and toxic signs like convulsions and diarrhea were observed.	[291]

(*continued on next page*)

Table 1 (*continued*)

Cancer type	Hydrogel	Drug	Loading efficiency	Stimulus	In vitro	In vivo	Administration route	Outcomes	Ref
	HA	CDDP	-	-	MKN45P cell	mice	Intraperitoneally	• For more than four days, CDDP was released from the hydrogel. • Significant reduction in the weight of • tumor • Gelation time decreased with increasing polymer concentration.	[292]
	PDLLA-PEG-PDLLA, PLEL	5-FU and CDDP	-	temperature	MKN45-luc cells	mice	intraoperative	• Approximately 62.43 % of 5-FU was released after 24 h and 92.42 % after 28 days. • During the 24 h and 28-day periods, DDP cumulatively released 33.35 % and 47.42 % • In the drug-loaded hydrogel, 5-FU and DDP had an initial drug ratio of 20:1. • The cumulative 5-FU and DDP release ratio during the 7-day release process was kept at about 40:1 • the most tumor suppressor effect	[293]
	PPZ	DTX	-	temperature	-	mice	intravenously or intraperitoneally	• DTX-gel-treated mice had significantly less tumor growth and an increase in survival rate than mice treated with DTX-sol IV or IP	[294]
	PRNP-gel	PTX	85 %	temperature	MKN−45 cells	xenograft	Intravenously and subcutaneously	• The cumulative release of PTX was 30 % after 6 days • Incubation at 37 °C or subcutaneous injection resulted in in situ gelation within 12 min	[295]
Melanoma	Kolliphor® P407	CUR	-	temperature	-	-	-	• In the viable epidermis (100–150 μm depth), CUR-loaded nanomicelles were localized. • At 48 h, the CUR amounts are 5.81 %, and at 72 h, they are 7.25 %.	[309]
	rGO-CMARX nanocomposite hydrogels	5-FU	after 24 h: 45.15 ± 1.79 % and 48 h: 57.37 ± 2.54 %,	pH	U−87 cells	-	-	• 93.10 % of drug release at pH 7.3. • 80.20 % of drug release at pH 6.4. • rGO and 5-FU played a synergistic role in anticancer activity	[310]
	HP-β-CD/ poloxamers 407 and 188	Cur	60.3 ± 0.4, 97.4 ± 0.8, 62.7 ± 2.6 %,	-	B16-F10 cells	-	-	• Melanoma cells were cytotoxic to Cur due to their blocking of cell proliferation in the G2/M stage and subsequent apoptosis. • Cyclodextrins have cone-shaped cavities that can embed the hydrophobic side chains of drugs.	[308]
	Sericin/Dextran	HRP and DOX	-	pH	C2C12 and HL7702 cells	C57BL/6 mice	subcutaneously	• As a result of the pH value for the test being close to sericin's	[311]

(*continued on next page*)

Table 1 (*continued*)

Cancer type	Hydrogel	Drug	Loading efficiency	Stimulus	In vitro	In vivo	Administration route	Outcomes	Ref
								isoelectric point, pH 3.8, the hydrogel showed relatively low swelling in the acidic condition. • After 12 days, a significant weight loss was observed • 70 days after injection, the degradation was nearly complete • During the 32nd day, more than 90 % of the encapsulated DOX from SDH−1 and SDH−2 was released.	
	DexMa-CsMa-BisAam; DexMa-GelMa-BisAam; and DexMa-X-Ma-BisAam	DOX	100 %	-	A431 epidermal cell	-	-	• Gelatin-based hydrogels had a lower percentage of viable cells. • In the hydrogel's architecture, natural polymers and synthetic components can be selected to control the release of DOX.	[312]
	CMC polymer	DOX	-	pH	HEK 293 T and A375 cells	-	-	• Cell viability reduced to 32–42 % • Due to the dissociation of the complex at a lower pH of 6.2, there was a faster release rate with weaker electrostatic binding interactions compared to pH 7.4.	[313]
	Carboxymethylcellulose–Silver/CA	DOX	-	-	HEK 293 T and A375 cells	xenograft	-	• More than 98 % of Ag was not released due to the relative stabilization of the hybrid network, caused by the incorporation of silver nanoparticles into the structures, along with chemical cross-linking. • In comparison to CMC membranes without AgNPs, the presence of AgNPs significantly increased cell death.	[314]
Bladder cancer	PLEL	GEM	-	temperature	MB49 cells	C57BL6 mice	intravesically	• 57.7 % and 90.8 % of GEM were released at 24 h and 10 d, respectively. • At 24 h and 96 h, CpG was 60.8 % and 94.2 %, respectively • on day 7; both of them were released entirely from PLEL. • A better immune response from the body's immune system was observed.	[318]
	CS/SBE-β-CD/Ag+	DOX	0.03 %	pH	MB49-luc and 293 T cells	mice	intravesically	• After 2 h, DOX released is 22 % • After 48 h, DOX released is 78 % • DOX released more drugs at a pH of 5.5 than at a pH of 7.4. • MB49 bladder tumor cells survived at only 17 % in the	[319]

(*continued on next page*)

Table 1 (*continued*)

Cancer type	Hydrogel	Drug	Loading efficiency	Stimulus	In vitro	In vivo	Administration route	Outcomes	Ref
								presence of CCA-DOX hydrogel, similar to the survival rate of free DOX (16 %). • CCA-DOX mice survived to day 12 in about 80 % of cases, with a gradual recovery of body weight after day 3.	
	HA-SH/PF127	DOX	87.5 %	temperature	T24 and MB49 cells	porcine	Intravesically	• DOX@HA-SH/PF127 nanogels could penetrate the bladder's mucus structure and penetrate the DOX without damaging the mucus or tissue. • Both T24 and MB49 cells were significantly cytotoxic by DOX@HA-SH/PF127 nanogels.	[320]
	D/DMP-F	Deguelin	4.9 %	temperature	ATCC cells	BALB/c mice	Intravesically	• T24 cells were inhibited by deguelin in a dose-dependent manner • DMP-F hydrogel composite was sustained released of deguelin by surface erosion of F127 gel at 37°C • The DMP-F gel partially dissolved in the urine 2 h after intravesical administration, but it remained pasted to the bladder wall after that time.	[321]
	HG-MNS	DOX	-	Magneto-thermally	T24 cell	swiss mice model	Intravesically	• Sustained release of DOX • Cell Petri dish exposed to RF for 1 h combined with HG-MNS-DOX caused severe cell death in 24 h, especially at higher fields • Even 6 h after exposure to a high field, more than 80 % of cells were found dead • Approximately 95 % of the cells died	[322]
	PVA/CS	DOX	15.5 %	Magneto-pH	TCCSUP and NIH/3T3 cells	C57BL/6 mice	intravenously	• As a result of the AMF, the DOX-mMSs are retained in the bladder for an extended period. • With pH-sensitive dissociation of CS and hydrazone bonds in DOX-mMSs, controlled drug release can be achieved by adjusting the pH of the urine in the bladder. • Encapsulation efficacy: 93.7 % • Cell viability of the DOX and DOX-mMSs groups after 12 h of incubation is 47.1 % and 44.6 %, respectively. Following 72 h of incubation, cell viability in the DOX-mMS group is 7.3 %	[323]

(*continued on next page*)

Table 1 (*continued*)

Cancer type	Hydrogel	Drug	Loading efficiency	Stimulus	In vitro	In vivo	Administration route	Outcomes	Ref
BCL1 leukaemia	HPMA	DOX, vinblastine and cyclosporine A	-	-	–	Balb/c mice	Intraperitoneally	• Growth with viability of cell: greater than 95 % • DOX released rate in the first 5 h is 60–70 %, and VLB is 90 % • The degradation time of hydrogels was 50 h • Within 24 h, VLB was released entirely, while 20 % of DOX remained • The mean survival of mice was 55 days • A drug's pharmacological activity is maintained in the bloodstream for at least 96 h.	[324]
oral cancer	PLGA-PEG-PLGA	DOX and Cel	64.46 %	Temperature and pH	KB, A549, HepG2, L929, and L−02 cells	BALB/c nude mice	Peritumorally (subcutaneously)	• Due to weak interactions between the drug and MOFs, DOX and Cel exhibited a burst release on the first day, followed by an 11-day sustained release. • In pH 6.5, over 80 % of DOX was delivered from Dox/Cel/MOFs or DOX /Cel/MOFs@Gel. • After 11 days at pH 7.4 and 6.5, 62.90 % and 65.77 % of the loaded Cel was released from the DOX/Cel/MOFs@Gel, but over 90 % of the loaded Cel was gradually released from the DOX/Cel/MOFs. • DOX/Cel/MOFs@Gel possess the highest anticancer potency in part due to localized steady dual drug release and synergistic effects of DOX and Cel.	[325]
	PLEL	GA	-	temperature	OSCC cell	mouse	intratumorally	• GA-MIC-GEL downregulated PD−1 expression, increased cytotoxic T cells, and reduced immunosuppressive cellular components, thereby boosting the anti-tumor immunity of OSCC-bearing mice. • The hematological and pathological examinations of GA-MIC-GEL indicated that it is biologically safe. • Within 24 s, GA-MIC-GEL formed hydrogel at 37 °C, enabling local delivery and sustained release of GA.	[326]
Head and Neck Cancer	ac-(RADA)4-CONH2 peptide hydrogel	CUR and DOX	-	-	HSC−3 cell	xenografted SCID mice	intratumorally	• In the nanofiber matrix, differential drug distribution is also displayed on the drug release rate, with the hydrophilic DOX releasing 80 %	[327]

(*continued on next page*)

Table 1 (*continued*)

Cancer type	Hydrogel	Drug	Loading efficiency	Stimulus	In vitro	In vivo	Administration route	Outcomes	Ref
								within 4 h. In contrast, in PBS pH 7.4, only 40 % of CUR was released. • On CUR over 19 days, the release profile was sustained • In the hydrogel matrix, neither drug interaction with nanofibers nor drug release was influenced by pH. • Upon initiation of the gelation process, both plain and dual drug-loaded samples displayed an initial lag phase lasting approximately 20 min, followed by a rapid growth phase of 10 min. • The peptide hydrogel-loaded CUR had a similar IC50 value to plain CUR, whereas the peptide hydrogel-loaded DOX had a significantly higher inhibitory effect with a 2.4-fold reduction in IC50.	
	CS/β-glycerophosphate	Erlotinib (Er) and Curcumin (Cm)	-	temperature	FaDu cell	xenograft HNSCC mouse	intratumorally	• Compared to free drugs, optEr/Cm-NP and optEr/Cm-NP-HG21 displayed enhanced cytotoxicity • A significant increase in apoptotic cell death • Considerable capacity to retard the tumor growth	[328]

TMC: Tamoxifen citrate, ADCC: antibody-dependent cellular cytotoxicity, GOFA: folic acid (FA)-conjugated GO, DOX: doxorubicin, HACPN: hyaluronic acid-chitosan-g-poly(N-isopropylacrylamide), PTX: Paclitaxel, GC: glycol chitosan, β-CD: beta-cyclodextrin, α-CD: α-Cyclodextrin, HA-FA: hyaluronic acid- folic acid, EMT: Epithelial-Mesenchymal Transition, PNC: PTX nanocrystals, PLGA-b-PEG-b-PLGA: poly-(D,L-lactide-co-glycolide)-block-poly-(ethylene glycol)-block-poly-(D,L-lactide-co-glycolide), NIR: near-infrared, DOC: Docetaxel, Epo: erythropoietin, BSA: bovine serum albumin, alginate-g-PNIPAAm: alginate-g-poly (N-isopropylacrylamide), CS/OD: chitosan/ oxidized dextran, MTX: methotrexate, 5-FU: Fluorouracil, PEI: polyethylenimine, CS-DA-OP: chitosan-grafted-dihydrocaffeic acid- oxidized pullulan, Cs: chitosan, AAc/AMPS: anionic polymers of (acrylic acid)-co-(2-acrylamido-2-methylpropane-sulfonic acid), MAA: monomers methacrylic acid, IA: itaconic acid, EGDMA: ethylene glycol dimethacrylate, GG: guar gum, PVA polyvinyl alcohol, DDDS: dual-drug delivery system, CMC: sodium carboxymethyl cellulose, Alg: alginate, CMC-Ald: oxidized carboxymethylcellulose, PAH: poly(aspartic hydrazide), 5′-GMP: 5′-guanosine monophosphate, NAP: 1,4,5,8-naphthalene tetracarboxylic acid tetra potassium salt, HP-β-CD-g-MAA: hydroxypropyl–β–cyclodextrin-based polymeric network, PNiMaTH: PNIPAM-Mal-TEGDE, PNiPenPH: PNIPAM-Pen-PEGDA, PNIPAAmMA: poly(*N*-isopropylacrylamide-co-methacrylic acid), MLTH: MRI-monitored long-term therapeutic hydrogel, mPEGPLGA: monomethoxy (polyethylene glycol)-poly (D, L-lactide-co-glycolide), TMZ: temozolomide, TGP: thermoreversible gelation polymer, PLGA: Poly lactic-co-glycolic acid, PEG-DMA: polyethylene glycol dimethacrylate, HA–Tyr: hyaluronic acid-tyramine, ES: Endostatin, HUVECs: human umbilical vascular endothelial cells, HIF-1α: hypoxia-inducible factor 1-alpha, VEGF-A: vascular endothelial growth factor A, AL: anlotinib, LLC: Lewis lung carcinoma, PDMP: PEG–PCL–PEG/DDP+ MPEG–PCL/PTX, PEG: polyethylene glycol, AuP: Gold(III) porphyrin, SCMC: sodium carboxymethyl cellulose, RNA NHs: RNA nanohydrogels, ROS: Reactive oxygen species, COFs: Covalent organic frameworks, NCTD-NPs: norcantharidin-loaded nanoparticles, PDMS: polydimethylsiloxane, PPG: polypropylene glycol, PECT: poly (ε-caprolactone-co-1,4,8-trioxa[4.6]spiro-9-undecanone)–poly (ethylene glycol)–poly (ε-caprolactone-co-1,4,8-trioxa[4.6]spiro-9-undecanone), RES: resveratrol, CDDP: cisplatin, ACC: amorphous calcium carbonate, PAA: poly (acrylic acid), CEC: N-carboxyethyl chitosan, PEGDA: dibenzaldehyde-terminated poly(ethylene glycol), SA/CS/HAP: Sodium alginate / chitosan / hydroxyapatite, A-Pul: aldehyded pullulan, ε-PL: ε-poly-L-lysine, BPEI: branched polyethylenimine, SWNT: Single wall carbon nanotube, PPZ: poly (organophosphazene), PRNP-gel: red blood cell membrane nanoparticles, rGO: reduced graphene oxide, CMARX: carboxymethylarabinoxylan, HRP: Horseradish peroxidase, SDH: sericin /dextran composite hydrogels, CA: citric acid, SBE-β-CD: anionic sulfobutyl ether β-cyclodextrin, HA-SH: hiolated hyaluronic acid, PF127: Pluronic F127, DMP: DOTAP and monomethoxy poly(ethylene glycol)–poly(ε-caprolactone) hybrid nanoparticles, MNS: Fe_3O_4 magnetic nanostructures, HPMA: hydroxypropyl)methacrylamide, Cel: celecoxib, GA: gambogic acid, 4aPEG-OPA: *o*-phthalaldehyde (OPA)-terminated 4-armed poly(ethylene glycol), PAMAM: Poly(amidoamine), AlgNB: Sodium alginate, SA: sodium alginate, GM: galactomannan, GNS: graphene sheets, AMF: applied magnetic field

Table 2
Completed and ongoing clinical trials of Cancer-related hydrogel-based formulations.

Drug	Cancer type	Enrollment	Study Type	Phase	Intervention	Ages	Study Start	Last Update Posted	ClinicalTrials.gov ID
VANTAS	Prostate Cancer	142	Observational	Completed	-	18 years and older	2011–01	2014–10–16	NCT01574846
	Prostate Cancer	12	Observational	Completed	Procedure: Ultrasound, CT, or MRI to locate the implant	45 years and older	2006–07	2024–01–02	NCT01013025
OncoGel	Glioblastoma Multiforme	4	Interventional	I/II (Terminated)	Drug: OncoGel (ReGel/PTX)	18 Years to 70 Years	2007–03	2022–06–22	NCT00479765
	Esophageal Cancer	137	Interventional	II	Drug: OncoGel (PTX gel), cisplatin, 5-FU Radiation: radiation therapy Procedure: esophageal resection	18 years and older	2008–01	2022–06–22	NCT00573131
SpaceOAR	Prostate Cancer	500	Interventional	Not Applicable	Device: SpaceOAR Vue System	18 years and older	2021–12–21	2024–11–27	NCT04905069
	Prostate Cancer	14	Observational	Completed	Device: SpaceOAR Hydrogel	Child, Adult, Older Adult	2022–11–03	2024–11–19	NCT05735652
	Localized T1-T2 Prostate Cancer	15	Interventional	Not Applicable	Device: SpaceOAR Treatment	Child, Adult, Older Adult	2022–08–18	2024–11–27	NCT05407714
	Prostate Cancer	222	Interventional	III	Device: SpaceOAR System	18 years and older	2012–01	2021–03–19	NCT01538628
	Prostate Cancer Patients Treated by Radiotherapy	119	Observational	Terminated	Device: SpaceOAR™ implantation	18 years and older	2013–11	2021–07–27	NCT01999660
	Prostate Cancer	30	Interventional	Not Applicable	Device: SpaceOAR Vue	Child, Adult, Older Adult	2024–03–08	2024–03–20	NCT05650021

5-FU: 5-fluorouracil; PTX: Paclitaxel; MRI: Magnetic resonance imaging; CT: Computed tomography

dose of histrelin acetate delivered by VANTAS® will be approximately 50 mcg over 12 months [331]. During the first week of treatment with VANTAS®, testosterone concentrations in the serum increased transiently. Thus, patients with vertebral metastases and/or urinary obstruction or hematuria are at risk of experiencing symptom exacerbation during the first few weeks of treatment. When these conditions are exacerbated, they can lead to neurological problems, such as weakness and/or paresthesia in the lower limbs, and worsened urinary symptoms [331].

The OncoGel product received FDA approval in 2007 [148]; it comprises a biocompatible gel called ReGel (23 % polymer by weight in water) containing PTX (6.0 mg/mL), which can be released in situ to treat different types of cancer without systemic side effects [332]. The gel disappears 4–6 weeks after the PTX is released [333]. A clinical trial (NCT00479765) was initiated following preclinical studies that showed improved survival in glioblastoma-bearing rodents treated with Oncogel®. It involved the local administration of Oncogel® to patients with recurrent gliomas who are eligible for gross total resection in a phase I/II clinical trial. Clinical trial termination was attributed to the sponsor's decision rather than safety or efficacy issues [334].

In a randomized phase 2b trial, patients diagnosed with localized or locoregional adenocarcinoma or squamous cell carcinoma (SCC) of the esophagus or gastroesophageal junction were selected as suitable candidates for preoperative neoadjuvant chemoradiotherapy. Participants were randomly assigned to receive either the standard of care (SOC) alone or SOC in conjunction with endoscopic ultrasound (EUS)-guided PTX injections. PTX was administered in 0.5- to 1-mL aliquots directly into the tumor. The neoadjuvant chemoradiotherapy regimen for the SOC group consisted of intravenous 5-FU administered during the first four days of weeks 1 and 5, in addition to intravenous cisplatin on the initial day of the same weeks, alongside radiotherapy delivered throughout five and a half weeks. The combination of SOC and PTX was deemed safe; however, it did not demonstrate any enhancement in overall survival or tumor response rates in patients with esophageal or gastroesophageal junction cancer (NCT00573131) [335]. Researchers investigated the effects of OncoGel in conjunction with oral TMZ or locally administered TMZ polymer in rats bearing intracranial gliosarcoma, both with and without radiotherapy. The administration of OncoGel at a concentration of 6.3 and TMZ polymer alone resulted in median survival times of 33 and 35 days, respectively, with 50 % of subjects surviving beyond 120 days (long-term survivors, LTS). The median survival duration increased to 36 days when oral TMZ was combined with radiotherapy, although no long-term survivors were observed in this group. Conversely, combining OncoGel with oral TMZ yielded a median survival time of 57 % longer than the target. In this rodent model of intracranial gliosarcoma, the local application of OncoGel in combination with either oral or locally delivered TMZ and/or radiotherapy significantly enhanced the proportion of long-term survivors and improved median survival compared to the administration of oral TMZ and radiotherapy alone or in combination [336].

In 2015, SpaceOAR®, a PEG-based hydrogel system, was FDA-approved. In prostate cancer radiotherapy, it creates a space that temporarily separates the anterior rectal wall from the prostate, thereby reducing radiation exposure. PEG powder was mixed with the diluent (Trilysine buffer) to form the precursor solution [337]. In a study, a pooled analysis of patients' quality of life (QOL) after prostate RT with up to 5 years of follow-up showed that the use of a rectal spacer preserved bowel function. With long-term follow-up, this QOL benefit was preserved (NCT01538628) [338]. Table 2 presents the completed and ongoing clinical trials involving hydrogel-based formulations related to cancer.

6. Challenges of using hydrogels for cancer therapy

Although hydrogel-based products have advanced significantly in research laboratories, they are still not readily available in clinical settings due to some limitations. To date, 16 oral drug delivery products are available, 17 vaginal drug delivery products, 16 buccal drug delivery products, and 7 transdermal drug delivery products [339]. Consequently, it is essential to carry out a thorough and detailed examination of the factors that hinder the advancement of hydrogel-based products.

6.1. Mechanical stability

Hydrogels are known to have a complex structure due to their hydrated nature, which makes the sterilization of hydrogels a significant challenge. A specific risk arises from storing some hydrogels in a hydrated state, which necessitates careful control over storage conditions. This includes reducing water evaporation and avoiding contact between the sample and any external media prior to the experiment. There may be challenges not present in dry biodegradable polymers, such as PLGA microspheres [19]. Moreover, dehydration must be performed after fabrication to prevent premature degradation during hydrogel storage and avoid the cleavage of drug-polymer linkages via hydrolysis. This treatment must not alter the structure of the hydrogel or its biological activity [19]. Hydrogel delivery systems frequently encounter substantial regulatory hurdles. Water content and network heterogeneity can also compromise the mechanical stability of hydrogels, limiting their practical application. To enhance the mechanical performance of hydrogels, double-network hydrogels have been developed, as well as chemically or ionically cross-linked hydrogels [340].

Gong et al. introduced “sacrificial weak bonds” to enhance the mechanical durability of double-network hydrogels. Polyelectrolyte networks are densely cross-linked, and polyacrylamide networks are loosely cross-linked in this approach. During sacrificial breakdown, the former absorbs energy and prevents crack propagation, thereby significantly enhancing the toughness of the hydrogel [341].

6.2. Loading and release of drugs

A primary limitation of hydrogel formulations is their gradual release of hydrophilic compounds, often over several hours or days. The mesh size of the hydrogel plays a crucial role in determining release kinetics. This mesh size is defined by the spacing between adjacent cross-links and the maximum size of proteins that can diffuse through the gel, which is influenced by the polymer concentration [342]. Confocal laser scanning microscopy can be employed to assess mesh size directly, whereas the diffusion of molecules is an indirect method for determining it. However, both of these techniques provide only approximate measurements of mesh sizes, thereby imposing certain limitations [343].

The release of drugs is primarily determined by diffusion and relies on several factors, including i) protein size, ii) hydrophilicity of the protein when mesh sizes are larger than the hydrodynamic radius of the protein, and iii) charge interactions between the matrix and the protein. Gel release rates are determined either by bulk degradation or surface degradation processes when mesh sizes are smaller than the hydrodynamic radius of proteins. The swelling and shrinking of hydrogels can also alter mesh size, resulting in a change in the release mechanism [343]. Drug loading capacities in hydrogel formulations for biologicals are typically limited to single-digit weight percentages, whereas high plasma concentrations are required to achieve therapeutic effects. The hydrogel formulation is beneficial for immunoglobulins with high potency, such as antibodies with dual affinity for retargeting [343].

6.3. Biocompatibility

In the polymerization of synthetic hydrogels and crosslinking of natural polymeric hydrogel precursors, toxic moieties and chemicals pose a significant challenge to their biocompatibility. Hydrogel preparation may also contain harmful ingredients such as stabilizers, unreacted monomers, initiators, emulsifiers, and organic solvents [344]. Therefore, the developed hydrogels should be purified before removing any unreacted hazardous chemicals. Dialysis or extensive solvent washing can be used to perform this purification [345].

6.4. Injectability

Improved ease of clinical usage is one of the most significant challenges. Designing physical gelators at precisely controlled temperatures and polymer concentrations would reduce the risk of premature gelation inside the needle. By developing strategies to release cross-linkers in a triggered manner inside the body, syringe clogging could be minimized for covalently cross-linked hydrogels. Another issue is related to localizing cross-linkers more effectively to avoid *in vivo* toxicity. To prevent the use of double-barreled syringes, it is suggested to mix the chemically reactive gel precursors in a single syringe [346]. It is possible to utilize injectable hydrogels for both drug delivery and tissue engineering applications by employing new physicochemical strategies or combining existing crosslinking techniques while simultaneously controlling the gelation process and the interactions between the gel and native tissues [346].

Different gelators can be used at varying concentrations or for varying periods to achieve mechanical strength in injectable hydrogels. Hydrogel-entrapped agent interactions can be controlled to improve drug release. The tensile strength of a drug-loaded hydrogel depends on the particular site and application, such as cartilage tissue, for which it is being used. Hydrophobic binding sites can be integrated into polymer networks using straightforward techniques such as solid molecular dispersion. This approach enhances drug loading capacity and inhibits the recrystallization of drugs in aqueous environments [347]. By incorporating vesicular carriers, such as nanoparticles, into the hydrogel matrix, it is possible to extend and control the release of drugs while minimizing the burst release commonly associated with particle-based delivery systems [348]. In hydrogel structures, drugs, proteins, and cells have been entrapped by polymerization reactions. Drugs may lose their functionality if dissolved in a polymerization mixture. In order to overcome these disadvantages, polymeric hydrogels encapsulating colloidal drug particles have been developed [349].

6.5. Regulatory issues

Hydrogels designed for the release of drugs or the encapsulation of drug-secreting cells are classified as combination products. This results in a regulatory approval process that extends over seven to ten years—substantially longer than the one- to five-year timeframe typically required for biomaterials and scaffolds without active agents. This prolonged approval period may negatively impact commercial viability as it reduces the effective duration of patent protection [350]. Overall, this long path is expected to incur substantial expenses, with costs ranging from $50 million to $800 million, thereby presenting considerable obstacles to commercialization [351].

7. Application of AI to hydrogel systems

Artificial intelligence (AI) can be applied to various aspects of hydrogels, such as material design and preparation process optimization, material characterization analysis, high-throughput screening, and performance monitoring. The use of these applications facilitates the advancement of hydrogel technology by improving the function and application effectiveness of hydrogels [352]. Computational simulations and modeling techniques started being applied to hydrogel research in the 1990s and early 2000s, respectively. Computational methods helped researchers predict swelling properties, mechanical responses, and drug

release kinetics of hydrogels under various conditions. In theory, hydrogels can be modelled using continuum mechanical concepts such as balancing laws, kinematics, and constitutive equations [353].

The synthesis of hydrogels to deliver drugs to specific targets in cancer treatment can be enhanced with the help of AI. Machine learning can be applied to better design natural and synthetic hydrogels by optimizing their physicochemical characteristics (e.g., porosity, swelling, and stimuli-responsiveness) to improve drug entrapment and sustained release. Through using AI-based predictive models, large data sets of polymer compositions and drug release profiles were studied, enabling the determination of novel hydrogel formulations that feature improved biocompatibility and tumor-specific targeting. Not only this method was faster than the experimental development process, but it was also more precise for hydrogel-based delivery systems, which showed remarkable potential as a method of personalized cancer treatments.

There are numerous potential benefits associated with applying AI to hydrogel design and preparation, including the following:

i) To achieve optimal hydrogel preparation outcomes, models can automatically adjust parameters during hydrogel preparation [354,355]. In a recent study, acrylamide-2-hydroxyethyl methacrylate and acrylamide-N-isopropylacrylamide hydrogels were optimized based on AI. A hydrogel made of these materials has great potential to be used for superabsorbents that have high swelling rates [356].
ii) AI could significantly impact hydrogel applications. Through AI's image processing and recognition capabilities, a patient's wound or lesion can be analyzed and diagnosed automatically, guiding the selection of suitable hydrogel materials.
iii) Hydrogel performance and application environment can be monitored using AI. It is possible to monitor parameters such as temperature, humidity, and pH value in real-time using sensor networks and data acquisition systems [357–360].
iv) Ionic thermo-sensitive hydrogels have been modeled using multiphysics, accounting for multiphase effects and thermal stimulus effects, and validated experimentally. The effect of temperature on the behavior of hydrogels can be investigated through multiphysics models, as can the impact of hydration and mechanical properties [361].
v) In order to advance the design of ideal drug release materials and to simulate their release behavior, AI has been applied [362,363]. To optimize its physical properties, response surface methodology (RSM) was used to synthesize a gel based on guar gum. This study assessed the concentration of the initiator, monomer, and cross-linker, as well as pH, reaction temperature, and reaction time. According to molecular dynamics simulations, the optimal swelling rate for effective drug release is 4903.87 % [364]. A hyaluronic acid-based hydrogel was also optimized using principal component analysis (PCA). To capture the complete release profile, this model considered multiple drug transport pathways through the gel. In order to further refine the hydrogel composition, data envelopment analysis was combined with PCA [365].
vi) Through the analysis of patient data and optimization of drug delivery parameters, AI plays a critical role in personalizing treatment schedules in hydrogel systems. By using AI algorithms, drug dosage, release rates, and targeting strategies can be predicted based on individual patient characteristics, resulting in more effective and personalized hydrogel therapies [366,367]. By optimizing algorithms, AI can enhance the performance and efficacy of drug sustained-release systems. AI algorithms can determine the optimal drug loading, hydrogel composition ratio, and preparation conditions in order to enhance therapeutic outcomes by extending or precisely controlling release rates [352].

8. Conclusions

The drug delivery systems that incorporate hydrogel are relatively new in the field of oncology and have provided a clear understanding of the improved therapeutic profile and reduced adverse effects associated with the disease in best practices. These sophisticated systems, which can respond to signals such as pH, temperature, and redox potential, have demonstrated the ability to enhance the concentrations of chemotherapeutic agents at the target site. However, many challenges still hinder these approaches from quickly translating into clinical work.

The first limitation concerns the mechanical strength of hydrogels, a primary issue in the development of hydrogels. Such factors include problems such as loss of drugs during hydration or storage due to the hygroscopic nature of these materials, which affects sterilization. Moreover, for example, the formation of double-network hydrogels is beneficial in enhancing the material's mechanical stability. However, at the same time, the material must be sufficiently compliant to work appropriately *in vivo*. This improves their mechanical strength and stability in the drug delivery profiles, addressing the challenges associated with the mechanical strength of hydrogel matrices. Further complications arise from the loading and release of drugs. The nature of hydrogels themselves may also limit the loading capacity of specific chemotherapeutic agents or drugs, such as those with high molecular weights and a tendency to form aggregates. The release rate is regulated by hydrophilicity and the size of the drugs; improving the properties of hydrogels is still ongoing, but the burst release effect remains a challenge in designing hydrogel-based sustained release systems. It is essential to conduct further studies and enhance the architecture of hydrogels so that the mesh size and chemical properties can be controlled to respond to different therapeutic agents.

Future developments may include shielded syringes for the hydrogel precursor ingredients or a two-compartment system to administer the agents. The processes of obtaining clearance for hydrogel drug formulations are time-consuming and often slow down the development of such products, as well as the research itself. These polymers are among the drug-device combination products, where both the drug and device require approval; therefore, the lengthy timelines problem must be solved. These new strategies that incorporate regulatory authorities in the pre-clinical stage may influence the optimal clinical use of such promising therapeutic platforms. In the future, interdisciplinary research and development may lead to the creation of a new and efficient hydrogel-based drug delivery system for cancer therapy.

Looking at the future, multi-stimuli-responsive hydrogels may be used to develop drug delivery systems that are both more precise and more effective. These smart hydrogels respond to a mixture of internal (e.g. pH, redox potential, enzymes) and external (e.g. temperature, light, magnetic field) stimuli with the potential to highly control and target specific release of therapeutic agents. Nonetheless, the more complex these systems, the more difficult it becomes to generate the fine-tuned and predictable behavior. Multi-stimuli integration may cause nonlinear and even unpredictable interactions that make it difficult to optimize release kinetics and therapeutic effects. As a result, the next steps include to establish reliable predictive models, optimize the design of smart materials with enhanced responsiveness, and offer reproducibility and scalability to aid clinical translation. With such obstacles overcome, multi-stimuli-responsive hydrogels would have a revolutionary impact in future cancer treatment. Finding effective optimization methods and predictive models to enhance hydrogel performance and preparation efficiency remains a major challenge. Combining advanced experimental techniques and computational simulation methods with materials science and chemical engineering is necessary to address these problems. By leveraging insights gleaned from collected data, AI can mitigate this challenge, enabling more focused and predictive experiments.

With advancements in materials, polymers, and clinical oncology, new hydrogel formulations can enhance drug delivery, minimize side

effects, and improve the efficacy of existing treatment methods. As more is learned about tumor microenvironments and *in vivo* imaging, the delivery of drugs to tumors could be more tightly regulated, and patient selection in clinical settings could be improved. Thus, hydrogel-based systems have great potential for enhancing cancer treatment; however, efforts should be made to overcome the current problems. The future evolution of sophisticated targeted drug delivery systems will involve utilizing new polymer materials, drug formulation approaches, legislation, and nanotechnology to bring these technologies from the research laboratory to clinical practice, dramatically changing the management of cancer patients.

CRediT authorship contribution statement

Fatemeh Davodabadi: Writing – review & editing, Writing – original draft, Methodology, Investigation, Conceptualization. **Francesco Baino:** Writing – review & editing, Supervision, Methodology, Investigation. **Saman Sargazi:** Writing – review & editing, Writing – original draft, Supervision, Methodology, Investigation, Conceptualization.

Declaration of Competing Interest

The authors declare that they have no known competing financial interests or personal relationships that could have appeared to influence the work reported in this paper.

Acknowledgments

This work received no funding.

Data Availability

No data was used for the research described in the article.

References

[1] F. Bray, et al., Global cancer statistics 2022: GLOBOCAN estimates of incidence and mortality worldwide for 36 cancers in 185 countries, CA a cancer journal clinicians 74 (3) (2024) 229–263.
[2] W. Cao, et al., Comparative study of cancer profiles between 2020 and 2022 using global cancer statistics (GLOBOCAN), J. Natl. Cancer Cent. 4 (2) (2024) 128–134.
[3] K. Desai, et al., Cancer statistics: the United States vs. Worldwide, American Society of Clinical Oncology, 2024.
[4] S. Chakraborty, T. Rahman, The difficulties in cancer treatment, ecancermedicalscience 6 (2012) ed16.
[5] A. Pourgholi, et al., Anticancer potential of silibinin loaded polymeric nanoparticles against breast cancer cells: insight into the apoptotic genes targets, Asian Pacific Journal Cancer Prevention APJCP 22 (8) (2021) 2587.
[6] X.H. Makhoba, et al., Potential impact of the multi-target drug approach in the treatment of some complex diseases, Drug Des. Dev. Ther. (2020) 3235–3249.
[7] G. Housman, et al., Drug resistance in cancer: an overview, Cancers 6 (3) (2014) 1769–1792.
[8] F. Davodabadi, et al., Cancer chemotherapy resistance: mechanisms and recent breakthrough in targeted drug delivery, Eur. J. Pharmacol. 958 (2023) 176013.
[9] A. Wicki, et al., Nanomedicine in cancer therapy: challenges, opportunities, and clinical applications, J. Control. Release 200 (2015) 138–157.
[10] F. Davodabadi, et al., Nanomaterials-Based targeting of long Non-Coding RNAs in cancer: a Cutting-Edge review of current trends, ChemMedChem 19 (8) (2024) e202300528.
[11] T. Sun, et al., Y. Xia engineered nanoparticles for drug delivery in cancer therapy angew, Chem. Int Ed. 53 (2014) 12320–12364.
[12] M.R. Hajinezhad, et al., Development of a new vesicular formulation for delivery of ifosfamide: evidence from in vitro, in vivo, and in silico experiments, Arab. J. Chem. 16 (9) (2023) 105086.
[13] M. Barani, et al., Preparation, characterization, cytotoxicity and pharmacokinetics of niosomes containing gemcitabine: in vitro, in vivo, and simulation studies, J. Drug Deliv. Sci. Technol. 84 (2023) 104505.
[14] F. Davodabadi, et al., Breast cancer vaccines: new insights into immunomodulatory and nano-therapeutic approaches, J. Control. Release 349 (2022) 844–875.
[15] F. Davodabadi, et al., Aptamer-functionalized quantum dots as theranostic nanotools against cancer and bacterial infections: a comprehensive overview of recent trends, Biotechnol. Prog. 39 (5) (2023) e3366.
[16] F. Davodabadi, et al., Unveiling the future of cancer treatment: a Cutting-Edge review on the role of nanotherapeutics in targeting long Non-Coding RNAs, ChemMedChem (2024) e202300528. -e202300528.
[17] A. Shamsabadipour, et al., Applying thermodynamics as an applicable approach to cancer diagnosis, evaluation, and therapy: a review, J. Drug Deliv. Sci. Technol. 86 (2023) 104681.
[18] M. Sepantafar, et al., Engineered hydrogels in cancer therapy and diagnosis, Trends Biotechnol. 35 (11) (2017) 1074–1087.
[19] J. Li, D.J. Mooney, Designing hydrogels for controlled drug delivery, Nat. Rev. Mater. 1 (12) (2016) 1–17.
[20] J. Mayr, C. Saldías, D.D. Díaz, Release of small bioactive molecules from physical gels, Chem. Soc. Rev. 47 (4) (2018) 1484–1515.
[21] J. Conde, et al., Local triple-combination therapy results in tumour regression and prevents recurrence in a colon cancer model, Nat. Mater. 15 (10) (2016) 1128–1138.
[22] W. Shen, et al., Sustained codelivery of cisplatin and paclitaxel via an injectable prodrug hydrogel for ovarian cancer treatment, ACS Appl. Mater. Interfaces 9 (46) (2017) 40031–40046.
[23] H. Awada, et al., A single injection of protein-loaded coacervate-gel significantly improves cardiac function post infarction, Biomaterials 125 (2017) 65–80.
[24] H. Ceylan, et al., 3D-printed biodegradable microswimmer for theranostic cargo delivery and release, ACS nano 13 (3) (2019) 3353–3362.
[25] J. Mu, et al., Development of endogenous enzyme-responsive nanomaterials for theranostics, Chem. Soc. Rev. 47 (15) (2018) 5554–5573.
[26] S.S. Said, S. Campbell, T. Hoare, Externally addressable smart drug delivery vehicles: current technologies and future directions, Chem. Mater. 31 (14) (2019) 4971–4989.
[27] T.T. Emi, et al., Pulsatile chemotherapeutic delivery profiles using magnetically responsive hydrogels, ACS Biomater. Sci. Eng. 4 (7) (2018) 2412–2423.
[28] F. Mushtaq, et al., Preparation, properties, and applications of gelatin-based hydrogels (GHs) in the environmental, technological, and biomedical sectors, Int. J. Biol. Macromol. 218 (2022) 601–633.
[29] D. Asai, et al., In situ depot formation of anti-HIV fusion-inhibitor peptide in recombinant protein polymer hydrogel, Acta Biomater. 64 (2017) 116–125.
[30] E.M. Nehls, A.M. Rosales, K.S. Anseth, Enhanced user-control of small molecule drug release from a poly (ethylene glycol) hydrogel via azobenzene/cyclodextrin complex tethers, J. Mater. Chem. B 4 (6) (2016) 1035–1039.
[31] M.A. Da Silva, C.A. Dreiss, Soft nanocomposites: nanoparticles to tune gel properties, Polym. Int. 65 (3) (2016) 268–279.
[32] R.A. Bini, et al., Soft nanocomposites of gelatin and poly (3-hydroxybutyrate) nanoparticles for dual drug release, Colloids Surf. B Biointerfaces 157 (2017) 191–198.
[33] L.E. Kass, J. Nguyen, Nanocarrier-hydrogel composite delivery systems for precision drug release, Wiley Interdiscip. Rev. Nanomed. Nanobiotechnology 14 (2) (2022) e1756.
[34] Y. Jiang, et al., Natural polymer-based stimuli-responsive hydrogels, Curr. Med. Chem. 27 (16) (2020) 2631–2657.
[35] K. Kim, Hybrid systems of gels and nanoparticles for cancer therapy: advances in multifunctional therapeutic platforms, Gels 11 (3) (2025) 170.
[36] A. Thumma, Introduction, classification and applications of 3D bioprinted hydrogels for cancer treatment: a review, RSC Pharm. (2025).
[37] M.M. Rana, H. De la Hoz Siegler, Evolution of hybrid hydrogels: Next-generation biomaterials for drug delivery and tissue engineering, Gels 10 (4) (2024) 216.
[38] W. Choi, D.S. Kohane, Hybrid nanoparticle–hydrogel systems for drug delivery depots and other biomedical applications, ACS nano 18 (34) (2024) 22780–22792.
[39] H. Choi, W.-S. Choi, J.-O. Jeong, A review of advanced hydrogel applications for tissue engineering and drug delivery systems as biomaterials, Gels 10 (11) (2024) 693.
[40] V. Mohammadzadeh, et al., Hydrogels as advanced drug delivery platforms for cancer immunotherapy: promising innovations and future outlook, J. Nanobiotechnol. 23 (1) (2025) 545.
[41] J. Chen, et al., Advances in hydrogel-based materials for breast cancer bone metastasis: from targeted drug delivery to bone microenvironment remodeling, Front. Pharmacol. 16 (2025) 1627883.
[42] H. Chang, et al., Advances in hybrid hydrogel design for biomedical applications: innovations in drug delivery and tissue engineering for gynecological cancers, Cell Biol. Toxicol. 41 (1) (2025) 1–31.
[43] J. George, et al., Neural tissue engineering with structured hydrogels in CNS models and therapies, Biotechnol. Adv. 42 (2020) 107370.
[44] K. Deligkaris, et al., Hydrogel-based devices for biomedical applications, Sens. Actuators B Chem. 147 (2) (2010) 765–774.
[45] M.H. Park, et al., Biodegradable thermogels, Acc. Chem. Res. 45 (3) (2012) 424–433.
[46] Y. Qiu, K. Park, Environment-sensitive hydrogels for drug delivery, Adv. Drug Deliv. Rev. 53 (3) (2001) 321–339.
[47] W. Xue, I.W. Hamley, M.B. Huglin, Rapid swelling and deswelling of thermoreversible hydrophobically modified poly (N-isopropylacrylamide) hydrogels prepared by freezing polymerisation, Polymer 43 (19) (2002) 5181–5186.
[48] L. Klouda, Thermoresponsive hydrogels in biomedical applications: a seven-year update, Eur. J. Pharm. Biopharm. 97 (2015) 338–349.
[49] R. Fan, et al., Thermosensitive hydrogels and advances in their application in disease therapy, Polymers 14 (12) (2022) 2379.
[50] T. Thambi, Y. Li, D.S. Lee, Injectable hydrogels for sustained release of therapeutic agents, J. Control. Release 267 (2017) 57–66.

[51] L.D. Taylor, L.D. Cerankowski, Preparation of films exhibiting a balanced temperature dependence to permeation by aqueous solutions—a study of lower consolute behavior, Journal Polymer Science Polymer Chemistry Edition 13 (11) (1975) 2551–2570.
[52] K. Zhang, K. Xue, X.J. Loh, Thermo-Responsive hydrogels: from recent progress to biomedical applications, Gels 7 (3) (2021) 77.
[53] A. Richter, et al., Review on hydrogel-based ph sensors and microsensors, Sensors 8 (1) (2008) 561–581.
[54] N.A. Peppas, et al., Hydrogels in biology and Medicine: from molecular principles to bionanotechnology, Adv. Mater. 18 (11) (2006) 1345–1360.
[55] Y. Zhao, et al., Smart hydrogel-based optical fiber SPR sensor for ph measurements, Sens. Actuators B Chem. 261 (2018) 226–232.
[56] Yetisen, A.K., et al., *Light-directed writing of chemically tunable narrow-band holographic sensors*. 2014.
[57] M. Rizwan, et al., Ph sensitive hydrogels in drug delivery: brief history, properties, swelling, and release mechanism, material selection and applications, Polymers 9 (4) (2017) 137.
[58] W. Cheng, Y. Liu, Redox-responsive hydrogels. Biopolymer-based composites, Elsevier, 2017, pp. 31–60.
[59] C. Dollendorf, M. Hetzer, H. Ritter, Polymeric redox-responsive delivery systems bearing ammonium salts cross-linked via disulfides, Beilstein J. Org. Chem. 9 (1) (2013) 1652–1662.
[60] E. Verheyen, et al., Protein macromonomers containing reduction-sensitive linkers for covalent immobilization and glutathione triggered release from dextran hydrogels, J. Control. Release 156 (3) (2011) 329–336.
[61] G. Deng, et al., Dynamic hydrogels with an environmental adaptive self-healing ability and dual responsive sol–gel transitions, ACS Macro Lett. 1 (2) (2012) 275–279.
[62] A.D. Baldwin, K.L. Kiick, Reversible maleimide–thiol adducts yield glutathione-sensitive poly (ethylene glycol)–heparin hydrogels, Polym. Chem. 4 (1) (2013) 133–143.
[63] P.M. Kharkar, A.M. Kloxin, K.L. Kiick, Dually degradable click hydrogels for controlled degradation and protein release, J. Mater. Chem. B 2 (34) (2014) 5511–5521.
[64] P.M. Kharkar, K.L. Kiick, A.M. Kloxin, Design of thiol-and light-sensitive degradable hydrogels using Michael-type addition reactions, Polym. Chem. 6 (31) (2015) 5565–5574.
[65] P.M. Kharkar, et al., Controlling the release of small, bioactive proteins via dual mechanisms with therapeutic potential, Adv. Healthc. Mater. 6 (24) (2017) 1700713.
[66] A. Petrelli, et al., Redox tunable delivery systems: sweet block copolymer micelles via thiol–(bromo) maleimide conjugation, Chem. Commun. 52 (82) (2016) 12202–12205.
[67] Y. Liang, K.L. Kiick, Liposome-cross-linked hybrid hydrogels for glutathione-triggered delivery of multiple cargo molecules, Biomacromolecules 17 (2) (2016) 601–614.
[68] L. Jiang, L. Wen, Photonic sensitive switchable materials. Biophotonics for medical applications, Elsevier, 2015, pp. 25–51.
[69] M. Bustamante-Torres, et al., Hydrogels classification according to the physical or chemical interactions and as stimuli-sensitive materials, Gels 7 (4) (2021) 182.
[70] F. Rizzo, N.S. Kehr, Recent advances in injectable hydrogels for controlled and local drug delivery, Adv. Healthc. Mater. 10 (1) (2021) 2001341.
[71] Y. Xing, B. Zeng, W. Yang, Light responsive hydrogels for controlled drug delivery, Front Bioeng. Biotechnol. 10 (2022) 1075670.
[72] I. Tomatsu, K. Peng, A. Kros, Photoresponsive hydrogels for biomedical applications, Adv. Drug Deliv. Rev. 63 (14-15) (2011) 1257–1266.
[73] K. Iwaso, Y. Takashima, A. Harada, Fast response dry-type artificial molecular muscles with [c2] daisy chains, Nat. Chem. 8 (6) (2016) 625–632.
[74] D. Miranda, J.F. Lovell, Mechanisms of light-induced liposome permeabilization, Bioeng. Transl. Med. 1 (3) (2016) 267–276.
[75] J. Liese, N.A. Hampp, Synthesis and photocleavage of a new polymerizable [2+2] hetero dimer for phototriggered drug delivery, J. Photochem. Photobiol. A Chem. 219 (2-3) (2011) 228–234.
[76] J.A. Shadish, C.A. DeForest, Site-selective protein modification: from functionalized proteins to functional biomaterials, Matter 2 (1) (2020) 50–77.
[77] C. Wang, et al., S, S-Tetrazine-Based hydrogels with visible light cleavable properties for on-demand anticancer drug delivery, Research (2020).
[78] M. Qiu, et al., Novel concept of the smart NIR-light–controlled drug release of black phosphorus nanostructure for cancer therapy, Proc. Natl. Acad. Sci. 115 (3) (2018) 501–506.
[79] A. Bordbar-Khiabani, M. Gasik, Smart hydrogels for advanced drug delivery systems, Int. J. Mol. Sci. 23 (7) (2022) 3665.
[80] A. Roy, K. Manna, S. Pal, Recent advances in various stimuli-responsive hydrogels: from synthetic designs to emerging healthcare applications, Mater. Chem. Front. 6 (17) (2022) 2338–2385.
[81] I. Carayon, et al., Electro-responsive hydrogels: macromolecular and supramolecular approaches in the biomedical field, Biomater. Sci. 8 (20) (2020) 5589–5600.
[82] C. Whiting, et al., Shear modulus of polyelectrolyte gels under electric field, J. Phys. Condens. Matter 13 (7) (2001) 1381.
[83] S. Ramanathan, L.H. Block, The use of chitosan gels as matrices for electrically-modulated drug delivery, J. Control. Release 70 (1-2) (2001) 109–123.
[84] S. Murdan, Electro-responsive drug delivery from hydrogels, J. Control. Release 92 (1) (2003) 1–17.
[85] Z. Li, et al., Magnetic-responsive hydrogels: from strategic design to biomedical applications, J. Control. Release 335 (2021) 541–556.
[86] E.C. Frachini, D.F. Petri, Magneto-responsive hydrogels: preparation, characterization, biotechnological and environmental applications, J. Braz. Chem. Soc. 30 (2019) 2010–2028.
[87] J. Zhang, Q. Huang, J. Du, Recent advances in magnetic hydrogels, Polym. Int. 65 (12) (2016) 1365–1372.
[88] J. Lei, Z. Zhou, Z. Liu, Side chains and the insufficient lubrication of water in polyacrylamide hydrogel—a new insight, Polymers 11 (11) (2019) 1845.
[89] E. Tanasa, et al., Novel nanocomposites based on functionalized magnetic nanoparticles and polyacrylamide: preparation and complex characterization, Nanomaterials 9 (10) (2019) 1384.
[90] L. Selzer, S. Odenbach, Effects of carbonyl iron particles on the rheological behavior of nanocomposite hydrogels, J. Magn. Magn. Mater. 501 (2020) 166394.
[91] M.L. Oyen, Mechanical characterisation of hydrogel materials, Int. Mater. Rev. 59 (1) (2014) 44–59.
[92] H. Kasgoz, et al., Structurally enhanced hydrogel nanocomposites with improved swelling and mechanical properties, J. Macromol. Sci. Part A 49 (1) (2012) 92–99.
[93] J. Jang, et al., Improving mechanical properties of alginate hydrogel by reinforcement with ethanol treated polycaprolactone nanofibers, Composites Part B Engineering 45 (1) (2013) 1216–1221.
[94] F. Crippa, et al., Dynamic and biocompatible thermo-responsive magnetic hydrogels that respond to an alternating magnetic field, J. Magn. Magn. Mater. 427 (2017) 212–219.
[95] C. Gila-Vilchez, et al., Anisotropic magnetic hydrogels: design, structure and mechanical properties, Philos. Trans. R. Soc. A 377 (2143) (2019) 20180217.
[96] H. Meharthaj, S.M. Sivakumar, A. Arockiarajan, Significance of particle size on the improved performance of magnetorheological gels, J. Magn. Magn. Mater. 490 (2019) 165483.
[97] X. Hu, et al., Adhesive tough magnetic hydrogels with high Fe3O4 content, ACS Appl. Mater. Interfaces 11 (10) (2019) 10292–10300.
[98] I.S. Protsak, Y.M. Morozov, Fundamentals and advances in Stimuli-Responsive hydrogels and their applications: a review, Gels 11 (1) (2025) 30.
[99] S. Ganguly, S. Margel, Design of magnetic hydrogels for hyperthermia and drug delivery, Polymers 13 (23) (2021) 4259.
[100] S. Ganguly, S. Margel, 3D printed magnetic polymer composite hydrogels for hyperthermia and magnetic field driven structural manipulation, Prog. Polym. Sci. 131 (2022) 101574.
[101] L. Vítková, et al., Magneto-responsive hyaluronan hydrogel for hyperthermia and bioprinting: magnetic, rheological properties and biocompatibility, APL Bioeng. 7 (3) (2023).
[102] D. Zhang, et al., Super hydrophilic semi-IPN fluorescent poly (N-(2-hydroxyethyl) acrylamide) hydrogel for ultrafast, selective, and long-term effective Mercury (II) detection in a bacteria-laden system, ACS Appl. Bio Mater. 2 (2) (2019) 906–915.
[103] H. Yang, et al., Engineering target-responsive hydrogels based on aptamer–target interactions, J. Am. Chem. Soc. 130 (20) (2008) 6320–6321.
[104] Y. Ma, et al., Target-responsive DNA hydrogel for non-enzymatic and visual detection of glucose, Analyst 143 (7) (2018) 1679–1684.
[105] Y. Dong, et al., Injectable and glucose-responsive hydrogels based on boronic acid–glucose complexation, Langmuir 32 (34) (2016) 8743–8747.
[106] X. Li, et al., Glucose-Responsive hydrogel optimizing fenton reaction to eradicate multidrug-resistant bacteria for infected diabetic wound healing, Chem. Eng. J. 487 (2024) 150545.
[107] T. Mateti, et al., A critical analysis of the recent developments in multi-stimuli responsive smart hydrogels for cancer treatment, Curr. Opin. Biomed. Eng. 25 (2023) 100424.
[108] X. Zhou, et al., A ph and magnetic dual-response hydrogel for synergistic chemo-magnetic hyperthermia tumor therapy, RSC Adv. 8 (18) (2018) 9812–9821.
[109] W. Du, et al., Injectable nanocomposite hydrogels for cancer therapy, Macromol. Biosci. 21 (11) (2021) 2100186.
[110] S. Deepthi, et al., Layered chitosan-collagen hydrogel/aligned PLLA nanofiber construct for flexor tendon regeneration, Carbohydr. Polym. 153 (2016) 492–500.
[111] S. Kupper, I. Kłosowska-Chomiczewska, P. Szumała, Collagen and hyaluronic acid hydrogel in water-in-oil microemulsion delivery systems, Carbohydr. Polym. 175 (2017) 347–354.
[112] F.I. Pareti, et al., Isolation and characterization of a collagen binding domain in human von willebrand factor, J. Biol. Chem. 261 (32) (1986) 15310–15315.
[113] J.-G. Hu, et al., Collagen hydrogel functionalized with collagen-targeting IFNA2b shows apoptotic activity in nude mice with xenografted tumors, ACS Biomater. Sci. Eng. 5 (1) (2018) 272–282.
[114] G. Mattheolabakis, et al., Hyaluronic acid targeting of CD44 for cancer therapy: from receptor biology to nanomedicine, J. Drug Target. 23 (7-8) (2015) 605–618.
[115] L. Lapcık Jr, et al., Hyaluronan: preparation, structure, properties, and applications, Chem. Rev. 98 (8) (1998) 2663–2684.
[116] J.H. Kim, et al., Hyaluronic Acid-Based nanomaterials for cancer therapy, Polymers 10 (10) (2018) 1133.
[117] A.S. Klar, et al., Tissue-engineered dermo-epidermal skin grafts prevascularized with adipose-derived cells, Biomaterials 35 (19) (2014) 5065–5078.
[118] O.M. Benavides, et al., Capillary-like network formation by human amniotic fluid-derived stem cells within fibrin/poly (ethylene glycol) hydrogels, Tissue Eng. Part A 21 (7-8) (2015) 1185–1194.
[119] O. Madkhali, G. Mekhail, S.D. Wettig, Modified gelatin nanoparticles for gene delivery, Int. J. Pharm. 554 (2019) 224–234.
[120] K. Yue, et al., Synthesis, properties, and biomedical applications of gelatin methacryloyl (GelMA) hydrogels, Biomaterials 73 (2015) 254–271.

[121] M. Foox, M. Zilberman, Drug delivery from gelatin-based systems, Expert Opin. Drug Deliv. 12 (9) (2015) 1547–1563.
[122] H. Samadian, et al., In vitro and in vivo evaluation of electrospun cellulose acetate/gelatin/hydroxyapatite nanocomposite mats for wound dressing applications, Artif. Cells Nanomed. Biotechnol. 46 (sup1) (2018) 964–974.
[123] M. Abbasian, et al., Scaffolding polymeric biomaterials: are naturally occurring biological macromolecules more appropriate for tissue engineering? Int. J. Biol. Macromol. 134 (2019) 673–694.
[124] S. Sargazi, et al., Chitosan nanocarriers for microRNA delivery and detection: a preliminary review with emphasis on cancer, Carbohydr. Polym. 290 (2022) 119489.
[125] G. Sandri, et al., Halloysite and chitosan oligosaccharide nanocomposite for wound healing, Acta Biomater. 57 (2017) 216–224.
[126] A. Montembault, C. Viton, A. Domard, Rheometric study of the gelation of chitosan in aqueous solution without cross-linking agent, Biomacromolecules 6 (2) (2005) 653–662.
[127] X. Zhang, Y. Lin, R.J. Gillies, Tumor ph and its measurement, J. Nucl. Med. 51 (8) (2010) 1167–1170.
[128] A. Punnia-Moorthy, Evaluation of ph changes in inflammation of the subcutaneous air pouch lining in the rat, induced by carrageenan, dextran and staphylococcus aureus, J. Oral. Pathol. Med. 16 (1) (1987) 36–44.
[129] R.O. Beauchamp, et al., A critical review of the toxicology of glutaraldehyde, Crit. Rev. Toxicol. 22 (3-4) (1992) 143–174.
[130] D.E. Anderson, B. Johnstone, Dynamic mechanical compression of chondrocytes for tissue engineering: a critical review, Front. Bioeng. Biotechnol. 5 (2017) 76.
[131] G.R. López-Marcial, et al., Agarose-based hydrogels as suitable bioprinting materials for tissue engineering, ACS Biomater. Sci. Eng. 4 (10) (2018) 3610–3616.
[132] A. Quarta, et al., Investigation on the composition of Agarose–Collagen I blended hydrogels as matrices for the growth of spheroids from breast cancer cell lines, Pharmaceutics 13 (7) (2021) 963.
[133] M.C. Catoira, et al., Overview of natural hydrogels for regenerative Medicine applications, Journal Materials Science Materials Medicine 30 (10) (2019) 115.
[134] Y.V. Bobryshev, Calcification of elastic fibers in human atherosclerotic plaque, Atherosclerosis 180 (2) (2005) 293–303.
[135] Z. Khavandgar, et al., Elastin haploinsufficiency impedes the progression of arterial calcification in MGP-deficient mice, J. Bone Miner. Res. 29 (2) (2014) 327–337.
[136] A. Pai, et al., Elastin degradation and vascular smooth muscle cell phenotype change precede cell loss and arterial medial calcification in a uremic mouse model of chronic kidney disease, Am. J. Pathol. 178 (2) (2011) 764–773.
[137] K. Draget, O. Smidsrød, G. Skjåk-Bræk, Biopolymers online, Wiley-VCH Verlag GmbH & Co. KGaA, 2005.
[138] K.I. Draget, C. Taylor, Chemical, physical and biological properties of alginates and their biomedical implications, Food Hydrocoll. 25 (2) (2011) 251–256.
[139] F. Brandl, F. Sommer, A. Goepferich, Rational design of hydrogels for tissue engineering: impact of physical factors on cell behavior, Biomaterials 28 (2) (2007) 134–146.
[140] H. Motasadizadeh, et al., Dual drug delivery system of teicoplanin and phenamil based on pH-sensitive silk fibroin/sodium alginate hydrogel scaffold for treating chronic bone infection, Biomater. Adv. 139 (2022) 213032.
[141] H. Enawgaw, et al., Synthesis of a cellulose-co-amps hydrogel for personal hygiene applications using cellulose extracted from corncobs, Gels 7 (4) (2021) 236.
[142] M.S. Rahman, et al., Recent developments of carboxymethyl cellulose, Polymers 13 (8) (2021) 1345.
[143] Y. Li, et al., Redox-responsive carboxymethyl cellulose hydrogel for adsorption and controlled release of dye, Eur. Polym. J. 123 (2020) 109447.
[144] W. Chen, et al., High-strength, tough, and self-healing hydrogel based on carboxymethyl cellulose, Cellulose 27 (2020) 853–865.
[145] N. Dadoo, et al., Synthesis and spatiotemporal modification of biocompatible and Stimuli-Responsive carboxymethyl cellulose hydrogels using Thiol-Norbornene chemistry, Macromol. Biosci. 17 (9) (2017) 1700107.
[146] Y. Gupta, et al., A review of carboxymethyl cellulose composite-based hydrogels in drug delivery applications, Results Chem. (2024) 101695.
[147] F. Wang, et al., Redox-responsive blend hydrogel films based on carboxymethyl cellulose/chitosan microspheres as dual delivery carrier, Int. J. Biol. Macromol. 134 (2019) 413–421.
[148] Z. Wang, et al., Poly ethylene glycol (PEG)-Based hydrogels for drug delivery in cancer therapy: a comprehensive review, Adv. Healthc. Mater. 12 (18) (2023) 2300105.
[149] A.K. Iyer, et al., Exploiting the enhanced permeability and retention effect for tumor targeting, Drug Discov. Today 11 (17-18) (2006) 812–818.
[150] A. Basu, et al., Poly(lactic acid) based hydrogels, Adv. Drug Deliv. Rev. 107 (2016) 192–205.
[151] E. Bakaic, N.M. Smeets, T. Hoare, Injectable hydrogels based on poly (ethylene glycol) and derivatives as functional biomaterials, RSC Adv. 5 (45) (2015) 35469–35486.
[152] A.B. Kutikov, J. Song, Biodegradable PEG-based amphiphilic block copolymers for tissue engineering applications, ACS Biomater. Sci. Eng. 1 (7) (2015) 463–480.
[153] H.J. Moon, et al., Temperature-responsive compounds as in situ gelling biomedical materials, Chem. Soc. Rev. 41 (14) (2012) 4860–4883.
[154] B. Jeong, et al., Biodegradable block copolymers as injectable drug-delivery systems, Nature 388 (6645) (1997) 860–862.
[155] M. Rahmati, Effect of PEG concentration on drug release from PLA-PEG copolymers: a molecular dynamics simulation study, J. Mol. Liq. 409 (2024) 125458.
[156] L. Yu, et al., The thermogelling PLGA–PEG–PLGA block copolymer as a sustained release matrix of doxorubicin, Biomater. Sci. 1 (4) (2013) 411–420.
[157] N.L. Elstad, K.D. Fowers, OncoGel (ReGel/paclitaxel)—Clinical applications for a novel paclitaxel delivery system, Adv. Drug Deliv. Rev. 61 (10) (2009) 785–794.
[158] M. Qiao, et al., Injectable biodegradable temperature-responsive PLGA–PEG–PLGA copolymers: synthesis and effect of copolymer composition on the drug release from the copolymer-based hydrogels, Int. J. Pharm. 294 (1-2) (2005) 103–112.
[159] L. Yu, J. Ding, Injectable hydrogels as unique biomedical materials, Chem. Soc. Rev. 37 (8) (2008) 1473–1481.
[160] M. Karimi, et al., Temperature-responsive smart nanocarriers for delivery of therapeutic agents: applications and recent advances, ACS Appl. Mater. Interfaces 8 (33) (2016) 21107–21133.
[161] A.R. Kim, S.L. Lee, S.N. Park, Properties and in vitro drug release of pH-and temperature-sensitive double cross-linked interpenetrating polymer network hydrogels based on hyaluronic acid/poly (N-isopropylacrylamide) for transdermal delivery of luteolin, Int. J. Biol. Macromol. 118 (2018) 731–740.
[162] D. Zhao, et al., The preparation of Green fluorescence-emissioned carbon dots/poly (N-isopropylacrylamide) temperature-sensitive hydrogels and research on their properties, Polymers 11 (7) (2019) 1171.
[163] M. Oak, R. Mandke, J. Singh, Smart polymers for peptide and protein parenteral sustained delivery, Drug Discov. Today. Technol. 9 (2) (2012) e131–e140.
[164] Y. Zhao, et al., pH-and temperature-sensitive hydrogel nanoparticles with dual photoluminescence for bioprobes, ACS nano 10 (6) (2016) 5856–5863.
[165] S. Ziane, et al., A thermosensitive low molecular weight hydrogel as scaffold for tissue engineering, Eur. Cells Mater. 23 (2012) 147–160.
[166] K. Thirupathi, et al., Ph and thermoresponsive PNIPAm-co-Polyacrylamide hydrogel for dual Stimuli-Responsive controlled drug delivery, Polymers 15 (1) (2023) 167.
[167] S. Graham, P.F. Marina, A. Blencowe, Thermoresponsive polysaccharides and their thermoreversible physical hydrogel networks, Carbohydr. Polym. 207 (2019) 143–159.
[168] J.Y. Chang, et al., Biopolymers· PVA hydrogels anionic polymerisation Nanocomposites, 153, Springer Science & Business Media, 2000.
[169] V.I. Lozinsky, et al., Polymeric cryogels as promising materials of biotechnological interest, TRENDS Biotechnol. 21 (10) (2003) 445–451.
[170] M.H. Alves, et al., Poly (vinyl alcohol) physical hydrogels: new vista on a long serving biomaterial, Macromol. Biosci. 11 (10) (2011) 1293–1313.
[171] F.A. Andersen, Amended final report on the safety assessment of polyacrylamide and acrylamide residues in cosmetics, Int. J. Toxicol. 24 (2005) 21–50.
[172] G. Chen, Y. Wang, J.L. Huang, Breast cancer following polyacrylamide hydrogel injection for breast augmentation: a case report, Mol. Clin. Oncol. 4 (3) (2016) 433–435.
[173] M. Teodorescu, M. Bercea, Poly (vinylpyrrolidone)–a versatile polymer for biomedical and beyond medical applications, Polym. Plast. Technol. Eng. 54 (9) (2015) 923–943.
[174] E. Biazar, et al., Biocompatibility evaluation of a new hydrogel dressing based on polyvinylpyrrolidone/polyethylene glycol, BioMed. Res. Int. 2012 (1) (2012) 343989.
[175] B.A. Butruk-Raszeja, et al., Athrombogenic hydrogel coatings for medical devices–examination of biological properties, Colloids Surf. B Biointerfaces 130 (2015) 192–198.
[176] E. Caló, V.V. Khutoryanskiy, Biomedical applications of hydrogels: a review of patents and commercial products, Eur. Polym. J. 65 (2015) 252–267.
[177] E.A. Kamoun, et al., Crosslinked poly (vinyl alcohol) hydrogels for wound dressing applications: a review of remarkably blended polymers, Arab. J. Chem. 8 (1) (2015) 1–14.
[178] A. Sobczak-Kupiec, et al., Studies on PVP-Based hydrogel polymers as dressing materials with prolonged anticancer drug delivery function, Materials 16 (6) (2023) 2468.
[179] T.A. Horbett, J.L. Brash, Proteins at interfaces: current issues and future prospects, ACS Publ. (1987).
[180] H. Chen, et al., Biocompatible polymer materials: role of protein–surface interactions, Prog. Polym. Sci. 33 (11) (2008) 1059–1087.
[181] P. Wyman, Hydrophilic coatings for biomedical applications in and ex vivo. Coatings for Biomedical Applications, Elsevier, 2012, pp. 3–42.
[182] W. Song, J. Xin, J. Zhang, One-pot synthesis of soy protein (SP)-poly (acrylic acid) (PAA) superabsorbent hydrogels via facile preparation of SP macromonomer, Ind. Crops Prod. 100 (2017) 117–125.
[183] W. Yuan, et al., Weak polyelectrolyte-based multilayers via layer-by-layer assembly: approaches, properties, and applications, Adv. Colloid Interface Sci. 282 (2020) 102200.
[184] M. Sohail, et al., Natural and synthetic polymer-based smart biomaterials for management of ulcerative colitis: a review of recent developments and future prospects, Drug Deliv. Transl. Res. 9 (2019) 595–614.
[185] S. Darvishan, et al., Gamma alumina coated-PAA/PVP hydrogel as promising quercetin nanocarrier: physiochemical characterization and toxicity activity, J. Drug Deliv. Sci. Technol. 84 (2023) 104500.
[186] P. Alexandridis, T.A. Hatton, Poly (ethylene oxide)□ poly (propylene oxide)□ poly (ethylene oxide) block copolymer surfactants in aqueous solutions and at interfaces: thermodynamics, structure, dynamics, and modeling, Colloids Surf. A Physicochem. Eng. Asp. 96 (1-2) (1995) 1–46.

[187] M. Piotrowski, et al., Study of the optimal composition and storage conditions of the Fricke–XO–Pluronic F–127 radiochromic dosimeter, Materials 15 (3) (2022) 984.
[188] M. Kozicki, et al., Preliminary study on a 3D lung mimicking dosimeter based on pluronic F-127 matrix, Radiat. Phys. Chem. 185 (2021) 109479.
[189] M. Zięba, et al., Polymeric carriers for delivery systems in the treatment of chronic periodontal disease, Polymers 12 (7) (2020) 1574.
[190] G. Cossellu, et al., Space-maintaining management in maxillary sinus lifting: a novel technique using a resorbable polymeric thermo-reversible gel, Int. J. Oral. Maxillofac. Surg. 46 (5) (2017) 648–654.
[191] E. Brambilla, et al., Poloxamer-Based hydrogel as drug delivery system: how polymeric excipients influence the Chemical-Physical properties, Polymers 14 (17) (2022) 3624.
[192] W.N. Chen, et al., Poloxamer 188 (P188), a potential polymeric protective agent for central nervous system disorders: a systematic review, Curr. Neuropharmacol. 20 (4) (2022) 799–808.
[193] D. Shastri, S. Prajapati, L. Patel, Design and development of thermoreversible ophthalmic in situ hydrogel of moxifloxacin HCl, Curr. Drug Deliv. 7 (3) (2010) 238–243.
[194] W. Gao, et al., Nanoparticle-hydrogel: a hybrid biomaterial system for localized drug delivery, Ann. Biomed. Eng. 44 (6) (2016) 2049–2061.
[195] M. Zhang, et al., Advanced application of stimuli-responsive drug delivery system for inflammatory arthritis treatment, Mater. Today Bio 14 (2022) 100223.
[196] E. Mauri, et al., Graphene-laden hydrogels: a strategy for thermally triggered drug delivery, Materials Science Engineering C 118 (2021) 111353.
[197] L.L. Palmese, et al., Multi-stimuli-responsive, liposome-crosslinked poly(ethylene glycol) hydrogels for drug delivery, J. Biomater. Sci. Polym. Ed. 32 (5) (2021) 635–656.
[198] Y.-X. Zhang, et al., Reduction-and pH-Sensitive lipoic acid-modified poly (l-lysine) and polypeptide/silica hybrid hydrogels/nanogels, Polymer 86 (2016) 32–41.
[199] Y. Shi, et al., Conductive “smart” hybrid hydrogels with PNIPAM and nanostructured conductive polymers, Adv. Funct. Mater. 25 (8) (2015) 1219–1225.
[200] L.L. Palmese, et al., Hybrid hydrogels for biomedical applications, Curr. Opin. Chem. Eng. 24 (2019) 143–157.
[201] F. Farjadian, et al., Smart nanogels as promising platform for delivery of drug, gene, and vaccine; therapeutic applications and active targeting mechanism, Eur. Polym. J. 219 (2024) 113400.
[202] V.S. Ghorpade, et al., Citric acid crosslinked carboxymethylcellulose-poly (ethylene glycol) hydrogel films for delivery of poorly soluble drugs, Int. J. Biol. Macromol. 118 (2018) 783–791.
[203] C. Gao, et al., Xylan-based temperature/ph sensitive hydrogels for drug controlled release, Carbohydr. Polym. 151 (2016) 189–197.
[204] Z. Liu, et al., Advances in the application of natural/synthetic hybrid hydrogels in tissue engineering and delivery systems: a comprehensive review, Int. J. Pharm. (2025) 125323.
[205] N. Chauhan, et al., Dexamethasone-loaded, injectable pullulan-poly (ethylene glycol) hydrogels for bone tissue regeneration in chronic inflammatory conditions, Materials Science Engineering C 130 (2021) 112463.
[206] H. Wang, et al., Doxorubicin conjugated phospholipid prodrugs as smart nanomedicine platforms for cancer therapy, J. Mater. Chem. B 3 (16) (2015) 3297–3305.
[207] J. Qu, et al., Antibacterial adhesive injectable hydrogels with rapid self-healing, extensibility and compressibility as wound dressing for joints skin wound healing, Biomaterials 183 (2018) 185–199.
[208] L. Yang, et al., Improving tumor chemotherapy effect using an injectable self-healing hydrogel as drug carrier, Polym. Chem. 8 (34) (2017) 5071–5076.
[209] W. Xie, et al., Injectable and self-healing thermosensitive magnetic hydrogel for asynchronous control release of doxorubicin and docetaxel to treat triple-negative breast cancer, ACS Appl. Mater. Interfaces 9 (39) (2017) 33660–33673.
[210] Y. Li, J. Rodrigues, H. Tomás, Injectable and biodegradable hydrogels: gelation, biodegradation and biomedical applications, Chem. Soc. Rev. 41 (6) (2012) 2193–2221.
[211] C.H. Takimoto, A. Awada, Safety and anti-tumor activity of sorafenib (Nexavar®) in combination with other anti-cancer agents: a review of clinical trials, Cancer Chemother. Pharmacol. 61 (2008) 535–548.
[212] E.I. Obeagu, G.U. Obeagu, Breast cancer: a review of risk factors and diagnosis, Medicine 103 (3) (2024) e36905.
[213] Y.-S. Sun, et al., Risk factors and preventions of breast cancer, Int. J. Biol. Sci. 13 (11) (2017) 1387.
[214] D.S. Shaker, et al., In situ thermosensitive tamoxifen citrate loaded hydrogels: an effective tool in breast cancer loco-regional therapy, J. Drug Deliv. Sci. Technol. 35 (2016) 155–164.
[215] X. Chen, et al., Injectable hydrogels for the sustained delivery of a HER2-targeted antibody for preventing local relapse of HER2+ breast cancer after breast-conserving surgery, Theranostics 9 (21) (2019) 6080–6098.
[216] X. Bi, et al., Polyamidoamine dendrimer-mediated hydrogel for solubility enhancement and anti-cancer drug delivery, J. Biomater. Appl. 38 (6) (2024) 733–742.
[217] Y.T. Fong, C.-H. Chen, J.-P. Chen, Intratumoral delivery of doxorubicin on Folate-Conjugated graphene oxide by In-Situ forming Thermo-Sensitive hydrogel for breast cancer therapy, Nanomaterials 7 (11) (2017) 388.
[218] I. Pandya, et al., Metal organic framework-based polymeric hydrogel: a promising drug delivery vehicle for the treatment of breast cancer, Int. J. Pharm. 658 (2024) 124206.
[219] C. Nieto, et al., Biodegradable gellan gum hydrogels loaded with paclitaxel for HER2+ breast cancer local therapy, Carbohydr. Polym. 294 (2022) 119732.
[220] T. Wang, et al., Injectable, adhesive albumin nanoparticle-incorporated hydrogel for sustained localized drug delivery and efficient tumor treatment, ACS Appl. Mater. Interfaces 16 (8) (2024) 9868–9879.
[221] P.M. Webb, S.J. Jordan, Global epidemiology of epithelial ovarian cancer, Nat. Rev. Clin. Oncol. 21 (5) (2024) 389–400.
[222] S. Nag, et al., Maintenance therapy for newly diagnosed epithelial ovarian cancer–a review, J. ovarian Res. 15 (1) (2022) 88.
[223] G.C. Jayson, et al., Ovarian cancer, lancet 384 (9951) (2014) 1376–1388.
[224] P. DiSilvestro, A.A. Secord, Maintenance treatment of recurrent ovarian cancer: is it ready for prime time? Cancer Treat. Rev. 69 (2018) 53–65.
[225] H. Hyun, et al., Photo-Cured glycol chitosan hydrogel for ovarian cancer drug delivery, Mar. Drugs 17 (1) (2019) 41.
[226] J.V. Lim, M.R. Nepacina, Y.-C. Hsu, The study of designing a controlled drug release using oxaliplatin-loaded hydrogel for ovarian cancer treatment, J. Taiwan Inst. Chem. Eng. (2024) 105326.
[227] C. Li, et al., Biocompatible supramolecular pseudorotaxane hydrogels for controllable release of doxorubicin in ovarian cancer SKOV-3 cells, RSC Adv. 10 (2) (2020) 689–697.
[228] S. Serini, et al., Characterization of a hyaluronic acid and folic acid-based hydrogel for cisplatin delivery: antineoplastic effect in human ovarian cancer cells in vitro, Int. J. Pharm. 606 (2021) 120899.
[229] G. Xu, et al., Improving the anti-ovarian cancer activity of docetaxel by self-assemble micelles and thermosensitive hydrogel drug delivery system, J. Biomed. Nanotechnol. 16 (1) (2020) 40–53.
[230] B. Sun, et al., Intraperitoneal chemotherapy of ovarian cancer by hydrogel depot of paclitaxel nanocrystals, J. Control. Release 235 (2016) 91–98.
[231] M. McKenzie, et al., Proof-of-concept of polymeric sol-gels in multi-drug delivery and intraoperative image-guided surgery for peritoneal ovarian cancer, Pharm. Res. 33 (2016) 2298–2306.
[232] S. Sargazi, et al., Induction of apoptosis and modulation of homologous recombination DNA repair pathway in prostate cancer cells by the combination of AZD2461 and valproic acid, EXCLI J. 18 (2019) 485.
[233] International., W.C.R.F. *Prostate cancer*. Available from: ⟨https://www.wcrf.org/diet-activity-and-cancer/cancer-types/prostate-cancer/⟩.
[234] M.K. Khang, et al., Preparation of a novel injectable in situ-gelling nanoparticle with applications in controlled protein release and cancer cell entrapment, RSC Adv. 8 (60) (2018) 34625–34633.
[235] M. Liu, et al., Injectable thermoresponsive hydrogel formed by alginate-g-poly (N-isopropylacrylamide) that releases doxorubicin-encapsulated micelles as a smart drug delivery system, ACS Appl. Mater. Interfaces 9 (41) (2017) 35673–35682.
[236] F. Bray, B. Stewart, C. Wild, World cancer report 2014, Transit. Hum. Dev. Glob. Cancer Burd. (2014).
[237] M.M. Fidler, I. Soerjomataram, F. Bray, A global view on cancer incidence and national levels of the human development index, Int. J. Cancer 139 (11) (2016) 2436–2446.
[238] Fund, W.C.R., *Continuous Update Project Expert Report 2018*: *Diet, Nutrition, Physical Activity and Colorectal Cancer*.
[239] Z. Liang, et al., A sequential delivery system based on MoS2 nanoflower doped chitosan/oxidized dextran hydrogels for colon cancer treatment, Int. J. Biol. Macromol. 233 (2023) 123616.
[240] X. Long, et al., Injectable 2D-MoS2-integrated bioadhesive hydrogel as Photothermal-Derived and Drug-Delivery implant for colorectal cancer therapy, Adv. Healthc. Mater. 14 (11) (2025) 2404842.
[241] Y. Liang, et al., pH-responsive injectable hydrogels with mucosal adhesiveness based on chitosan-grafted-dihydrocaffeic acid and oxidized pullulan for localized drug delivery, J. Colloid Interface Sci. 536 (2019) 224–234.
[242] M.M. Ghobashy, A.M. Elbarbary, D.E. Hegazy, Gamma radiation synthesis of a novel amphiphilic terpolymer hydrogel pH-responsive based chitosan for colon cancer drug delivery, Carbohydr. Polym. 263 (2021) 117975.
[243] O. Abdullah, et al., Synthesis of hydrogels for combinatorial delivery of 5-fluorouracil and leucovorin calcium in colon cancer: optimization, in vitro characterization and its toxicological evaluation, Polym. Bull. 76 (2019) 3017–3037.
[244] A. Zarbab, et al., Synthesis and characterization of guar gum based biopolymeric hydrogels as carrier materials for controlled delivery of methotrexate to treat colon cancer, Saudi J. Biol. Sci. 30 (8) (2023) 103731.
[245] Y. Sheng, et al., Dual-drug delivery system based on the hydrogels of alginate and sodium carboxymethyl cellulose for colorectal cancer treatment, Carbohydr. Polym. 269 (2021) 118325.
[246] S. Tahmasebi, R. Mohammadi, Green synthesis of pH-sensitive magnetic bio-nanocomposite hydrogel based on galactomannan and sodium alginate for targeted colorectal cancer drug delivery, Journal Science Advanced Materials Devices 10 (2) (2025) 100892.
[247] M.U. Minhas, et al., Synthesis and characterization of biodegradable hydrogels for oral delivery of 5-fluorouracil targeted to colon: screening with preliminary in vivo studies, Adv. Polym. Technol. 37 (1) (2018) 221–229.
[248] K.M. Rao, et al., Ph sensitive halloysite-sodium hyaluronate/poly (hydroxyethyl methacrylate) nanocomposites for colon cancer drug delivery, Appl. clay Sci. 97 (2014) 33–42.
[249] S. Sarkar, et al., A self-healable and injectable hydrogel for pH-responsive doxorubicin drug delivery in vitro and in vivo for colon cancer treatment, Mater. Today Chem. 30 (2023) 101554.

[250] N. Batool, et al., Orally administered, biodegradable and biocompatible Hydroxypropyl–β–Cyclodextrin grafted Poly(methacrylic acid) hydrogel for ph sensitive sustained anticancer drug delivery, Gels 8 (3) (2022) 190.
[251] L. Yin, et al., Carboxymethylcellulose based self-healing hydrogel with coupled DOX as camptothecin loading carrier for synergetic colon cancer treatment, Int. J. Biol. Macromol. 249 (2023) 126012.
[252] G. Carreño, et al., Development of "on-demand" thermo-responsive hydrogels for anti-cancer drugs sustained release: rational design, in silico prediction and in vitro validation in colon cancer models, Materials Science Engineering C 131 (2021) 112483.
[253] J. Ferlay, M. Colombet, F. Bray, Cancer incidence in five continents, CI5plus: IARC CancerBase no. 9, International Agency for Research on Cancer, Lyon, France, 2018.
[254] R. Karim, et al., Nanocarriers for the treatment of glioblastoma multiforme: current state-of-the-art, J. Control. Release 227 (2016) 23–37.
[255] C. Bastiancich, et al., Anticancer drug-loaded hydrogels as drug delivery systems for the local treatment of glioblastoma, J. Control. Release 243 (2016) 29–42.
[256] M. McKenzie, et al., Hydrogel-based drug delivery systems for poorly water-soluble drugs, Molecules 20 (11) (2015) 20397–20408.
[257] F.W. Lin, et al., Rapid in situ MRI traceable Gel-forming Dual-drug delivery for synergistic therapy of brain tumor, Theranostics 7 (9) (2017) 2524–2536.
[258] S. Jaiswal, et al., A non-covalently cross-linked self-healing hydrogel for drug delivery: characterization, mechanical strength, and anti-cancer potential, N. J. Chem. 48 (35) (2024) 15670–15686.
[259] J.I. Kim, et al., MRI-monitored long-term therapeutic hydrogel system for brain tumors without surgical resection, Biomaterials 33 (19) (2012) 4836–4842.
[260] Y. Xu, et al., Polymer nanocomposites based thermo-sensitive gel for paclitaxel and temozolomide co-delivery to glioblastoma cell, J. Nanosci. Nanotechnol. 15 (12) (2015) 9777–9787.
[261] T. Fourniols, et al., Temozolomide-loaded photopolymerizable PEG-DMA-based hydrogel for the treatment of glioblastoma, J. Control. Release 210 (2015) 95–104.
[262] T. Arai, et al., Novel local drug delivery system using thermoreversible gel in combination with polymeric microspheres or liposomes, Anticancer Res. 30 (4) (2010) 1057–1064.
[263] M. Thun, et al., Stages of the cigarette epidemic on entering its second century, Tob. Control 21 (2) (2012) 96–101.
[264] A. Wéber, et al., Lung cancer mortality in the wake of the changing smoking epidemic: a descriptive study of the global burden in 2020 and 2040, BMJ Open 13 (5) (2023) e065303.
[265] D.M. Parkin, F. Bray, S. Devesa, Cancer burden in the year 2000. The global picture, Eur. J. Cancer 37 (2001) 4–66.
[266] R. Alonso, et al., Lung cancer incidence trends in Uruguay 1990–2014: an age-period-cohort analysis, Cancer Epidemiol. 55 (2018) 17–22.
[267] N. Wang, et al., Anti-tumor effect of local injectable hydrogel-loaded endostatin alone and in combination with radiotherapy for lung cancer, Drug Deliv. 28 (1) (2021) 183–194.
[268] T. Anirudhan, M. Mohan, M. Rajeev, Modified chitosan-hyaluronic acid based hydrogel for the pH-responsive Co-delivery of cisplatin and doxorubicin, Int. J. Biol. Macromol. 201 (2022) 378–388.
[269] C. Chittasupho, et al., Biopolymer hydrogel scaffolds containing doxorubicin as a localized drug delivery system for inhibiting lung cancer cell proliferation, Polymers 13 (20) (2021) 3580.
[270] Q. Gao, et al., Intratumoral injection of anlotinib hydrogel enhances antitumor effects and reduces toxicity in mouse model of lung cancer, Drug Deliv. 27 (1) (2020) 1524–1534.
[271] Z. Wu, et al., Thermosensitive hydrogel used in dual drug delivery system with paclitaxel-loaded micelles for in situ treatment of lung cancer, Colloids Surf. B Biointerfaces 122 (2014) 90–98.
[272] P. Lee, et al., A multifunctional hydrogel delivers gold compound and inhibits human lung cancer xenograft, Pharm. Res. 36 (2019) 1–10.
[273] J. Li, et al., A triple-combination nanotechnology platform based on multifunctional RNA hydrogel for lung cancer therapy, Sci. China Chem. 63 (2020) 546–553.
[274] T. Meng, et al., Delivery of small-molecule drugs and protein drugs by injectable acid-responsive self-assembled COF hydrogels for combinatorial lung cancer treatment, ACS Appl. Mater. Interfaces 15 (36) (2023) 42354–42368.
[275] W.T. London, K.A. Mcglynn, Liver cancer, Cancer Epidemiol. Prev. (2006) 763–786.
[276] B. Gao, et al., Intratumoral administration of thermosensitive hydrogel co-loaded with norcantharidin nanoparticles and doxorubicin for the treatment of hepatocellular carcinoma, Int. J. Nanomed. (2021) 4073–4085.
[277] P. Ma, et al., Hybrid polydimethylsiloxane (PDMS) incorporated thermogelling system for effective liver cancer treatment, Pharmaceutics 14 (12) (2022) 2623.
[278] M. Peng, et al., Thermosensitive injectable hydrogel enhances the antitumor effect of embelin in mouse hepatocellular carcinoma, J. Pharm. Sci. 103 (3) (2014) 965–973.
[279] Q. Wen, et al., Therapeutic efficacy of thermosensitive pluronic hydrogel for codelivery of resveratrol microspheres and cisplatin in the treatment of liver cancer ascites, Int. J. Pharm. 582 (2020) 119334.
[280] Z. Liu, et al., Shear-responsive injectable supramolecular hydrogel releasing doxorubicin loaded micelles with pH-sensitivity for local tumor chemotherapy, Int. J. Pharm. 530 (1-2) (2017) 53–62.
[281] S. Mansha, et al., Development of pH-Responsive, thermosensitive, antibacterial, and anticancer CS/PVA/Graphene blended hydrogels for controlled drug delivery, Gels 10 (3) (2024) 205.
[282] F. Raza, et al., Paclitaxel-loaded ph responsive hydrogel based on self-assembled peptides for tumor targeting, Biomater. Sci. 7 (5) (2019) 2023–2036.
[283] C. Xu, et al., Biodegradable nanoparticles of polyacrylic acid–stabilized amorphous CaCO3 for tunable pH-responsive drug delivery and enhanced tumor inhibition, Adv. Funct. Mater. 29 (24) (2019) 1808146.
[284] J. Qu, et al., pH-responsive self-healing injectable hydrogel based on N-carboxyethyl chitosan for hepatocellular carcinoma therapy, Acta Biomater. 58 (2017) 168–180.
[285] M.F. Abou Taleb, A. Alkahtani, S.K. Mohamed, Radiation synthesis and characterization of sodium alginate/chitosan/hydroxyapatite nanocomposite hydrogels: a drug delivery system for liver cancer, Polym. Bull. 72 (2015) 725–742.
[286] C. Cheng, et al., Development of a dual drug-loaded hydrogel delivery system for enhanced cancer therapy: in situ formation, degradation and synergistic antitumor efficiency, J. Mater. Chem. B 5 (43) (2017) 8487–8497.
[287] C.P. Howson, T. Hiyama, E.L. Wynder, The decline in gastric cancer: epidemiology of an unplanned triumph, Epidemiol. Rev. 8 (1) (1986) 1–27.
[288] W.F. Anderson, et al., The changing face of noncardia gastric cancer incidence among US non-Hispanic whites, JNCI Journal National Cancer Institute 110 (6) (2018) 608–615.
[289] M. Arnold, et al., Is gastric cancer becoming a rare disease? A global assessment of predicted incidence trends to 2035, Gut 69 (5) (2020) 823–829.
[290] M. Zhou, et al., Doxorubicin-loaded single wall nanotube thermo-sensitive hydrogel for gastric cancer chemo-photothermal therapy, Adv. Funct. Mater. 25 (29) (2015) 4730–4739.
[291] K. Qian, et al., Evaluation of cisplatin-hydrogel for improving localized antitumor efficacy in gastric cancer, Pathol. Res. Pract. 215 (4) (2019) 755–760.
[292] S. Emoto, et al., Intraperitoneal administration of cisplatin via an in situ cross-linkable hyaluronic acid-based hydrogel for peritoneal dissemination of gastric cancer, Surg. Today 44 (2014) 919–926.
[293] W. Chen, et al., Sustained co-delivery of 5-fluorouracil and cis-platinum via biodegradable thermo-sensitive hydrogel for intraoperative synergistic combination chemotherapy of gastric cancer, Bioact. Mater. 23 (2023) 1–15.
[294] T.S. Han, et al., Improvement of anti-cancer drug efficacy via thermosensitive hydrogel in peritoneal carcinomatosis in gastric cancer, Oncotarget 8 (65) (2017) 108848–108858.
[295] H. Qian, et al., Therapy for gastric cancer with peritoneal metastasis using injectable albumin hydrogel hybridized with paclitaxel-loaded red blood cell membrane nanoparticles, ACS Biomater. Sci. Eng. 5 (2) (2019) 1100–1112.
[296] Y. Lei, et al., Inhibition of MGMT-mediated autophagy suppression decreases cisplatin chemosensitivity in gastric cancer, Biomed. Pharmacother. 125 (2020) 109896.
[297] J.U. Bertrand, et al., Melanoma risk and melanocyte biology, Acta Derm. Venereol. 100 (11) (2020).
[298] J. Pastwińska, et al., Targeting EGFR in melanoma–the sea of possibilities to overcome drug resistance, Biochimica et Biophysica Acta (BBA)Reviews Cancer 1877 (4) (2022) 188754.
[299] R.I. Hartman, J.Y. Lin, Cutaneous melanoma—a review in detection, staging, and management, Hematol. /Oncol. Clin. 33 (1) (2019) 25–38.
[300] Y. Ding, et al., Single-cell sequencing analysis related to sphingolipid metabolism guides immunotherapy and prognosis of skin cutaneous melanoma, Front. Immunol. 14 (2023) 1304466.
[301] A. Alkilani, M. McCrudden, R. Donnelly, Transdermal drug delivery: innovative pharmaceutical developments based on disruption of the barrier properties of the stratum corneum, Pharmaceutics 7 (2015) 438–470.
[302] F.-Y. Wang, et al., Transdermal drug delivery systems for fighting common viral infectious diseases, Drug Deliv. Transl. Res. 11 (4) (2021) 1498–1508.
[303] H. Labie, M. Blanzat, Hydrogels for dermal and transdermal drug delivery, Biomater. Sci. 11 (12) (2023) 4073–4093.
[304] B. Kim, et al., Transdermal delivery systems in cosmetics, Biomed. Dermatol. 4 (2020) 1–12.
[305] A. Ahsan, et al., An overview of hydrogels and their role in transdermal drug delivery, Int. J. Polym. Mater. Polym. Biomater. 70 (8) (2021) 574–584.
[306] R. Johnson, N.Y. Wang, Drug delivery systems for wound healing, Curr. Pharm. Biotechnol. 16 (7) (2015) 621–629.
[307] Y. Ni, et al., Lipopeptide liposomes-loaded hydrogel for multistage transdermal chemotherapy of melanoma, J. Control. Release 351 (2022) 245–254.
[308] Y. Sun, et al., Transdermal delivery of the in situ hydrogels of curcumin and its inclusion complexes of hydroxypropyl-β-cyclodextrin for melanoma treatment, Int. J. Pharm. 469 (1) (2014) 31–39.
[309] V. Paganini, et al., Nanostructured strategies for melanoma Treatment—Part II: targeted topical delivery of curcumin via Poloxamer-Based thermosensitive hydrogels, Pharmaceuticals 18 (3) (2025) 337.
[310] S. Nazir, et al., Nanocomposite hydrogels for melanoma skin cancer care and treatment: In-vitro drug delivery, drug release kinetics and anti-cancer activities, Arab. J. Chem. 14 (5) (2021) 103120.
[311] J. Liu, et al., Sericin/dextran injectable hydrogel as an optically trackable drug delivery system for malignant melanoma treatment, ACS Appl. Mater. Interfaces 8 (10) (2016) 6411–6422.
[312] A. Luca, et al., New methacrylated biopolymer-based hydrogels as localized drug delivery systems in skin cancer therapy, Gels 9 (5) (2023) 371.
[313] S.M. Carvalho, et al., Synthesis and in vitro assessment of anticancer hydrogels composed by carboxymethylcellulose-doxorubicin as potential transdermal delivery systems for treatment of skin cancer, J. Mol. Liq. 266 (2018) 425–440.
[314] N.S. Capanema, et al., Hybrid hydrogel composed of carboxymethylcellulose–silver nanoparticles–doxorubicin for anticancer and

antibacterial therapies against melanoma skin cancer cells, ACS Appl. Nano Mater. 2 (11) (2019) 7393–7408.
[315] Accessed April 13, 2022; Available from: ⟨http://gco.iarc.fr/today/home⟩.
[316] *Survival Rates for Bladder Cancer (n.d.)*. Accessed May 20, 2021; Available from: ⟨https://www.cancer.org/cancer/bladder-cancer/detection-diagnosis-staging/survival-rates.html⟩.
[317] 2014., A.G.C.f.D.C.a.P.U. *The Health Consequences of Smoking—50 Years of Progress*. Available from: ⟨https://www.ncbi.nlm.nih.gov/books/NBK179276/⟩.
[318] J. Liu, et al., Intravesical chemotherapy synergize with an immune adjuvant by a thermo-sensitive hydrogel system for bladder cancer, Bioact. Mater. 31 (2024) 315–332.
[319] C. Zhang, et al., Polysaccharide based supramolecular injectable hydrogels for in situ treatment of bladder cancer, Chin. Chem. Lett. 35 (1) (2024) 108556.
[320] F. Li, et al., Mucoadhesive thiolated hyaluronic Acid/Pluronic F127 nanogel formation via Thiol–Maleimide click reaction for intravesical drug delivery, ACS Appl. Bio Mater. 7 (3) (2024) 1976–1989.
[321] K. Men, et al., Delivering instilled hydrophobic drug to the bladder by a cationic nanoparticle and thermo-sensitive hydrogel composite system, Nanoscale 4 (20) (2012) 6425–6433.
[322] M.K. Jaiswal, et al., Magneto-thermally responsive hydrogels for bladder cancer treatment: therapeutic efficacy and in vivo biodistribution, Colloids Surf. B Biointerfaces 136 (2015) 625–633.
[323] P. Yin, et al., Chitosan/polyvinyl alcohol-based magnetic hydrogel microspheres with controlled retention and regulated drug release for intravesical instillation, Int. J. Biol. Macromol. 287 (2025) 138412.
[324] M. Šťastný, et al., HPMA-hydrogels containing cytostatic drugs: kinetics of the drug release and in vivo efficacy, J. Control. Release 81 (1) (2002) 101–111.
[325] G. Tan, et al., A multifunctional MOF-based nanohybrid as injectable implant platform for drug synergistic oral cancer therapy, Chem. Eng. J. 390 (2020) 124446.
[326] X. Chen, et al., Local delivery of gambogic acid to improve anti-tumor immunity against oral squamous cell carcinoma, J. Control. Release 351 (2022) 381–393.
[327] C. Karavasili, et al., Synergistic antitumor potency of a self-assembling peptide hydrogel for the local co-delivery of doxorubicin and curcumin in the treatment of head and neck cancer, Mol. Pharm. 16 (6) (2019) 2326–2341.
[328] M. Haider, et al., Erlotinib and curcumin-loaded nanoparticles embedded in thermosensitive chitosan hydrogels for enhanced treatment of head and neck cancer, Int. J. Pharm. 666 (2024) 124825.
[329] G. Carreño, et al., Development of "on-demand" thermo-responsive hydrogels for anti-cancer drugs sustained release: rational design, in silico prediction and in vitro validation in colon cancer models, Materials Science Engineering C 131 (2021) 112483.
[330] A. Mandal, et al., Hydrogels in the clinic, Bioeng. Transl. Med. 5 (2) (2020) e10158.
[331] *VANTAS*® Available from: ⟨https://www.accessdata.fda.gov/drugsatfda_docs/label/2014/021732s015lbl.pdf⟩.
[332] G.A. DuVall, et al., Phase 2: a dose-escalation study of OncoGel (ReGel/paclitaxel), a controlled-release formulation of paclitaxel, as adjunctive local therapy to external-beam radiation in patients with inoperable esophageal cancer, AntiCancer Drugs 20 (2) (2009) 89–95.
[333] H. Cho, J. Gao, G.S. Kwon, PEG-b-PLA micelles and PLGA-b-PEG-b-PLGA sol-gels for drug delivery, J. Control Release 240 (2016) 191–201.
[334] M. Ahmed, et al., Overcoming the blood brain barrier in glioblastoma: status and future perspective, Rev. Neurol. 179 (5) (2023) 430–436.
[335] J.M. DeWitt, et al., EUS-guided paclitaxel injection as an adjunctive therapy to systemic chemotherapy and concurrent external beam radiation before surgery for localized or locoregional esophageal cancer: a multicenter prospective randomized trial, Gastrointest. Endosc. 86 (1) (2017) 140–149.
[336] A.K. Vellimana, et al., Combination of paclitaxel thermal gel depot with temozolomide and radiotherapy significantly prolongs survival in an experimental rodent glioma model, J. NeuroOncol. 111 (3) (2013) 229–236.
[337] *SpaceOAR*®. Available from: ⟨https://www.accessdata.fda.gov/cdrh_docs/reviews/DEN140030.pdf⟩.
[338] Z.A. Seymour, et al., Long-term follow-up after radiotherapy for prostate cancer with and without rectal hydrogel spacer: a pooled prospective evaluation of bowel-associated quality of life, BJU Int. 126 (3) (2020) 367–372.
[339] S. Cascone, G. Lamberti, Hydrogel-based commercial products for biomedical applications: a review, Int. J. Pharm. 573 (2020) 118803.
[340] B. Liu, K. Chen, Advances in Hydrogel-Based drug delivery systems, Gels 10 (4) (2024) 262.
[341] J.P. Gong, et al., Double-network hydrogels with extremely high mechanical strength, Adv. Mater. 15 (14) (2003) 1155–1158.
[342] T. Vermonden, R. Censi, W.E. Hennink, Hydrogels for protein delivery, Chem. Rev. 112 (5) (2012) 2853–2888.
[343] L.M. Ickenstein, P. Garidel, Hydrogel formulations for biologicals: current spotlight from a commercial perspective, Ther. Deliv. 9 (3) (2018) 221–230.
[344] S.J. Bryant, C.R. Nuttelman, K.S. Anseth, Cytocompatibility of UV and visible light photoinitiating systems on cultured NIH/3T3 fibroblasts in vitro, J. Biomater. Sci. Polym. Ed. 11 (5) (2000) 439–457.
[345] I.M. El-Sherbiny, M.H. Yacoub, Hydrogel scaffolds for tissue engineering: progress and challenges, Glob. Cardiol. Sci. Pract. 2013 (3) (2013) 38.
[346] T.R. Hoare, D.S. Kohane, Hydrogels in drug delivery: progress and challenges, Polymer 49 (8) (2008) 1993–2007.
[347] P. Zahedi, P.I. Lee, Solid molecular dispersions of poorly water-soluble drugs in poly (2-hydroxyethyl methacrylate) hydrogels, Eur. J. Pharm. Biopharm. 65 (3) (2007) 320–328.
[348] L. Ying, et al., In vitro evaluation of lysozyme-loaded microspheres in thermosensitive methylcellulose-based hydrogel, Chin. J. Chem. Eng. 15 (4) (2007) 566–572.
[349] D. Gulsen, A. Chauhan, Dispersion of microemulsion drops in HEMA hydrogel: a potential ophthalmic drug delivery vehicle, Int. J. Pharm. 292 (1-2) (2005) 95–117.
[350] K.L. Spiller, G. Vunjak-Novakovic, Clinical translation of controlled protein delivery systems for tissue engineering, Drug Deliv. Transl. Res. 5 (2015) 101–115.
[351] E. Hunziker, et al., Translation from research to applications, Tissue Eng. 12 (12) (2006) 3341–3364.
[352] Z. Li, et al., AI energized hydrogel design, optimization and application in biomedicine, Mater. Today Bio 25 (2024) 101014.
[353] I. Negut, B. Bita, Exploring the potential of artificial intelligence for hydrogel development—A short review, Gels 9 (11) (2023) 845.
[354] Y. Shokrollahi, et al., Finite element-based machine learning model for predicting the mechanical properties of composite hydrogels, Appl. Sci. 12 (21) (2022) 10835.
[355] C. Boztepe, A. Künkül, M. Yüceer, Application of artificial intelligence in modeling of the doxorubicin release behavior of ph and temperature responsive poly (NIPAAm-co-AAc)-PEG IPN hydrogel, J. Drug Deliv. Sci. Technol. 57 (2020) 101603.
[356] M. Islamkulov, S. Karakuş, C. Özeroğlu, Design artificial intelligence-based optimization and swelling behavior of novel crosslinked polymeric network hydrogels based on acrylamide-2-hydroxyethyl methacrylate and acrylamide-N-isopropylacrylamide, Colloid Polym. Sci. 301 (3) (2023) 259–272.
[357] S. Wang, Z. Sun, Hydrogel and machine learning for soft robots' sensing and signal processing: a review, J. Bionic Eng. 20 (3) (2023) 845–857.
[358] M. Seifermann, et al., High-throughput synthesis and machine learning assisted design of photodegradable hydrogels, Small Methods 7 (9) (2023) 2300553.
[359] M. Berezo, et al., Predicting chronic wound healing time using machine learning, Adv. Wound care 11 (6) (2022) 281–296.
[360] Y. Liang, J. He, B. Guo, Functional hydrogels as wound dressing to enhance wound healing, ACS nano 15 (8) (2021) 12687–12722.
[361] H. Li, et al., Multiphysics modelling of volume phase transition of ionic hydrogels responsive to thermal stimulus, Macromol. Biosci. 5 (9) (2005) 904–914.
[362] G. Lamberti, Parametric simulation of drug release from hydrogel-based matrices, J. Pharm. Pharmacol. 64 (1) (2012) 48–51.
[363] F.A. Radu, et al., Modeling of drug release from collagen matrices, J. Pharm. Sci. 91 (4) (2002) 964–972.
[364] I. Salahshoori, et al., Cisplatin uptake and release assessment from hydrogel synthesized in acidic and neutral medium: an experimental and molecular dynamics simulation study, J. Mol. Liq. 344 (2021) 117890.
[365] R.P.K. Pannala, U. Juyal, J. Kodavaty, Optimization of hydrogel composition for effective release of drug, Chem. Prod. Process Model. 18 (6) (2023) 969–975.
[366] N. Albayati, et al., AI-Driven innovation in skin kinetics for transdermal drug delivery: overcoming barriers and enhancing precision, Pharmaceutics 17 (2) (2025) 188.
[367] G.K. Jena, et al., Artificial intelligence and machine learning implemented drug delivery systems: a paradigm shift in the pharmaceutical industry, J. BioX Res. 7 (2024) 0016.